AD-766 841

SELECTED MATERIAL FROM SOVIET TECHNICAL LITERATURE, JUNE, 1973

Stuart G. Hibben

Informatics, Incorporated

Prepared for:

Advanced Research Projects Agency
Air Force Office of Scientific Research

21 August 1973

informatics inc

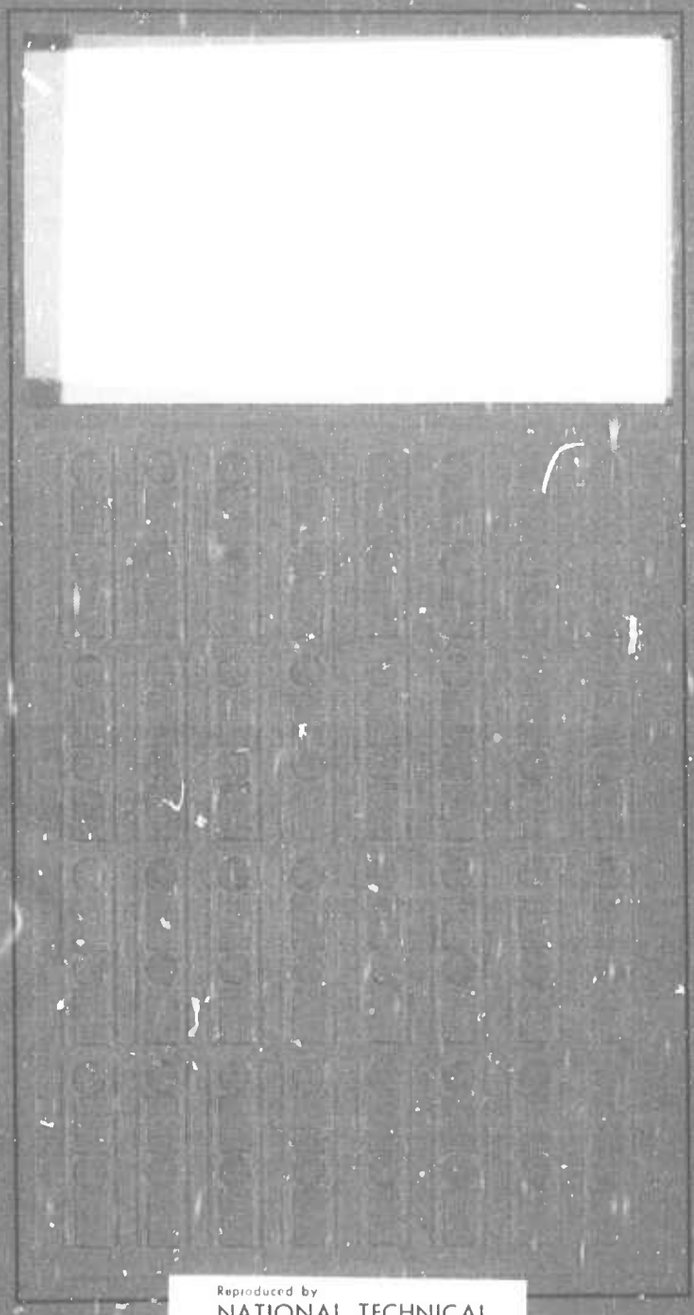

189

SELECTED MATERIAL FROM SOVIET TECHNICAL LITERATURE

June, 1973

Sponsored by

Advanced Research Projects Agency

ARPA Order No. 1622-4

August 21, 1973

ARPA Order No. 1622-4
Program Code No: 62701E3F10
Name of Contractor:
Informatics Inc.
Effective Date of Contract:
January 1, 1973
Contract Expiration Date:
December 31, 1973
Amount of Contract: $343,363

Contract No. F44620-72-C-0053, P00001
Principal Investigator:
Stuart G. Hibben
Tel: (301) 770-3000 or
(301) 779-2850
Program Manager:
Klaus Liebhold
Tel: (301) 770-3000
Short Title of Work:
"Soviet Technical Selections"

This research was supported by the Advanced Research Projects Agency of the Department of Defense and was monitored by the Air Force Office of Scientific Research under Contract No. F44620-72-C-0053. The publication of this report does not constitute approval by any government organization or Informatics Inc. of the inferences, findings, and conclusions contained herein. It is published solely for the exchange and stimulation of ideas.

informatics inc
Systems and Services Company
6000 Executive Boulevard
Rockville Maryland 20852
(301) 770-3000 Telex 89-521

Approved for public release; distribution unlimited.

UNCLASSIFIED

Security Classification

DOCUMENT CONTROL DATA - R & D

(Security classification of title, body of abstract and indexing annotation must be entered when the overall report is classified)

1 ORIGINATING ACTIVITY (Corporate author) Informatics Inc. 6000 Executive Boulevard Rockville, Maryland 20852	2a. REPORT SECURITY CLASSIFICATION UNCLASSIFIED 2b. GROUP

3 REPORT TITLE

Selected Material from Soviet Technical Literature, June, 1973

4. DESCRIPTIVE NOTES (Type of report and inclusive dates)

Scientific . . . Interim

5 AUTHOR(S) (First name, middle initial, last name)

Stuart G. Hibben

6 REPORT DATE August 21, 1973	7a. TOTAL NO. OF PAGES ~~184~~ 189	7b. NO. OF REFS - - -
8a. CONTRACT OR GRANT NO F44620-72-C-0053, P00001 b. PROJECT NO c. 1622-4 d. 62701E3F10	9a. ORIGINATOR'S REPORT NUMBER(S) 9b. OTHER REPORT NO(S) (Any other numbers that may be assigned this report) AFOSR - TR - 73 - 1598	

10 DISTRIBUTION STATEMENT

Approved for public release; distribution unlimited.

11 SUPPLEMENTARY NOTES Tech. Other	12. SPONSORING MILITARY ACTIVITY Air Force Office of Scientific Research 1400 Wilson Boulevard (NPG) Arlington, Virginia 22209

13 ABSTRACT

This report includes abstracts and bibliographic lists on contractual subjects that were completed in June, 1973. The major topics are: laser technology, effects of strong explosions, geosciences, particle beams, and material sciences. Sections on energy technology and miscellaneous interest items are included.

Laser coverage is generally limited to high power effects; all current laser material is routinely entered in the quarterly laser bibliographies.

An index identifying source abbreviations and a first-author index to the abstracts are appended.

1a

DD FORM 1 NOV 68 1473

UNCLASSIFIED

INTRODUCTION

This report includes abstracts and bibliographic lists on contractual subjects that were completed in June, 1973. The major topics are: laser technology, effects of strong explosions, geosciences, particle beams, and material sciences. Sections on energy technology and miscellaneous interest items are included.

Laser coverage is generally limited to high power effects; all current laser material is routinely entered in the quarterly laser bibliographies.

An index identifying source abbreviations and a first-author index to the abstracts are appended.

TABLE OF CONTENTS

1. Laser Technology

A. Abstracts

L. I. Mirkin. Mechanical deformation and destruction of metals from effects of a laser beam with a 10^{-3} second pulse duration. FiKhOM, no. 1, 1973, 31-33.

Deformation and fracture of metallic materials from the effects of laser pulses were studied in a number of single and polycrystalline technical grade metals, ferrous and nonferrous alloys, and refractory metal carbides. Irradiation was with a focused GDS-30M laser beam of $\sim 10^{-3}$ sec. pulse duration with variable beam defocusing. Plastic deformation from irradiation effects was detected in metals, e.g., Cu-15% Pt alloy in an ordered state, by optical micrography and interferometry methods. Typical cracks are exhibited in tungsten and chromium as the result of the presence of impurities at the grain boundaries and a sharp focusing in the absence of a molten zone. Cracks in the presence of a molten zone, e.g. in D16T duralumin, are attributed to thermal stresses generated by crystallization.

In cast iron and metal-carbide-metal compositions, e.g., tungsten carbide-cobalt alloy, cracks propagate very rapidly through both components, because of different coefficients of thermal expansion and weak bonds between crystals. Usually mechanical deformation from effects of millisecond laser pulses is not the main cause of fracture; nonuniform thermal expansion is believed to be the fracture mechanism common to the different materials.

Mirkin, L. I. Feasibility of displacement of atoms in a solid from the effects of a pulsed laser. IVUZ Fiz, no. 2, 1973, 106-108.

In a companion paper to the preceding one, x-ray diffraction data are presented of an ordered Cu-Pt alloy with 25 at %Pt (Cu_3Pt) before and after irradiation with GOS-30M laser pulses of 30 j output energy and 10^{-3} sec. duration. The alloy was selected for study of structure changes via very small displacement of atoms from equilibrium positions, because of its extremely stable superstructure in annealed state. The x-ray diffraction patterns show a total elimination of the cubic superstructure and an increase in intensity of the base line of fcc structure, after a short-time irradiation. The latter effect is attributed to breaking down of large crystal blocs due to a rapid heating and cooling. Micrographs of the thermal effect zone show a polygon structure which is the result of alloy deformation (disordering) with accompanying decrease in microhardness. Thus an ordered alloy is suitable for the study of atom displacement in solid state from the effects of a 10^{-3} sec. laser pulse.

Mirkin, L. I. Contact melt zone on a ferrite-graphite interface from the effect of laser pulses. FiKhOM, no. 1, 1973, 143-145.

A micrographic study is reported of the solid-phase diffusion effects in laser-irradiated gray and malleable cast irons containing ferrite and graphite, the latter of different geometries. Irradiation was with focused laser pulses of 30 j energy and 10^{-3} sec. duration. The irradiated zone was studied with optical and electronic scanning microscopes

at 100,000 X maximum magnification. Micrographs of both gray and malleable cast irons show a zone of partial graphite dissolution between the quenched liquid state (austenite-martensitic) zone and the zone with the original structure. Dimensional analysis of the graphite dissolution zone indicated that this zone may attain 10μ size in malleable cast iron with spheroidal graphite, but does not exceed 2-3μ in gray cast iron containing lamellar graphite. Calculations based on carbon diffusion coefficient in solid and liquid iron showed that, during laser irradiation, diffusion zone boundary shift was three orders of magnitude higher than theoretical shift in solid iron, and one order higher in liquid iron.

The observed phenomena are tentatively explained by contact melting at the iron-graphite interface, which occurs at the m.p. of a eutectic (1,150° C). The mechanism of the observed phenomenon is discussed. The observed significant acceleration of graphite diffusion in comparison to theoretical diffusion is the result of phase transitions during diffusion. In addition, there is cleavage of graphite lamellas and the wedge effect of the liquid formed on the contact surfaces by rapid heating. Also, liquid penetration into porous graphite according to the filtration mechanism in porous media plays a significant role. Confirmation of this latter mechanism of dissolution is seen in the observed difference in dimensions of dissolution zones between the cast irons with spheroidal and lamellar graphite. In the former, crystal adherence to the surrounding iron matrix is weaker than in the latter.

Libenson, M. N., and M. N. Nikitin.
Diffusion of atoms from film to substrate under laser irradiation. FiKhOM, no. 1, 1973, 9-14.

Diffusion of atoms through the film-substrate interface during film heating by a pulsed laser beam is treated theoretically, with allowance for temperature dependence D(T) of the diffusion coefficient. The importance of diffusion is emphasized when making patterns in a film by vaporizing it with laser beam, without affecting the substrate.

The boundary value problem of atom diffusion into the substrate subsurface layer is solved on the assumption that concentration of diffusing atoms at the interface is constant during irradiation time t. The number N(t) of diffused atoms through a unit area during time t and the depth ℓ_D of the diffusion layer are then formulated as functions of $\int D(\theta), d\theta$ and D(t) and the equivalent time $t_e \leq t$ during which D(t) has approximately maximum value, respectively. The formulas show that at a given radiation flux, diffusion layer formation is in effect completed in a short period, when T of the film is near its maximum. Calculations of the minimum number $N_{min}(\tau)$ of atoms diffused into the substrate at a time $t = \tau$ of complete vaporization of the film, the required radiation flux density, and pulse duration τ_o, show that the optimum conditions of film vaporization by a rectangular pulse are a very high T and a τ_o typical for giant laser pulses.

Basov, N. G., A. R. Zaritskiy, S. D. Zakharov, O. N. Krokhin, P. G. Kryukov, Yu. A. Matveyets, Yu. V. Senatskiy, and A. I. Fedosimov. Generation of powerful light pulses at 1.06 and 0.53μ and its application to plasma heating. I. Experimental studies of radiation reflection during laser plasma heating at two wavelengths. IN: Sb. Kvantovaya elektronika, no. 5(11), 1972, 63-71.

Calorimetric, spectroscopic, oscilloscopic, direction shift, and polarization measurement data are given for laser radiation reflected by the plasma of a solid target heated by nanosecond laser pulses at power densities above 10^{14} w/cm^2. The 10^{-9} sec. pulses, with a 10^{-9} sec. repetition rate, were generated at 1.06 and 0.53μ by a mode-locked Nd glass laser and its second harmonic, respectively, in the apparatus described by the authors in the no. 6(12), 1972 issue of the title periodical.

The data obtained present the first known attempt at the study of plasma generated by laser heating of a solid target. It was established that energy losses due to reflection are decreased by one order of magnitude from conversion of 1.06μ laser radiation to the second harmonic. Hence, the 0.53μ radiation absorption by the plasma is three times as strong as absorption of the 1.06μ radiation. It is concluded that the use of even higher harmonics of Nd laser radiation may be advantageous for plasma heating for nuclear fusion purposes.

Vlasov, R. A., K. P. Grigor'yev, I. I. Kantorovich, and G. S. Romanov. Mechanism of shock ionization from optical breakdown of transparent dielectrics. FTT, no. 2, 1973, 444-448.

Some previously overlooked or unclarified problems are taken into account in a theoretical treatment of the avalanche shock ionization of transparent dielectrics by a high-power laser beam. The problems are treated of a more accurate calculation of the photon absorption cross-section $\sigma(\epsilon)$ by an electron of the conduction band, and energy losses of nonequilibrium electrons owing to electron-phonon interactions. Formulas are derived for $\sigma_a(\epsilon)$ and $\sigma_i(\epsilon)$ in cases of electron interactions with the acoustic and optical lattice vibrations, respectively. Necessary and sufficient criteria of the electron avalanche development are formulated from the energy and particle balance, and solution of a kinetic equation for $n(\epsilon)$ in a diffusion approximation with allowance for energy losses due to acoustic phonon generation. The formula derived for threshold density q_o of radiation flux was used to evaluate q_o of leucosapphire breakdown by Nd-glass laser pulses of $\tau \sim 10^{-8}$ sec. The q_o value thus obtained is in satisfactory agreement with the latest Soviet experimental q_o data in the absence of self-focusing.

Vyskrebentsev, A. I., and Yu. P. Rayzer. Simple theory of breakdown in monatomic nonlight gases in fields from low to optical frequency range. ZhPMTF, no. 1, 1973, 40-47.

A simplified approximate theory of avalanche breakdown is developed for monatomic nonlight gases, e.g., Ar or Xe. Simple universal

numerical formulas for the averaged ionization frequency ν_i breakdown field threshold E are derived by solving a set of equations for the electron energy ϵ distribution function, $n(\epsilon, t)$. Simplifications were made by substituting the potentials $I_1^* \cong I^* + 1$ eV and $I_1 \cong I + 1$ eV for the atom excitation potential I^* and ionization potential I, assuming the constancy the collisional excitation frequency ν^* in the $I_1^* < \epsilon < I_1$ range; the frequency ν_m of elastic collisions; and the characteristic time τ_d of electron diffusion at a ν_d frequency, from the electric field. The authors define β and $1-\beta$ to be probabilities of atom ionization and excitation by inelastic electrons, and assume the electrons to have zero energy after inelastic collision or atom ionization.

The transcendental equation thus derived for ν_i defines dimensionless ν_i/ν^* as the universal function $F(\nu_E/\nu^*)$, where $\nu_E = 1/\tau_E$ is the frequency of energy cumulation by an electron during time τ_E necessary to acquire energy I_1 sufficient for multiplication. The numerical value of ν_i/ν^* was calculated for $\beta = 0.2$ (breakdown in a d.c. field, from high frequencies, SHF, and 10.6 μ CO_2 laser radiation) and for $\beta = 1$ (breakdown from optical frequencies). The ν_i/ν^* versus ν_E/ν^* plots are shown. In the case of $\nu^* \leq \nu_E$, the equation for ν_i at $\beta = 1$ gives $\nu_i = 0.8\nu_E$, which is the case of breakdown from a ruby laser. When $\nu^* \geq \nu_E$, the asymptotic solution of the equation gives

$$\nu_i = \nu_E \alpha \beta a^2, \qquad \alpha = 2a \exp\left(-\frac{a-1}{a}\sqrt{6\nu^*/\nu_E}\right) \tag{1}$$

where $\alpha = j(I_1)/j(I_1^*)$ and $a = \sqrt{I_1/I_1^*}$. Thus ν_i is determined, with $a^2 - 1$ approximation, by ν_E and β. The compact formula

$$E^2 = 5.7 \cdot 10^{-16} I_1 (\omega^2 + \nu_m^2) \frac{\nu^*}{\nu_m} \Phi(\eta)$$
$$\eta = (\nu_d + \nu_i)/\nu^*, \qquad \nu_d = 5.8 \cdot 10^{11} I^*/\nu_m A^2 \tag{2}$$

where ω is the field frequency, $\Phi(\eta)$ is the inverse of the F function and Λ is the diffusion length, was derived for E in different gases at different ω, pressures, and dimensions. At $\nu_t \leq \nu_d$ and $\nu_i \approx \nu_d$ ("stationary" breakdown), Eq. (2) applies to breakdown in d.c. field, and from HF, SHF, and CO_2 laser IR radiations. At a low p or $\omega^2 \geq \nu_m^2$, E/ω is a function of $p\Lambda$. At a high p or at a low ω, e.g., in d.c. field, the threshold field increases somewhat slower than p and its dimensional dependence is logarithmic (log $p\Lambda$). The E(p) plots calculated from (2) for Ar and Xe at different frequencies are in reasonably good agreement with earlier experimental data. Thus Eq. (2) can be useful for evaluating E in the absence of experimental data.

Teslenko, V. S. Photohydrodynamic parameters of a laser breakdown in liquids. IN: Sbornik. VI Vses. Konf. po. nelineyn. optike. Minsk, 1972, 81. (RZh Radiot, 2/73, no. 2Ye213)

Acoustic shock wave energy and the energy lost in expanding the cavitation gap are measured for a series of liquids (water, glycerin, benzene) as a function of single-pulsed ruby laser radiation energy delivered (Q = 0-1 joule, τ = 5-70 nsec). Results are plotted in graphs, which may be approximated by $Q_1 = K_1 Q$, $Q_2 = K_2 Q$; where K_1, K_2 are photohydrodynamic coefficients. The results obtained enable determination of the cavity size as a function of delivered optical energy Q.

Grigor'yev, B. A. Simplification of one-dimensional problems of thermal conductivity from pulsed radiative heating of flat bodies. TVT, no. 1, 1973, 133-137.

Using a simplified model of a laser-heated surface, the author develops a differential equation of thermal conductivity in the target material. This is solved for dimensionless excess temperature $\theta_{\psi(s)}$ of a semi-infinite body and the excess temperature ϑ_{ψ} of an infinite plate. The heat is generated in the body or the plate by absorption of a monochromatic radiation according to the Bouguer law.

Two simplified solutions to the cited problems are discussed: substitution of the surface heat flux for the internal heat source, and determination of the local excess temperatures θ^{o}_{ψ} and $\theta^{o}_{\psi(J)}$ from locally released heat, without allowance for thermal conductivity. Relative errors $\Delta g(J)$ $\Delta\psi(J)$ of the excess temperature determinations by two simplified methods are analysed. The maximum possible error $\Delta^{*}_{J}(0)$ is evaluated as a function of the Bouguer (B) and Fourier (F) numbers. A rapid graphical method is developed for selection of the most appropriate approximation, using F-B diagrams which represent the families of orthogonal, exponential, and exponential-power functions. The first approximation method is suitable for metallic bodies and requires solution or superposition of solutions of a hyperbolic equation of thermal conductivity with a heat source. The second method would apply to thermal insulators, especially for transparent bodies.

B. Recent Selections

i. Beam Target Effects

Anisimov, S. I., and B. I. Makshantsev. Rol' pogloshchayushchikh neodnorodnostey v opticheskom proboye prozrachnykh sred. (Preprint). (The role of absorbing inhomogeneity in an optical breakdown of transparent media.) Chernogolovka, 1972, 10 p. (KL Dop vyp, 4/73, no. 7811).

Askar'yan, G. A. Particle motion in a laser beam. UFN, v. 110, no. 1, 1973, 115-116.

Askar'yan, G. A., V. A. Namiot, and M. S. Rabinovich. Using supercompression of material by reactive pressure for obtaining microcrystallic masses of fissionable materials, to generate super-strong magnetic fields, and for particle acceleration. ZhETF P, v. 17, no. 10, 1973, 597-600.

Grasyuk, A. Z., I. G. Zubarev, V. V. Lobko, Yu. A. Matveyets, A. B. Mironov, and O. B. Shatberashvili. Relationship of two-photon absorption in GaAs to light pulse duration. ZhETF P, v. 17, no. 10, 1973, 584-587.

Sinitsyn, A. P., V. A. Krivilev, Yu. V. Sidorin, and V. A. Upadyshev. Stresses in rods resulting from electromagnetic radiation. PM, v. 9, no. 5, 1973, 109-114.

Strekalov, V. N. Quantum kinetic equation and variation in threshold conditions for impact ionization by light. FTT, no. 5, 1973, 1373-1377.

Sultanov, M. A., and V. A. Ageyev. Investigating the destruction of polymeric films due to laser radiation. DAN TadSSR, v. 16, no. 4, 1973, 25-28.

Volod'kina, V. L., K. I. Krylov, M. P. Libenson, and V. T. Prokopenko. Heating an oxidizing metal by CO_2 laser radiation. DAN SSSR, v. 210, no. 1, 1973, 66-69.

Zhiryakov, B. M., N. N. Rykalin, A. A. Uglov, and A. K. Fannibo. Laws governing material ejection from a laser radiation interaction zone. IN: Sb. Kvantovaya elektronika, no. 1(13), 1973, 119-121.

ii. Beam Plasma Interaction

Anan'in, O. B., Yu. A. Bykovskiy, Yu. P. Kozyrev, and A. S. Tsybin. Obtaining laser plasma ion acceleration in a cyclotron. ZhETF P, v. 17, no. 9, 1973, 460-463.

Goncharov, V. K., L. Ya. Min'ko, Ye. S. Tyunina, and A. N. Chumakov. Experimental study of optical properties of an erosion laser plasma in the interaction zone. IN: Sbornik. Kvantovaya elektronika, no. 1(13), 1973, 56-62.

Kaliski, S. Averaged equations of laser implosive compression of D-T plasma with ablation of the heavy envelope, with fusion heat being taken into consideration. IN: ibid., 35(307)-45(316).

Kaliski, S. On a simplified case of thermal concentric compression of matter with ablation, using an averaged description. Bulletin de l'Academie Polonaise des Science, serie des sciences techniques, v. 21, no. 4, 1973, 45(317)-53(325).

Yampol'skiy, Yu. P. Izlucheniye lazera i khimicheskaya reaktsiya. (Laser radiation and chemical reactions). Moskva, Izd-vo Znaniye, 1973, 64 p.

Zhuravlev, V. A., and G. D. Petrov. Two-photon optical scattering spectra in an electron plasma. OiS, v. 34, no. 5, 1973, 1012-1015.

2. Effects of Strong Explosions

A. Abstracts

Zlatin, N. A., A. A. Kozhushko, V. A. Lagunov and V. A. Stepanov. Method of measuring pressure in a discharge channel during electrical impulse breakdown of solid dielectrics. ZhTF, no. 12, 1972, 2618-2620.

Experimental determination is described of pressure p in a discharge channel formed by electrical breakdown of plexiglass. Breakdown was induced by applying 650 kV voltage pulses to electrodes imbedded in a plexiglass specimen. Propagation of the breakdown-initiated waves and development of the specimen fracture was recorded by high speed motion picture camera and a Schlieren photographic system. Typical frames are shown of the electric breakdown at discharge current periods of 1.1 and 5.7 μsec.

The pictures were used to calculate p by two methods. The first method consisted of measuring propagation rate of the leading shock wave generated by the first voltage pulse, then determining shock wave amplitude at the time of separation from the channel walls, i.e., p on the walls, using the computed values of the shock wave propagation rate at t = 0 and the shock adiabat of plexiglass. A second method, applicable in the case when material strength is negligible, uses the experimental initial growth rate of the channel radius, which is equated to the mass velocity behind the shock wave front. Both methods gave approximately the same p value of about 30 kbar.

Rabinovich, V. A., L. M. Burshteyn, and N. M. Akulova. Thermodynamic properties of solid para-hydrogen at 0 to 25° K temperatures and 1 to 500 bar. IN: Sbornik. Teplofizicheskiye svoystva veshchestv pri nizkikh temperaturakh, Moskva, 1972, 31-39. (RZhKh, 3/73, no. 3B683). (Translation).

The equation of state for solid parahydrogen is formulated on the basis of thermodynamic correlations. The method of establishing the equation of state from thermal and caloric experimental data is developed. The equation was used to calculate thermodynamic properties of solid para-hydrogen within a specified range of parameters, and to plot the phase diagram. The calculated detailed thermodynamic data are tabulated.

Romanov, I. D., and V. V. Sten'gach. Sensitivity of PETN to electrical sparks. ZhPMTF, no. 6, 1972, 152-155.

Experimental data are given on the effect of PETN and discharge circuit characteristics on sensitivity of PETN to electric sparks. Sensitivity is defined as the amount of energy W_{50} released in the spark gap which is sufficient to detonate 50% of the explosive charge. Study of sensitivity is important for development of safety measures and regulations of the practical uses of explosives. In the experiments, frequency of explosions was determined as a function of released energy. Explosions were initiated by discharge of a capacitance connected across the spark gap. The electrodes were mounted in a chamber into which PETN

was pressed. At a 0.05 μH minimum inductance of the discharge circuit, 90% of stored energy was released in the spark gap during 10^{-8} sec. The experimental plots show that W_{50} increases, i.e., sensitivity decreases, with an increase in PETN crystal size from 2.4 to 100 μ, an increase in its density from 0.9 to 1.40 g/cm^3, or increase in its moisture content from 0 to 3%. The tabulated data show that W_{50} decreases from 27.0 to 4.5 mj when the temperature is raised from 203° to 323° K. The spark gap length dependence of W_{50} exhibits a minimum at a 0.2-0.3 mm gap (Fig. 1).

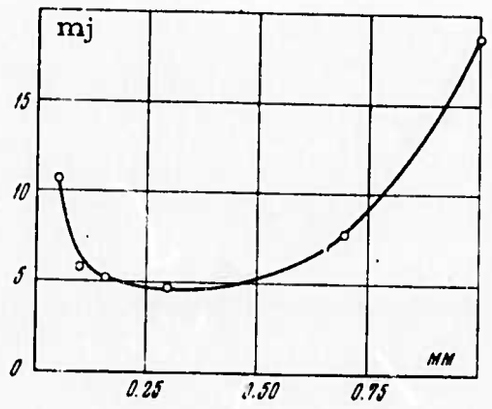

Fig. 1. Energy W_{50} versus electrode gap length: PETN average crystal size-2-3μ, density - 1.1 g/cu. cm.

An increase in W_{50} from 6.5 to 500 mj was observed when inductance was increased from 0.05 to 0.68 μH. A large increase in the energy release rate with decrease of inductance is the result of an increase in shock wave velocity. Detonation initiation in PETN is explained in terms of generation of a shock wave by powerful spark discharge and the thermal effect of electric discharge. Thermal effect is evidenced by the increase in W_{50} with the decrease in temperature, humidifying of PETN, or shortening of the interelectrode gap to less than 0.2 mm.

Barmin, A. A., and Ye. A. Pushkar'.
Adiabats of ionizing shock waves in an inclined magnetic field. MZhiG, no. 6, 1972, 102-106.

For the case of an arbitrarily oriented magnetic field, the conditions on an ionizing shock wave are established, taking into account certain supplementary relations dependent on the structure of the shock wave. Using Ohm's Law and the continuity of a tangent of the electric field resultant, the authors obtain the conservation laws for mass, momentum and energy. Dimensionless variables are introduced and the unknown magnetic field parameters are expressed in terms of the pressure jump ΔP, magnetic field jump Δh and V_{x2}^2 where V_{x2} is the velocity behind the shock wave. The relation connecting Δh, ΔP and V_{x2}^2 is derived, which is used for determining the adiabats. Qualitative character of the adiabat for normal ionizing shock waves is illustrated both for subsonic and supersonic slow shock waves. The behavior of the adiabat for an ionizing shock wave in an oblique magnetic field, both for subsonic and supersonic waves, is also presented.

Zhikhareva, T. V., and G. K. Tumakayev.
Temperature of electron gas in precursors.
ZhTF, no. 12, 1972, 2602-2604.

Temperature T_e of electron gas in front of a shock wave in argon and xenon is calculated as a function of distance y from the front for Mach numbers M = 10-22. Calculations were made using a set of kinetic equations of electron gas and populations of the $^1P_1$ and $^3P_1$ resonance states of A and Xe, and the energy balance equation of electron gas. In the latter equation, allowance is made for thermal effect of the

$^1P_1$ and $^3P_1$ de-excitation by elastic electron-atom collisions and energy losses in the atom ground state excitation and in ionization of excited atoms. The calculated $T_e(y)$ plots show that, for long y, the T_e relative variations are insignificant due to the energy elastic scattering. In contrast the T_e increase near the shock front in A and Xe is significant, hence the excited atoms ionization must be accounted for. $T_e(y)$ plots are given, accounting for either step-by-step or direct ionization of excited atoms. The latter calculation gave the lower estimate of T_e. Energy losses by excitation of the ground state atoms are connected with the resonance radiation diffusion, which was taken into account in calculation of the $0 \rightarrow i$ state excitation rate. In summary, a strong deviation from the electron-atom thermodynamic equilibrium is established in a cold inert gas ahead of the shock wave front. It follows that T_e in plasma can be much higher than the atom temperature.

Novitskiy, Ye. Z., O. A. Kleshchevnikov, V. N. Mineyev, and A. G. Ivanov. Shock wave depolarization of $BaTiO_3$, $PbTiO_3$, and $LiNbO_3$ ferroelectric crystals. FTT, no. 1, 1973, 310-311.

The effect of shock compression on polarization characteristics of the subject crystals was studied experimentally. Plane shock waves from detonation of an explosive charge in contact with a steel grid acted as the compressive load. Analysis of the oscilloscope traces of depolarization current i(t) generated by shock loading indicated that depolarization of all studied crystals by weak elastic waves (p_1 = 12-20 kbar) decreases with increase in ferroelectric hardness. The integral electric charge Q generated during propagation of a shock wave in a sample amounted to $\sim 0.1 P_s$ and

$<10^{-3} P_s$ for $BaTiO_3$ and $PbTiO_3$ or $LiNbO_3$, respectively, where P_s is spontaneous polarization. The following second compression wave (P_2 = 110 kbar) generated Q = 0.9-1.0P_s in the external circuit when using $PbTiO_3$ and $LiNbO_3$ crystals. The current i(t) during propagation of the second wave in $LiNbO_3$ increased significantly, a fact which indicates an increase to 10^2 ϵ_o in dielectric constant of the crystal behind the shock front.

Pilyugin, N. N. Radiant heat flux distribution on a spherical surface in hypersonic streamline flow of an inviscid radiative gas. ZhPMTF, no. 6, 1972, 44-49.

Flow of a hypersonic, inviscid, thermally nonconductive radiative gas flow around a sphere is analyzed in a Newtonian approximation to calculate radiant heat flux q_o to a sphere of radius R. A set of equations which describe gas flow between a detached shock wave and the sphere is solved under the condition of stagnation. The final solution to the gas dynamic problem is obtained in an approximation of volumetric de-excitation by introducing the dimensionless parameter b of radiative energy losses. Thus all gas dynamic parameters of the shock layer, including shock wave separation y_s are formulated as functions of b. The formulas for b and the enthalpy are used to derive the expression of q_R in a two-dimensional layer of thickness equal to y_s, assuming the shock layer to be thin. Analysis of this expression led to the conclusion that in a weakly radiant gas ($b \leq 1$), q_R is proportional to R and decreases fairly rapidly with increase in the angle θ of observation. In a strongly radiant gas ($b \geq 1$), q_R is equal to half the kinetic incoming gas flow and is independent of R. In both cases, the ratio of q_R at $\theta \neq 0$ vs. q_R to the stagnation point is independent of b and R. Earlier numerical calculations of q_R and y_s are in satisfactory agreement with the cited conclusions.

Arutyunyan, G. M. Calculating critical point pressure during shock wave impact on a supersonic configuration. MZhiG, no. 6, 1972, 94-101.

The interaction of a shock wave with a blunt symmetric body moving at supersonic velocity is analyzed. The principal aim of the article is to show that under certain conditions the pressure of a primary reflection at the critical point of a blunt body can be determined on the basis of one-dimensional shock wave theory. Two limiting cases of one-dimensional gas flow behind the shock wave are considered: 1) The parameters of the gas are those of the shock wave, which moves with the velocity of the blunt body; 2) The parameters of the gas are the same as the parameters behind the shock, where the flow velocity is equal to the velocity of the moving blunt body. It can be assumed that the difference between the maximum value of the real pressure at the critical point and the pressure determined by one of these two one-dimensional flow schemes will be smaller than the difference between the pressures determined on the basis of the two one-dimensional flow schemes. The value

$$\eta = p_+ / p_- \qquad (1)$$

where p_- and p_+ are pressures of reflection at critical point calculated on the basis of the first and second one-dimensional schemes respectively, is considered as a measure of the maximum error stipulated by the application of the one-dimensional shock wave theory. Calculation of η depends on solution of a sixth degree algebraic equation and can be solved only by numerical methods. Analytic expressions for the maximum η are derived in the case when Mach number M increases without bound. The applicability domains for these asymptotic expressions of error η are analyzed and the results obtained are presented in graphs. Conditions under which secondary reflections of shock waves at the critical point are possible are also examined.

Pavlov, V. G. Using approximations of thermodynamic functions in gas dynamic calculations. MZhiG, no. 6, 1972, 173-176.

It is pointed out that in the analysis of hypersonic flows, the model of an ideal gas with constant thermal capacity cannot be used because the equation describing the physicochemical processes in high temperature gas must be added to the system of gas dynamic equations. The obtained thermodynamic functions can be represented only by means of very cumbersome tables and therefore are very inconvenient for computer calculations.

The thermodynamic functions are approximated with a certain error, which affects the calculation accuracy. In the present article the effect of these errors on the calculation of Prandtl-Mayer supersonic gas flow around a blunt cone is analyzed. It is shown how the relative error in pressure of Prandtl-Mayer flow can be derived. This error is proportional to the total approximation error ϵ, the turn angle $\theta - \theta_o$ and increases with the increase of Mach number. At small $\theta - \theta_o$ angles this error is also small, however at $(\theta - \theta_o) \sim 1$ the error can exceed the approximation error by several times. Calculated results for several hypothetical cases are given graphically.

Golovachev, Yu. P. Convective and radiative heating during hypersonic flow around blunt bodies. MZhiG, no. 6, 1972, 169-175.

In a study pertinent to reentry problems, the effect of radiation and absorption of energy in a boundary layer upon the radiation heating, and the effect of radiation upon the thermal flow at the leading

critical point of a blunt body is analyzed. In view of the wide range of conditions for entering the Earth atmosphere, calculations of viscous and nonviscous flows with and without radiation are carried out. It is assumed that the gas in a shock layer is in a state of local thermodynamical equilibrium, and that pressure variation across the shock layer can be neglected. A system of equations with corresponding boundary conditions is developed describing the motion of a viscous radiating gas in the neighborhood of leading critical leading point of a blunt body. The equations of motion of a nonviscous radiating gas can be obtained from these equations. Characteristics of these equations as well as of boundary conditions are analyzed.

The calculation of viscous and nonviscous flows is reduced to the solution of a system of two nonlinear ordinary differential equations of the second and first order, respectively. Methods of finite differences and of successive approximations were applied to the solution of these equations. Calculation were carried out for T_S = 10,000; 12,500, and 15,000° K. The radius of bluntness and the pressure in the shock layer were varied within the ranges $0.15m \leq r \leq 3$ m and 0.1 atm $\leq p \leq 10$ atm. The calculation results are given in the form of four graphs, and are discussed for each assumed set of conditions.

Petrov, N. G. Errors in explosion modelling. Gornyy zhurnal, no. 12, 1972, 49-51.

The sources of errors are discussed in modelling explosions in rocks on the basis of dimensional and similarity theories. Most errors are attributed to inaccurate physical reproduction of the rock fracture process. The modelling errors analysis, based on the fundamental principles of explosion physics, led to the conclusion that substitution of artificial models

for natural material is the main source of errors, since physical characteristics of the fracture process are thereby distorted. In any given case, the experimental model design has to be based on scientific analysis of physical aspects of explosion and fracture. The geometric modelling of fracture and crushing of cohesive soil and rocks developed by G. I. Pokrovskiy is outlined as the most accurate method. The method can be applied to both natural and artificial materials. In the latter case, only approximate modelling of the fracture volume is possible, on condition of strict geometric similarity of dimensionless characteristics. The outlined method of modelling artificial materials can be used to study the effects of charge disposition, fuse delay magnitude, and related characteristics.

Zhilenkov, V. N. Method of determining extent of cracks in rock. Otkr izobr, no. 2, 1973, no. 362209. (Translation).

This author's certificate introduces a method of determining the extent of a crack opening in rock by measuring flow rate of a liquid pumped into the bore-hole in the rock. According to the inventor the accuracy of the measurement is increased by successive displacements of an elastic balloon inside the bore-hole with simultaneous pumping of liquid into the balloon. Flow rate of the pumped liquid is measured at the moment the balloon bursts at the crack mouth.

Azarkevich, Ye. I. Application of similarity theory in calculating characteristics of electric explosion of conductors. ZhTF, no. 1, 1973, 141-145.

A fairly simple and precise method is presented for calculating an LC circuit which includes an exploding conductor, by means of similarity theory. The multi-factor dependence of the current intensity i is reduced to two-variables dependence by introducing dimensionless time τ, current amplitude y, and resistance m into known equations for i, R, and the "specific effect" h(t).

In the initial phase of an electric explosion, when R of the exploding conductor is a single-valued function of h, the dimensionless τ_M, y_M, and m_M values at i maximum can be expressed as functions of two similarity criteria: dimensionless $m_o = \rho_o \ell / zs$ and $p = W_o / zs^2$ amp x coul/ mm^4, where ρ_o, ℓ, and s are the initial resistivity, length, and cross-section of the exploding conductor, $z = \sqrt{LC}$ is the wave impedance of the circuit, and W_o is the initial energy of the capacitor. All cited functions are described by the empirical formulas $x = A(10^{-6}\ pm_o^{1/3})^{\alpha}$ where x is the unknown quantity, A and α are the constants. Analysis of experimental data of different authors for Cu, Al and Ag indicated that m_o and p criteria are applicable over a wide range of initial conditions. Accuracy of y_m and τ_M determination is ± 15%; that of $\epsilon_M = W_M / W_o$ is ± 30%. The cited empirical formulas can be used in designing devices and planning experiments with electric explosion.

Baykov, A. P., A. M. Iskol'dskiy, and Yu. Ye. Nesterikhin. Electric explosion of wires at a high rate of energy input. ZhTF, no. 1, 1973, 136-140.

Experiments with electrically exploding tungsten wires are described, which were designed to verify the feasibility of suppressing low-mode magnetohydrodynamic instabilities by increasing energy input W to a value near the sublimation energy. In the experiments the rate of dW/dt was increased from 10^{10} to 10^{11} j/g.sec. Voltage at the wire was monitored by an ultrahigh-speed oscilloscope with a special CR tube. Explosions were recorded photographically, synchronously with the oscilloscope traces. Typical voltage traces and photographs of the wire luminescence indicate that at $dW/dt > 10^{10}$ j/g.sec., the low-mode MHD instabilities are absent during the first 35 nsec following the explosion of a wire with diam = 1.2×10^{-3} cm. in water or air. The R(t) of the wire during the first 25 nsec depends on the wire properties and geometry only. The W and dW/dt dependences of the wire R revealed a steady decrease in R* at $W^* \approx 5.3 \times 10^{-3}$ j, i.e. near the m.p. of tungsten, when dW/dt is increased. The criterion of this effect is formulated as the near equality of the energy of fusion to dW/dt during the time necessary for the unloading wave to reach the wire axis. The cited experimental data can be used in development of the large-area distributed detonators based on exploding foils.

Zhdanov, V. A., V. F. Konusov, and A. V. Zhukov. Equations of state for copper, silver, gold, aluminum, nickel, and lead. IVUZ Fiz, no. 1, 1973, 66-70.

Semiempirical equations of state for metals with a cubic lattice were derived from the expression of a function of metal bond energy together

with experimental lattice constants, elastic moduli, and the equation of state for hydrostatic compression. The condition was also formulated of thermodynamic stability of crystal lattice. The equations of state thus derived can be used to analyze mechanical characteristics of the cubic crystal lattice under complex stress, and over the entire region of elastic deformation. The parameters of mechanical failure of cubic lattices can be evaluated with the use of the thermodynamic stability condition. The cited possibilities were illustrated by the analysis of uniform extension. In this case, the tensor equations of state and the thermodynamic stability conditions are reduced to a single equation which correlates negative pressure P with density ρ and to three inequalities, respectively. The tabulated P and ρ values at which lattices of the six metals become thermodynamically unstable show that lattice strength is about 0.2 of the shear modulus value, when ρ decreases by 10%. Typical equations of state for Cu, Ag, and Au are plotted in P/C_{44} - ρ coordinates.

Kanunnikov, L. A., and I. G. Mikhaylov. Feasibility of calculating a second virial coefficient for polyatomic gases on the basis of acoustic data. VLU, no. 22, 1972, 144-146.

Theoretical analysis shows that the second virial coefficient B(T) of polyatomic gases, e.g., freons, can be calculated exclusively from the experimental velocity c of sound data, if temperature T is at least of the order of room temperature. This indirect method of calculation is preferable to the direct method using the more cumbersome P-V-T measurements. The method is detailed for the case of F-21 freon. First the function b(T) in the known c(P) formula was calculated for the range of

T = 350-450° K using experimental low frequency c data from the literature. Then, assuming $\gamma_{av} = C_p/C_v = 1.135$ and b(T) in polynomial form, the formula

$$B_c(T) = 325 - \frac{261\,000}{T} \tag{1}$$

was obtained. Calculation by a direct method using the experimental density ρ data gave the empirical formula

$$B_\rho(T) = 370 - \frac{268\,000}{T}. \tag{2}$$

The $B_c(T)$ and $B_\rho(T)$ plots calculated from (1) and (2) are shown to be in good agreement. The plots are extrapolated to 290° K.

Malyshev, V. V. Equation of state for UF_6 at densities to 0.0180 g/cm^3 and temperatures to 367° K. Atomnaya energiya, v. 34, no. 1, 1973, 42-44.

Isochores for UF_6 in the 296-367° K range and saturated vapor pressure curve $p_s(T)$ are plotted from experimental p-T data at constant volume. The experimental p_s data are approximated by the equation

$$\lg p_s = 12{,}2250 - \frac{2808{,}8}{T} - 0{,}0025309\,T, \tag{1}$$

with accuracy better than 0.5%. Densities ρ_v of saturated UF_6 vapors and heats of sublimation r of solid UF_6 are tabulated for T = 296-327.6° K. The ρ_v and r data were determined by extrapolating isochores to the $p_s(T)$ curve and from the Clausius-Clapeyron equation using Eq. (1), respectively. The

error of r determination was less than 0.7%. The experimental p-ρ-T data thus obtained for UF_6 vapors in the region remote from the critical point are described by the equation of state in the form

$$p\mu/\rho RT = 1 + \left(3{,}94 - \frac{2{,}197 \cdot 10^3}{T}\right)\rho. \qquad (2)$$

The difference between the experimental data and those calculated from (2) is not over 0.2-0.3%.

Fortov, V. Ye. Equation of state for condensed media. ZhPMTF, no. 6, 1972, 156-166.

Formulation of a complete thermodynamic equation of state for condensed media is described. The caloric equation of state

$$E^q(P, V) = \sum_{k+l \leqslant q} \sum e_{kl} V^k P^l \qquad (1)$$

where E is the internal energy, is used to calculate dP/dV and dT/dV, which are expressed by ordinary differential equations. Eq. (1) formulated on the basis of dynamic experimental data can be used for hydrodynamic calculations. Additional equations T = T(P, V) which are derived from the second law of thermodynamics, complete the thermodynamic description of a given system without imposing limitations on the properties, nature, or phase composition of the studied medium. Equations of state for Cu, W, and LiF were then formulated using the cited universal method together with experimental shock compression data. The Hugoniot adiabats calculated for Cu, W, and LiF from (1) and the Rankine-Hugoniot equation show agreement with the independent experimental data. Temperature $T(V/V_o)$ and $\gamma(P)$ plots

calculated by the cited method also agree well with the corresponding data calculated from the Mie-Gruneisen theoretical model. Statistical analysis by the Monte Carlo method revealed a 5-8% error in T determination of the shock adiabat for condensed media of porosity m = 1.

Tolokonnikov, L. A., and G. T. Volodin.
Calculating point explosions in various active media. PM, v. 9, no. 1, 1973, 15-19.

Dimensionless density y, velocity z, and pressure h are calculated for a perfect, inviscid gas set in motion by a point explosion with finite energy E_o in the center of motion symmetry. The point explosion problem is formulated by a set of two ordinary first order differential equations. The equations were derived from differential gas dynamic equations using integral equations of mass conservation and E_o. The derived equations, with the initial condition in asymptotic form, were solved by numerical integration using the Runge-Kutta method. Numerical values were thus obtained for the functions R(q) and $\sigma(q)$, where $R = r_2/r_o$ is the dimensionless radius of the shock wave, $q = (\varkappa p_1/\rho_1)^{\frac{1}{2}}/D$, $\varkappa$ is the adiabatic exponent, $D = dr_2/dt$,

$$\sigma_\nu = 2\pi(\nu - 1) + (\nu - 2)(\nu - 3) \qquad (1),$$

and ν is the parameter of motion symmetry (ν = 1, 2, and 3 for plane, cylindrical, and spherical symmetry, respectively). The R(q) functions are plotted for ν = 1, 2, and 3, $\varkappa$ = 1.4 and the energy densities Q_1 at the shock front = -4.2×10^4 to 4.2×10^4 j/kg. The dimensionless y, z, and h values calculated from the R(q) and $\sigma(q)$ values exhibit a significant dependence of the solution on ν, $\varkappa$, and Q_1 parameters.

Sinkevich, O. A., and O. S. Popel'. Possibility of generating a secondary shock wave from one-dimensional dispersion of actual detonation products in a medium with counterpressure. IN: Trudy Moskovskogo energeticheskogo instituta, no. 115, 1972, 21-32 (RZhMekh, 1/73, no. 1B159). (Translation).

The calculation is presented of the place of origin and propagation of a secondary shock wave, from one-dimensional dispersion of condensed explosive detonation products into a gaseous medium under a finite pressure. The calculation was simplified by assuming the Poisson adiabatic exponent to be equal to three, which means that nonisentropicity of flow behind the secondary shock wave was not accounted for in the calculations. For this reason the calculations are valid only for the initial interval of detonation products motion.

B. Recent Selections

i. Shock Wave Effects

Afanasenkov, A. N., and I. M. Voskoboynikov. Sensitivity of ballistite powder in shock wave initiation. FGiV, no. 2, 1973, 331-332.

Andreyev, A. F., and A. E. Meyyerovich. The structure of shock waves. ZhETF, v. 64, no. 5, 1973, 1640-1652.

Gendugov, V. M. Heating of a thermally conducting liquid behind a shock wave during combustion in a boundary layer. FGiV, no. 2, 1973, 291-295.

Gerasimenko, L. I. Effect of preliminary cold prehardening on shock wave hardening of nickel foils. IN: Trudy Volgogradskogo politekhnicheskogo instituta, no. 4, 1972, 100-105. (RZh Metallurgiya, 5/73, no. 51437).

Koldunov, S. A., K. K. Shvedov, and A. N. Dremin. Disintegration of porous explosives by shock waves. FGiV, no. 2, 1973, 295-304.

Lahe, A. Conversion of a symmetrical wave deformation process in a plate into an asymmetric one during shock wave formation. IAN Est, v. 22, no. 2, 1973, 216-219.

Mali, V. I. Flow of metals with a hemispherical groove due to shock waves. FGiV, no. 2, 1973, 282-286.

Pashkov, P. O. Phase transformations in solids during treatment by strong shock waves. IN: Trudy Volgogradskogo politekhnicheskogo instituta, no. 4, 1972, 129-140. (RZh Metallurgiya, 5/73, no. 51279)

Sobolenko, T. M., T. S. Teslenko, and A. F. Shalygin. Effect of shock waves on grain-oriented rolled materials and coarse-grained metals. FGiV, no. 2, 1973, 315-322.

Tolstykh, A. I. Numerical method of solving the Navier-Stokes equation for a compressible gas over a wide range of Reynolds numbers. DAN SSSR, v. 210, no. 1, 1973, 48-51.

Vompe, G. A. Kinetics of the thermal decomposition of ammonia at high temperatures. ZhFKh, no. 5, 1973, 1269-1270.

ii. Hypersonic Flow

Katayev, D. I., and A. A. Mal'tsev. Spectroscopy of non-volatile compound vapors, supercooled in supersonic flow. ZhETF, v. 64, no. 5, 1973, 1527-1537.

Ryabokon', M. P. Supersonic wind tunnel. Author's certificate, USSR no. 377659, published July 5, 1971. (Otkr izobr, 18/73, 18).

iii. Soil Mechanics

Beysebayev, A. M., M. F. Shnayder, N. A. Ten, and A. Ya. Veselov. Massovyye vzryvy na podzemnykh rudnikakh. (Mass explosions in underground mines). Alma-Ata, Nauka, 1973, 207 p. (KL, 23/73, no. 17617)

Borovikov, V. A. Blasting by micro-charges as a method for controlling explosion energy. IVUZ Gorn, no. 3, 1973, 52-60.

Khanukayev, A. N. Fizicheskiye protsessy pri otboyke gornykh porod vzryvom. (Physical processes during rock breaking by explosion.) Izd-vo Nedra. (NK, 21/73, to be published late 1974).

Klochkov, V. F., Yu. K. Pasichenko, and M. S. Yarokhno. Selecting optimum parameters of explosion contour during opening of a horizontal mine. Gornyy zhurnal, no. 5, 1973, 44-46.

Kuznetsov, G. V., and V. P. Ulybin. Parameters of air waves during explosions in mines. Gornyy zhurnal, no. 5, 1973, 46-48.

Pokrovskiy, G. I. Vozvedeniye plotin napravlennym vzryvom. (Erecting a dam by guided explosion). Nedra. (NK, 21/73, to be published late 1974).

Proyektirovaniye vzryvnykh rabot. (Planning explosion works). Izd-vo Nedra. (NK, 21/73, to be published late 1974).

Simanov, V. G., and V. A. Bezmaternykh. Variations in pressure of explosion products in a shaft with the inherent fissility of massifs. IVUZ Gorn, no. 3, 1973, 61-67.

Smolyanitskiy, A. A. Prokhodka geologorazvedochnykh kanav vzryvom. (Opening geological exploration trenches by explosion). Nedra (NK, 22/73, to be published late 1974)

Sposoby povysheniya bezopasnosti vzryvnykh rabot v ugol'nykh shakhtakh. (Method of increasing safety of explosive works in coal mines). Moskva, 1972,42 p. (KL Dop vyp, 4/73, no. 8389)

iv. Exploding Wire

Baykov, A. P., A. Ye. Voytenko, A. M. Iskol'dskiy, and Yu. Ye. Nesterikhin. Initiation of explosion along the charge surface. FGiV, no. ?, 1973, 323-325.

Baykov, A. P., V. A. Belago, A. M. Iskol'dskiy, L. S. Gerasimov, and Yu. Ye. Nesterikhin. Studying the electrical explosion of foils. FGiV, no. 2, 1973, 286-291.

Dolmatov, K. I. Plasmoids generated by electric wire explosion in air. IAN Uzb, no. 2, 1973, 57-59.

v. Equations of State

Artyukhovskaya, L. M., Ye. T. Shimanskaya, and Yu. I. Shimanskiy. Experimental investigation of characteristics of the equation of state for heptane close to the critical point. ZhETF, v. 64, no. 5, 1973, 1679-1687.

vi. Miscellaneous Effects of Explosions

Atroshchenko, E. S., Yu. L. Krasulin, B. I. Lipovatyy, V. S. Sedykh, and E. G. Spiridonov. Explosive compression of electrotechnical materials. IN: Trudy Volgogradskogo politekhnicheskogo instituta, no. 4, 1972, 229-237. (RZhKh, 10/73, 10M32)

Deribas, A. A. Certain phenomena occurring during high-speed collision of solids. FGiV, no. 2, 1973, 268-281.

Donukis, T. L., G. I. Savvakin, P. V. Titov, and L. G. Khandros. Hardening of austenitic ferromanganese alloys by explosion. IN: Metallofizika. Resp. mezhved. sb., no. 36, 1971, 72-75. (RZh Metallurgiya, 5/73, no. 5I170).

Goreniye i vzryv. [Materialy tret'yego vsesoyuznogo simpoziuma po goreniyu i vzryvu. 5-10 iyulya 1971 g.] (Combustion and explosions. Proceedings of the third All-Union symposium on combustion and explosion, July 5-10 1971). Moskva, Nauka, 1972, 802 p. (RBL, 1 /73, no. 748)

Gushchin, V. I. Zadachnik po vzryvnym rabotam. (Theoretical problems in explosion operations). Moskva, Izd-vo Nedra, 1972, 160 p. (LC-VKP)

Jeziorski, L., W. Ziewiec, and Z. Blazejowski. Effect of short-duration annealing on structural changes in Armco iron after explosive deformation. IN: Zesz. nauk. P. Czest., no. 68, 1970 (1972), 147-162. (RZh Metallurgia, 5/73, no. 5I146)

Merzhanov, A. G., A. P. Posetsel'skiy, A. M. Stolin, and A. S. Shteynberg. Experimental realization of a hydrodynamic thermal explosion. DAN SSSR, v. 210, no. 1, 1973, 52-54.

Popov, R. Yu. and Yu. I. Tuzhilkin. A model estimate of the linear correlation of explosion signals propagating in the sea. Akusticheskiy zhurnal, no. 3, 1973, 411-419.

Razvitiye teorii i praktiki vzryvnogo dela. Sbornik. (The development of the theory and practice of explosion technology. Collection of papers). Moskva, Izd-vo Nedra, 1972, 239 p. (LC-VKP)

Spivak, A. A. Compression waves in a solid medium from detonation of an explosive charge in air. FGiV, no. 2, 1973, 263-268.

3. Geoscience

A. Abstracts

Komissiya mnogostoronnego sotrudnichestva Akademiy nauk sotsialisticheskikh stran..., et al. Stroyeniye zemnoy kory tsentral'noy i yugo-vostochnoy Yevropy; po dannym vzryvnoy seysmologii (Crustal structure of central and southeastern Europe; based on explosion seismology data). Kiyev, Izd-vo Naukova dumka, 1971, 5-181.

The material presented below consists of extracts from individually authored chapters and sections of the above monograph. The remaining chapters and sections of this book (pp. 182-284) will appear in the next issue of the monthly report.

INTRODUCTION

At the 1963 VI Congress of the Carpatho-Balkan Geological Association, its Geophysical Commission passed a resolution to initiate coordinated studies of the deep crustal structure in the Carpatho-Balkan system and adjacent regions. For this purpose the following eight international profiles were planned:

I. Kharkov - Melitopol' - Black Sea (USSR);
II. Baturin - Kishinev (USSR) - Brani (Rumania) - Maritsa (Bulgaria);
III. Ostrog - Dolina - Beregovo (USSR) - Debrecen - Szeged (Hungary) - Dubrovnik (Yugoslavia);
IV. Debrecen - Kaposvar (Hungary);
V. Warsaw - Zakopane (Poland) - Kosice (Czechoslovakia) - Debrecen (Hungary);
VI. Debrecen (Hungary) - Brno - Prague (Czechoslovakia) - Weimar (German Democratic Republic);
VII. Kaliningrad (USSR) - Poznan (Poland) - Prague (Czechoslovakia);
VIII. Rostov - Kirovograd - L'vov (USSR) - Swietokrzyzskie Mountains (Poland).

In 1966, the European Seismological Commission, at its congress in Copenhagen, established a working group on the explosion seismology projects in Europe.

In 1966, the Commission for Multilateral Collaberation between the Academies of Sciences of Socialist Countries established a working group on deep seismic sounding.

The original program was expanded by adding five more profiles:

IX. Azov Sea - Black Sea (Nogaysk - Sinop peninsula in Turkey);

X. Black Sea (Caucasus) - Bulgaria (Varna) - Yugoslavia (Makresh);

XI. Black Sea (Crimea - Danube River delta) - Rumania (Galati - Vrancea) - Hungary (to the intersection with Profile IV);

XII. SSR - Rumania - Bulgaria (between Profiles II and III);

XIII. Southwestern Black Sea - Bulgaria (Burgas - Rhodope Mountains) - Yugoslavia (to the Adriatic Sea).

In addition, many countries (USSR, Yugoslavia, Hungary) planned national profiles in order to study specific geological structures.

The location of the DSS profiles completed by January 1971 are shown in Figure 1.

The field work and interpretation of profile sectors located in the border areas were conducted jointly.

The deep seismic studies were conducted using the technique of continuous profiling to obtain fully correlated systems of time-distance curves for the waves from all main crustal interfaces. Discrete observation systems were employed only at the initial stage and in poorly accessible regions.

The distribution of the completed 13,300 km of profiles is as follows: 1) Bulgaria - 670 km; 2) Hungary - 1200 km; 3) German Democratic Republic - 200 km; 4) Poland - 1050 km; 5) Rumania - 200 km; 6) USSR - 5100 km; 7) Czechoslovakia - 600 km; 8) Yugoslavia - 700 km; and 9) Black and Azov Seas - 3700 km.

It is mentioned that, in recent years, East Germany has been using the "Zemlya" seismic recording system for a large volume of its crustal-study programs.

The present monograph represents the first attempt at summarizing the results of crustal studies in central and southeastern Europe. The monograph includes the description of all international profiles. An attempt is made to determine the correlation between deep and near-surface geological structures, as well as to give an explanation of the evolution of certain geological megastructures.

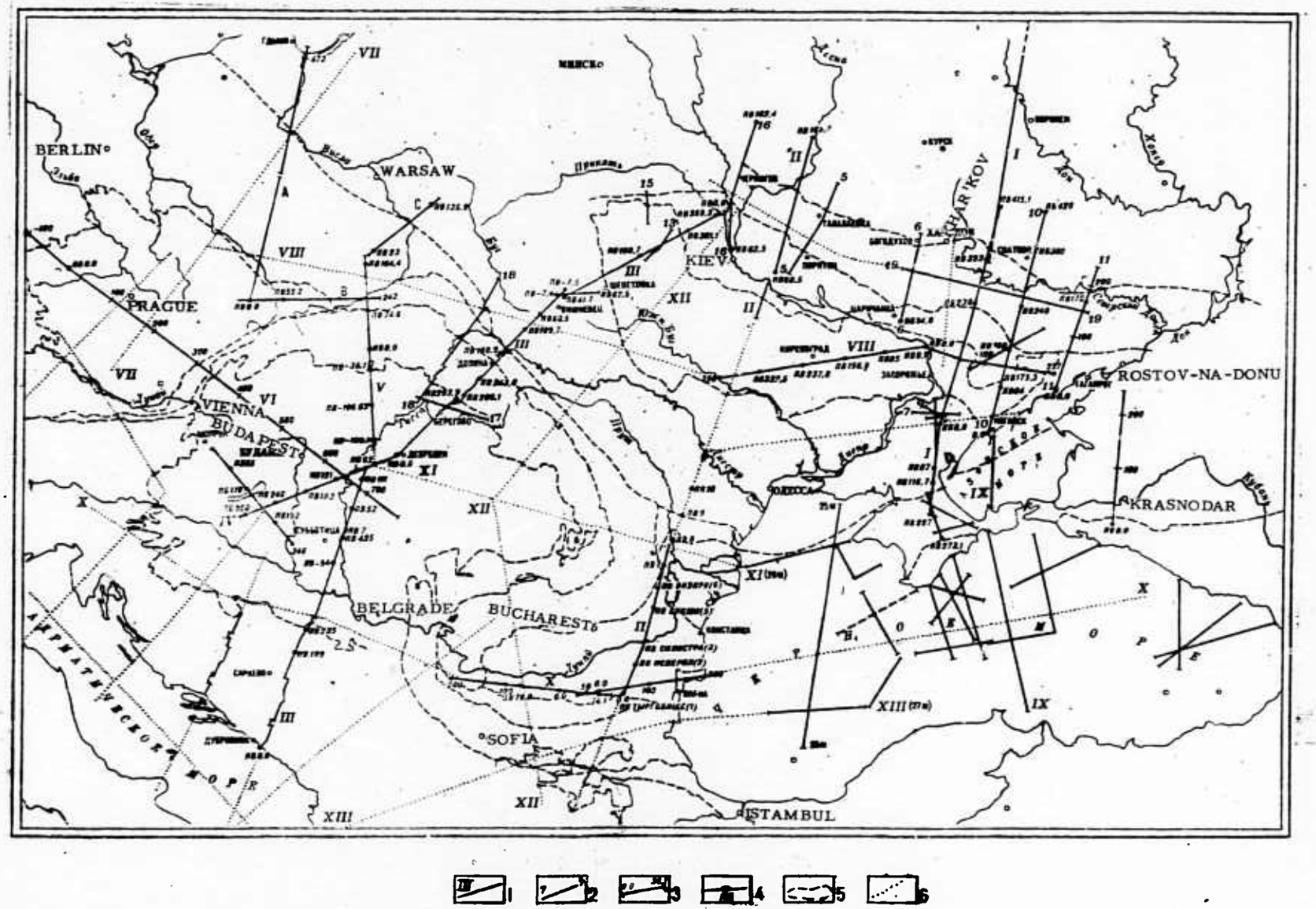

Fig. 1. Location of DSS Profiles in Central and Southeastern Europe.

1 - International profiles; 2 - national profiles; 3 - profile end and marker points; 4 - shot points; 5 - boundaries of geological regions; 6 - planned profiles.

Chapter I. Brief summary of the geological characteristics of central and southeastern Europe.

Khain, V. Ye., and V. I. Slavin

The region under investigation encompasses the southwestern part of the ancient East European platform, the eastern margins of the Central European Hercynides and the central part of the South European Alpides.

The major structural elements of the East European platform within the territory surveyed are the Russian plate and the Ukrainian shield. The Russian plate includes the Baltic syneclise, the Belorussian - Voronezh belt of anteclises and the Pripyat - Donets belt of aulacogenes.

The northernmost structure of the Caledonian Baltic syneclise trends southwest to northeast. It borders the Baltic shield on the northwest and the Belo russian - Voronezh belt of anteclises on the south. The maximum depth to the basement (3 km) occurs in the Bay of Gdansk.

The next large structure to the south is the Belorussian - Voronezh belt which consists of the Mazurian-Belorussian and Voronezh anteclises. They form a single submeridional belt of the uplifted basement of the Russian plate, which developed in the Hercynian orogenesis. Parallelling this belt, to the south lies the belt of depressions called the Pripyat-Donets belt of aulacogenes. It includes Podlyas - Brest syneclise (Lower Paleozoic) on the west, the Pripyat aulacogene (Devonian), and the Dnepr-Donets aulacogene (Devonian). The last mentioned proceeds into the Donets intracratonal miogeosyncline (Donbass region) on the east.

South of the Pripyat - Donets system of depressions, lies the Ukrainian shield, formed from a metamorphosed sedimentary - volcanic complex of Precambrian, Archean and Lower-Proterozoic age, intruded by granitic masses of the same age.

The central European Hercynide region consists of several structures with east-north-east trend: the Subvariscicum (foredeep); the Rhenohercynicum (outer miogeosyncline), the central German uplift; the Saxothuringicum (eogeosyncline); and the Bohemian massif with its Moldanubicum (median massif). The Moldanubicum is composed of deeply metamorphosed Precambrian formations and intruded by Hercynian granites. Within the central part of the Bohemian massif, a narrow geosynclinal trough (Prague synclinorium) occurs.

All these zones are traced toward the east to the Elbe lineation. Beyond this point, their north-northeast trend changes to east-southeast. The foredeep in front of the Hercynides diminishes sharply or is absent here. The Rhenohercynicum terminates with the structure of the Swietokrzyzskie Mountains and the Crakow rise. The Central German uplift is traced under the Cis-Sudetic monoclise, and the Saxothuringicum extends beyond the Elbe lineation up to the Sudetic Mountains.

Part of the region under investigation includes the Danish-Polish folded zone (anteclise), situated southwest of the East European platform and north of the Central European Hercynides. It is bordered by the North Sea syneclise (also known as the Stettin trough) on the west and southwest respectively.

In addition to these structures, the Central Dobruja and the complex Crimean Steppes belong to the Hercynides. The folded system of Dobruja, together with the ancient Misian plate, is situated between the convex segment of the Carpatho-Balkan arc on the west and the East European platform on the north. Within the folded system of Dobruja, there is a succession of zones of Baykalian, Hercynian, and early Cimmerian folding, from southwest to northeast, respectively. On the north, the Dobruja system is bordered by a foredeep.

The Crimean Mountains have an intermediate position between the Epi-Hercynian Scythian plate and Alpine belt of folding.

More than half of the territory under consideration is occupied by the Alpine Mediterranean folded belt. Within this belt, the Carpathians, Balkanides, and Dinarides are bordered by foredeeps and separated by an intramontane depression (Pannonian) and median massifs (Serbo-Macedonian, Rhodope).

The Carpathian folded system consists of three different parts, i.e., western, eastern and southern Carpathians.

The western Carpathians extend from the Danube River (Bratislava-Vienna section) to the Czechoslovakia-Poland-USSR border. They consist of the Outer and Inner Carpathians, which are divided by the Pennine lineation. They are separated from the Hercynides by a relatively shallow foredeep (2.5-3.0 km). In the Outer (flysch) Carpathians, there are a number of overthrusts with a northwest-southeast strike. The Inner Carpathians consist of longitudinal and transversal uplifts and depressions. The eastern Carpathians are located within USSR territory and also consist of the outer and inner groups. These are bordered by a 10-15-km-deep foredeep. The southern Carpathians extend from the southwestern bend of the Carpathian arc to the Balkanides. The foredeep and the outer (flysch) zone are much less evident here. The metamorphosed complex of the Inner Carpathians is uplifted here.

After the southern Carpathians change their trend into nearly meridional and intersect the Danube River, they join the northwestern end of the Balkanides. The Balkanides are crossed by numerous post-Paleogene faults and have very complex structure. South of them lies the uplifted Rhodope median massif.

The Serbian-Macedonian median massif extends west from the Carpatho-Balkans and Rhodope massif. It is a narrow horst-like uplift of the metamorphosed basement. West of this extends the very complex Vardar fault zone. To the north, in Serbia, it borders the Inner Dinarides while in the south, it borders the Pelagonian massif.

The western part of the Balkan peninsula is occupied by the Dinarides and their southern extension, the Helenides. The Yugoslavian Dinarides consist of inner and outer groups.

The Pannonian depression is situated between the eastern Alps, the western Carpathians, the Bihar Mountains, the southern Carpathians, and the Dinarides. The depth to the basement is 5 km.

The Black Sea basin has a very definite structure. In its central part, suboceanic crust is observed.

Chapter II. Results of deep seismic sounding by country:

People's Republic of Bulgaria

Dachev, Khr., Iv. Petkov, Tsv. Velchev, E. Andonova, and S. Mikhaylov.

Crustal studies in Bulgaria were conducted along international profiles II* and X (see Fig. 1). Profile X (Makresh-Black Sea) intersects the following structures of the Misian plate: the Lom depression, the North Bulgarian uplift, and the Varna depression.

The observation system used on the Bulgarian sector of international profile X was intended for continuous tracing of the crystalline basement surface (6.2 - 12-km-spaced shot points) and deep crustal interfaces (40, 70 and 100-km-spaced shot points).

The seismic instrumentation used included SS-30-60-58 and PSS-60 seismic recording systems and NS-3 and UNS-6 seismometers, spaced 50 and 100 m apart.

Explosives were detonated in water and in boreholes. The charges, ranging from 350 to 1500 kg, were set off in groups of 10-15 shot holes, 15-20 m deep.

The following wave groups were recorded: P^{oc} - associated with interfaces within the sedimentary layer; P_0^K - interfaces within the crystalline basement surface; P^K - interfaces within the consolidated crust; and P^M_{refl} - the Moho discontinuity. Results for profile X (see Fig. 2) indicate that the crustal thickness in the Misian plate varies from 30 to

---

* Profile II is incomplete

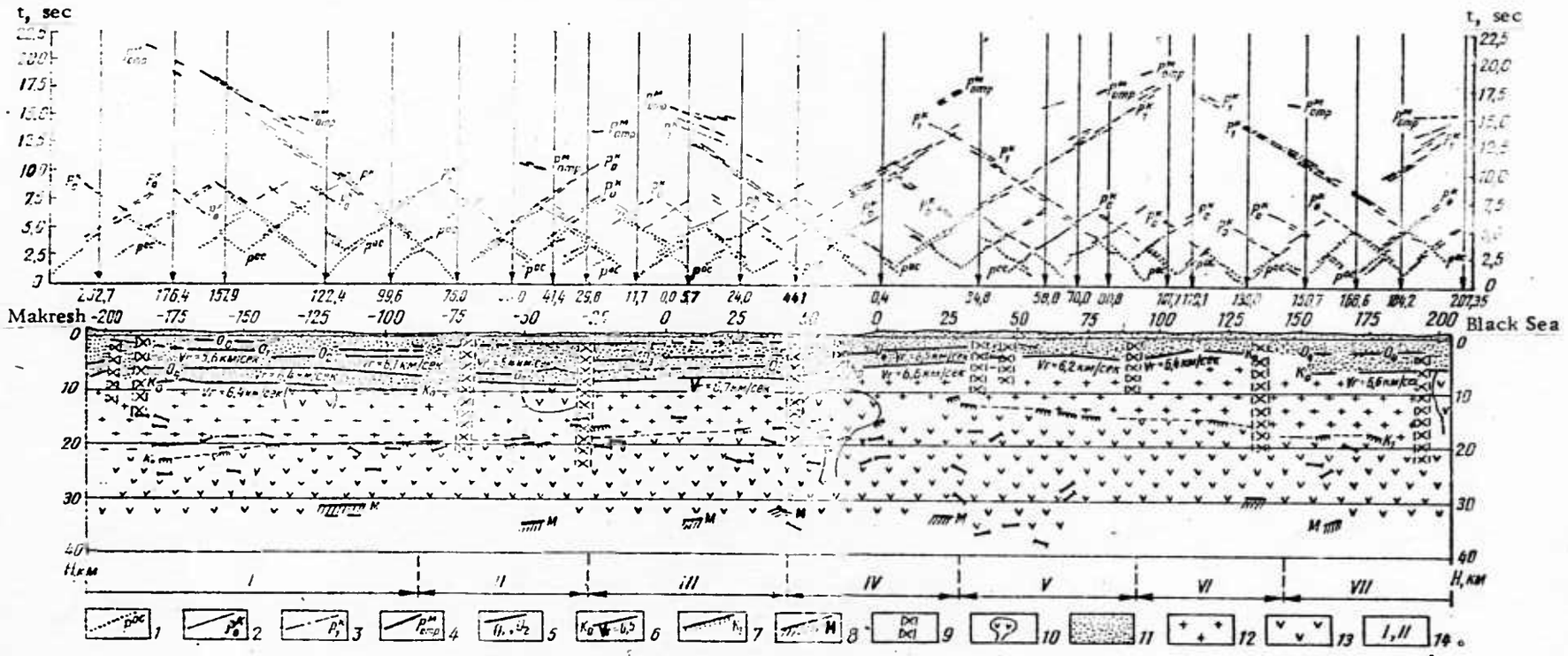

Fig. 2. System of Time-Distance Curves and the Seismogeological Section along Profile X (Makresh-Black Sea).

Time-distance curves for waves from: 1- interfaces within sedimentary cover; 2- consolidated crust surface; 3- basaltic layer surface; 4- Moho discontinuity, wide-angle reflections; Interfaces: 5- interfaces within the sedimentary cover; 6- crystalline basement surface; 7- Conrad discontinuity; 8- Moho discontinuity; 9- abyssal faults; 10- intrusions; 11- sedimentary layer; 12- granitic layer; 13- basaltic layer; 14- tectonic blocks and regions: I- Lom depression, II- Plevna block; III- Maslarevo block, IV- Popovo block, V- Khitrin block, VI- Vetrin block, VII-Varna depression.

35-37 km. The crust is distinctly differentiated into two parts: the upper granitized and the lower basaltified. The Conrad discontinuity has complex relief, and its depth varies from 12-15 to 20-25 km. The eastern part of the plate is bounded by abyssal faults.

The crystalline basement surface (interface K_0) with V_r = 6.4-6.8 km/sec has gentle relief in the western part of the profile, where the depths to the basement vary from 10 to 9.0-7.5 km. In the eastern part of the profile, the basement surface rises to depths of 2.5-4.0 km.

The Conrad (K_1) and Moho discontinuities are determined from an incomplete system of time-distance curves, taking into account gravity and magnetic data.

The Conrad discontinuity forms an anticlinal structure, with the uppermost part confined to the western arm of the North Bulgarian uplift. The thickness of the granitic layer varies significantly from 15-17 km at the western end, 8-10 km at the center, and 12-15 km at the eastern end of the profile.

The Moho discontinuity (determined from single time-distance curves) occurs at a depth of 31-33 km in the western and at 35-37 km in the eastern part of the profile.

Hungarian People's Republic

Mituch, E., and K. Posgay

Crustal studies in Hungary were conducted along international profiles III, IV, V, VI and along national profile Sopron - Balaton Lake - Danube (see Fig. 3) all within the Pannonian depression.

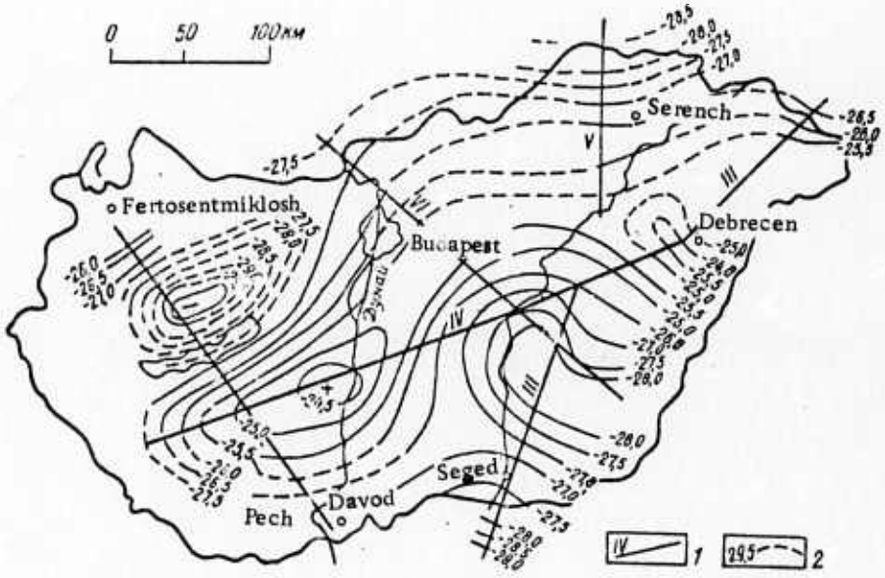

Fig. 3. Isopach Map of the Crust in Hungary

1 - DSS profiles; 2 - isopachs, in km.

Seismic observations were performed using techniques of: 1) continuous linear profiling; d) discrete linear profiling; and 3) nonlinear profiling along parallel profiles. The following wave groups were identified: P^{oc} - associated with interfaces within the Tertiary complex and folded basement; P_0^K - associated with the granitic layer surface; P_1^K - associated with the Conrad discontinuity; and P_{refl}^M and P^M - wide-angle-reflections and head waves from the Moho discontinuity.

Velocity distribution for the crust in the Pannonian depression is shown in Figure 4 (determined by the Kondrat'yev method). The average

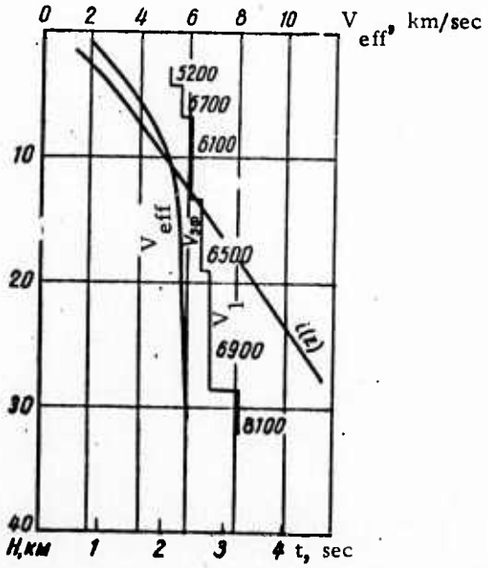

Fig. 4. Distribution of the Effective and Layer Velocities.

velocity to the Moho discontinuity (5.85 - 6.1 km/sec) was determined from wide-angle reflection data. Along profile IV, three major seismic interfaces (see Fig. 5) are found: K_0 (surface of the granitic layer) with V_r = 6.1 km/sec; K_1 (surface of the basaltic layer) with V_r = 6.8; km/sec and M (Moho discontinuity) with V_r = 8.1 km/sec.

The surface of the granitic layer occurs at depths of 4-9 km. The surface of the basaltic layer is traced only on the northeast sector of the profile at a depth of about 19 km. The Moho discontinuity depth varies insignificantly from 24.4 km in the Danube river area to 27 km northeast thereof.

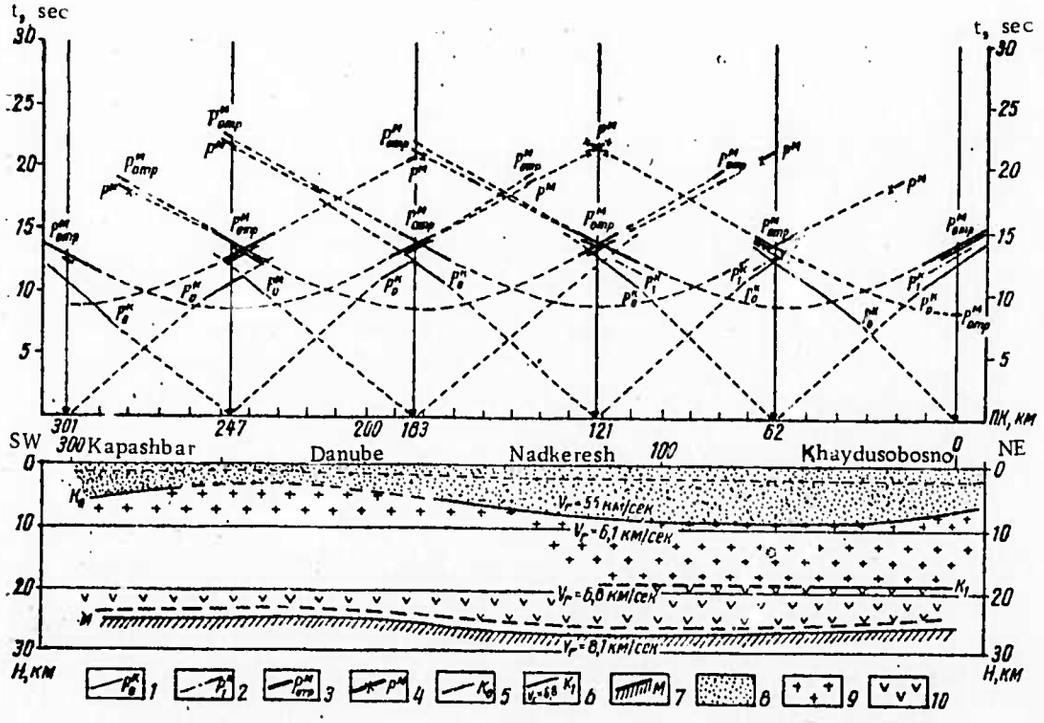

Fig. 5. System of Time-Distance Curves and Seismogeological Section along Profile IV.

Time distance curves for waves from: 1- basement surface; 2- Conrad discontinuity; 3 - Moho discontinuity, wide-angle reflections; 4 - Moho discontinuity, refracted; Interfaces: 5 - basement surface; 6 - Conrad discontinuity; 7 - Moho discontinuity; 8 - sedimentary layer; 9 - granitic layer; 10 - basaltic layer.

As seen in Figure 6, the Moho discontinuity gradually dips in a southwesterly direction from a depth of 26 to 29 km. A nonconformity between the Moho discontinuity and the basement surface is outlined.

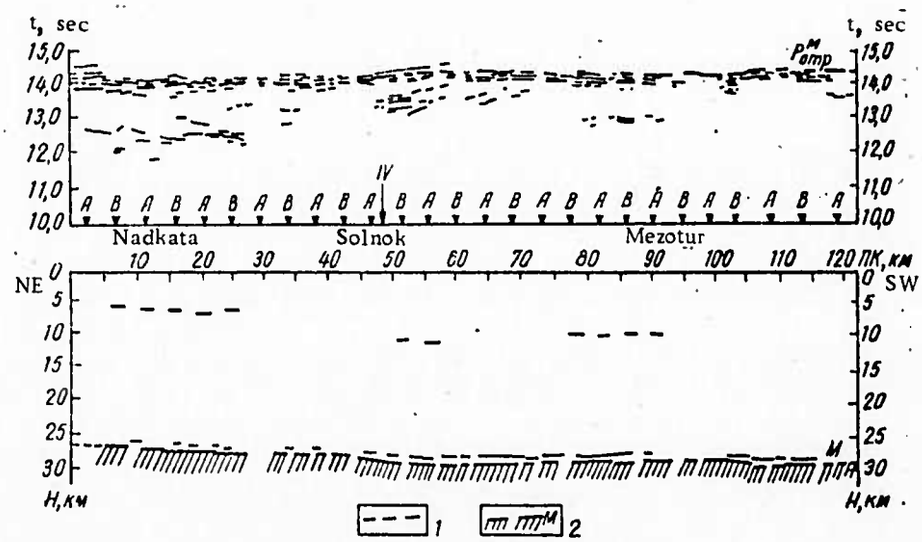

Fig. 6. System of Nonlinear Time-Distance Curves and Seismic Section along Profile VI.

1 - nonlinear time-distance curves for wide-angle reflections from Moho discontinuity; 2 - Moho discontinuity.

The central part of the Hungarian sector of international profile III (see Fig. 7) coincides with the northeastern part of profile IV (see Fig. 3 above). The northeastern leg of this profile extends into the Soviet Union, while the southern leg meets the Yugoslavian sector of international profile III.

The surface of the granitic layer with V_r = 6.1 km/sec (K_0 interface) is overlain by the folded basement surface along almost the entire profile. The deeper interfaces, with V_r = 6.5 km/sec and 6.9 km/sec (K_1), are traced only sporadically. The Moho discontinuity depth varies from 24.0 km (west of Debrecen) to 30.0 km. The Moho discontinuity

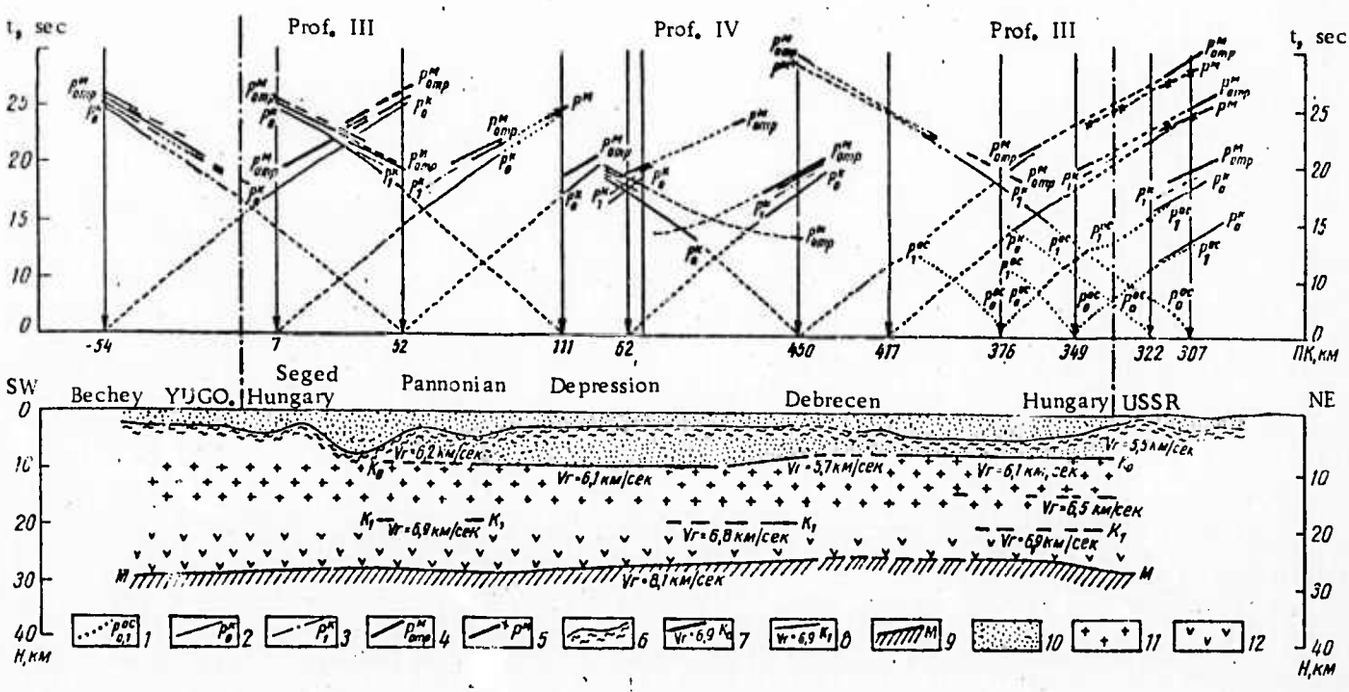

Fig. 7. System of Time-Distance Curves and Seismogeological Section along the Hungarian Sector of International Profile III.

Time-distance curves for waves from: 1- interfaces within the sedimentary cover; 2- crystalline basement surface; 3- basaltic layer surface; 4- Moho discontinuity, refracted; Interfaces: 6- folded basement surface; 7- crystalline basement surface; 8- Conrad discontinuity; 9- Moho discontinuity; 10- sedimentary layer; 11- granitic layer; 12- basaltic layer.

descends northeastward, reaching depths of 50-60 km in the Eastern Carpathians and Cis-Carpathian foredeep in the USSR territory, and also southward, reaching a depth of 31 km in Yugoslavia. Thus, the Pannonian depression is characterized by an anomalously thin crust.

The Sopron - Balaton Lake - Danube profile (see Fig. 8) crosses the Bakony hills where there is an exposed folded basement.

The basement surface (unspecified type), with V_r = 5.9-6.0 km/sec (interface K_0) at depths of about 5.0 km, is traced reliably on the southeastern part of the profile. Interface K_1 with V_r = 7.0-7.1 km/sec (probably the Conrad discontinuity), at depths of 19-20 km, is traced sporadically. The depth to the Moho discontinuity, which is represented by two interfaces, varies significantly over the profile. The maximum depth is confined to the Bakony hills, where it forms a synclinal bend.

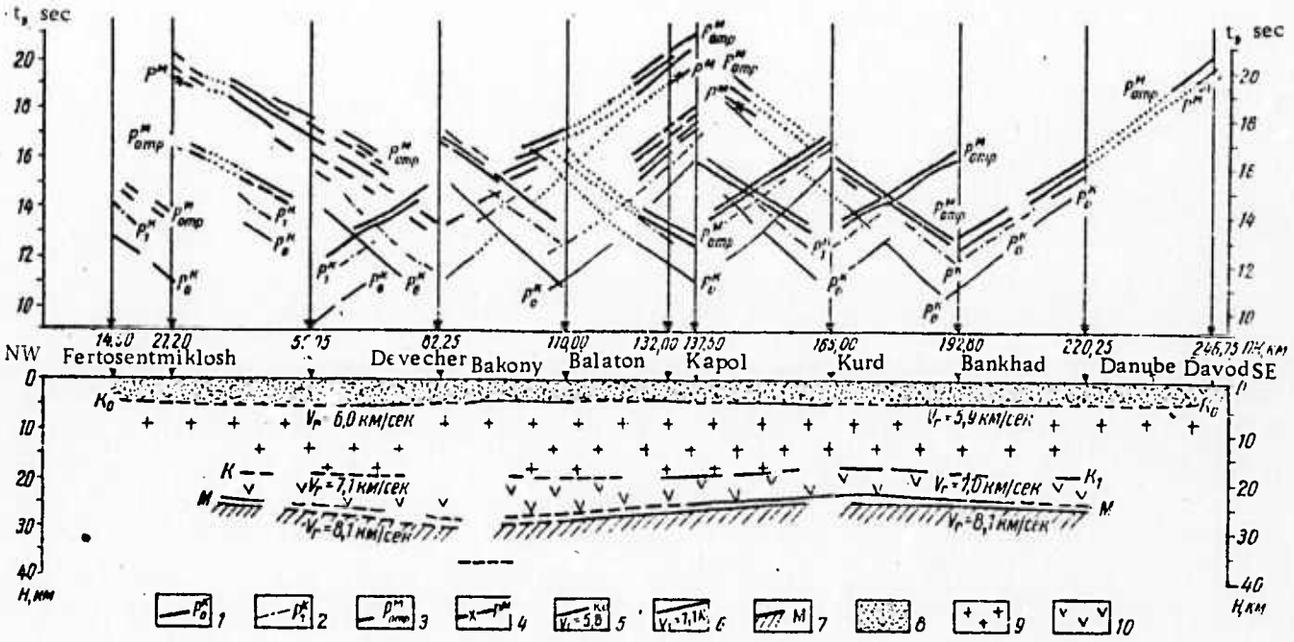

Fig. 8. System of Time-Distance Curves and Seismogeological Section along Sopron - Lake Baltaton - Danube Profile.

Time-distance curves for waves from: 1- basement surface; 2- Conrad discontinuity; 3 - Moho discontinuity, wide-angle reflections; 4 - Moho discontinuity, refracted; Interfaces: 5- basement surface; 6 - Conrad discontinuity; 7 - Moho discontinuity; 8 - sedimentary layer; 9 - granitic layer; 10 - basaltic layer.

According to preliminary results for profile V (see Fig. 9) refraction surface K_0 (probably the basement surface) with V_r = 6.1 km/sec occurs at an average depth of 5 km. A refraction surface with V_r = 7 km/sec is traced only discretely at depths of 20-20.5 km. The Moho discontinuity, represented by two interfaces, gradually dips towards Czechoslovakia.

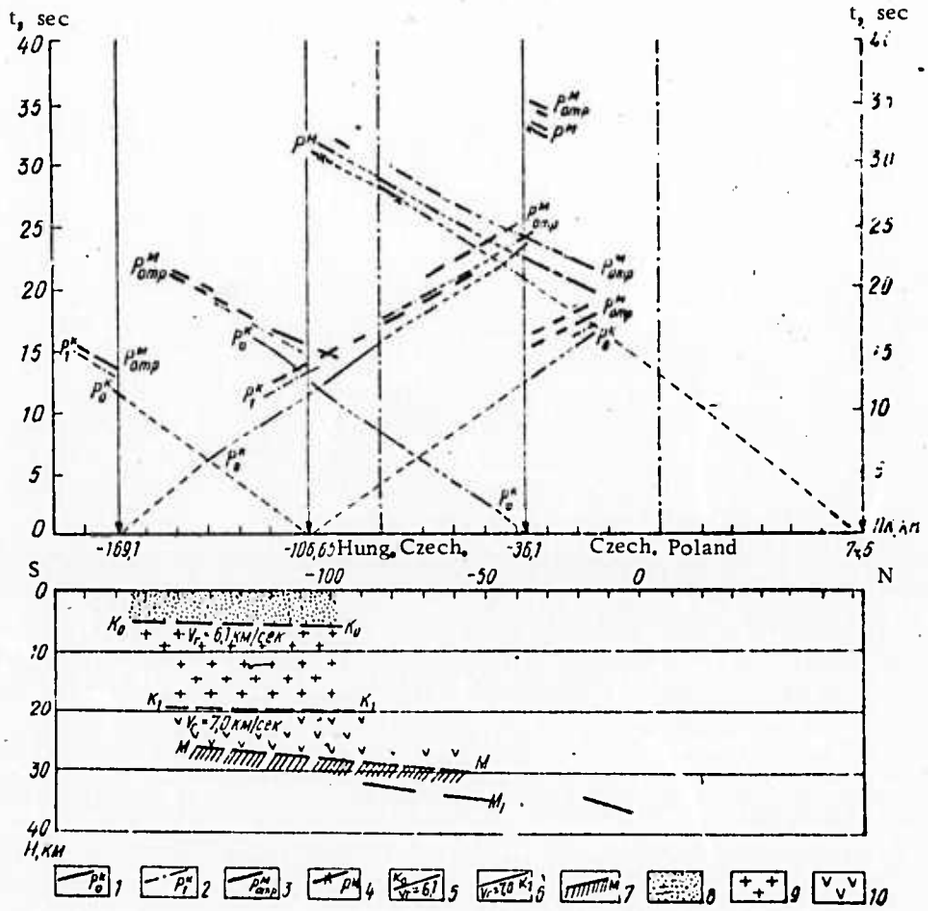

Fig. 9. System of Time-Distance Curves and Seismogeological Section along Profile V in the Hungarian-Czechoslovakian Border Zone.

Time-distance curves for waves from: 1- basement surface; 2- Conrad discontinuity; 3 - Moho discontinuity, wide-angle reflections; 4- Moho discontinuity, refracted. Interfaces: 5- basement surface; 6- Conrad discontinuity; 7- Moho discontinuity; 8- sedimentary layer; 9- granitic layer; 10- basaltic layer.

The isopach map for the crust in Hungary is shown in Fig. 3 above. The Pannonian depression is characterized by a thin crust (from 24-25 to 30.5 km) and a thin basaltic layer.

German Democratic Republic

Knothe, Ch.

Crustal studies in East Germany were conducted along international profile VI (200-km long segment) crossing the Hercynian folded regions transversally to their strike (see Fig. 10).

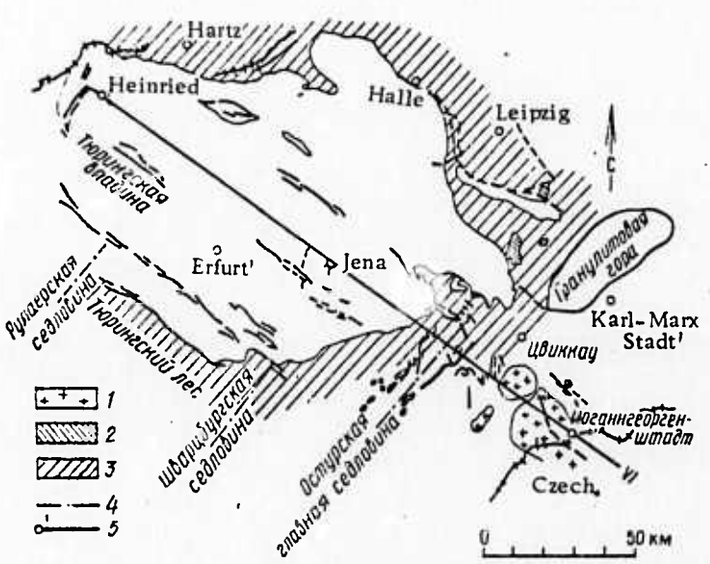

Fig. 10. Location of International Profile VI in the GDR.

1- acid migmatites; 2- basic migmatites; 3- Paleozoic sediments; 4- axes of regional geological structures; 5- DSS profile.

Seismic observations along profile VI were made by means of an observations system intended for continuous tracing of crustal intervaces. Three shot points were located in Germany and three in Czechoslovakia.

NS-3 seismometers having a natural frequency of about 4.5 Hz were arranged at 150 m intervals.

Charges of 800-1200 kg were fired in 25 - 40-m-deep holes, usually grouped in 8-10 boreholes and in shallow water reservoirs at depths of 4-5 m. The recorded wave field is characterized by the following wave groups: P^{oc} - associated with interfaces within the sedimentary layer; $P^{K}_{0,\ 1,\ 2}$ - associated with the basement surface and interfaces within the consolidated crust; and P^{M} - associated with the Moho discontinuity (P^{M} - head wave and P^{M}_{refl}).

The crustal velocity characteristics are determined from near-vertical and wide-angle refracted waves, as well as from well-logging data and reflection surveys of the sedimentary cover.

The velocities in the sedimentary cover were determined to be 3.0 and 3.75 km/sec.

The effective velocity determined from wide-angle and near-vertical reflections are: 5.5 km/sec to interface K_0; 5.6 km/sec to K_1; 5.85 km/sec to K_2; and 5.93 km/sec to the Moho discontinuity. The velocity distribution inferred from curvilinear time-distance curves of refracted waves by the Kondrat'yev method is shown in Figure 11. The velocity distribution inferred from discontinuous curvilinear time-distance curves of refracted waves by the Giese method is shown in Figure 12. This velocity-depth curve is characterized by a low velocity zone.

The crustal thickness along profile IV (see Fig. 13) varies from 28 to 32 km. The eastern sector of the Thuringian depression is characterized by an inverse relief of the upper and lower crustal interfaces.

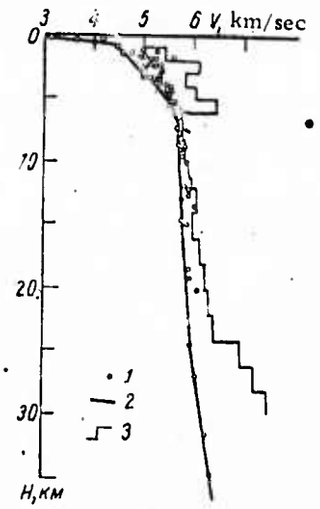

Fig. 11. Velocity-Depth Curve Determined by the Kondrat'yev Method.

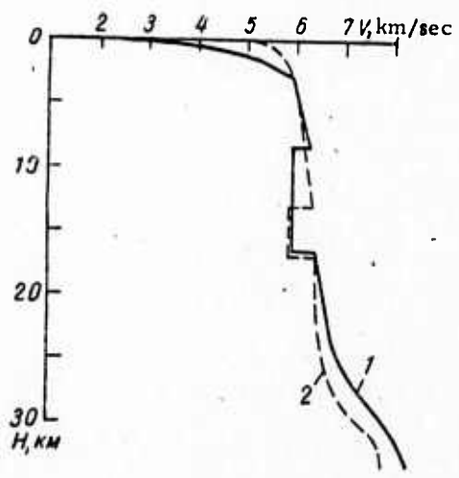

Fig. 12. Velocity-Depth Curve Determined by the Giese Method.

Interfaces within the consolidated crust are traced only discretely.

The Moho discontinuity forms a depression occurring at a depth of 32 km in the area of the German - Czechoslovakian border and rising both northwestward and southeastward.

Interface K_1 (possibly the Conrad discontinuity) occurs at depths of 11-12 km in the sourtheastern part of the Thuringian depression, subsiding in the northwest to a depth of 13 km. Interface K_2, which may coincide with the lower boundary of the low-velocity zone, occurs at a depth of about 20 km.

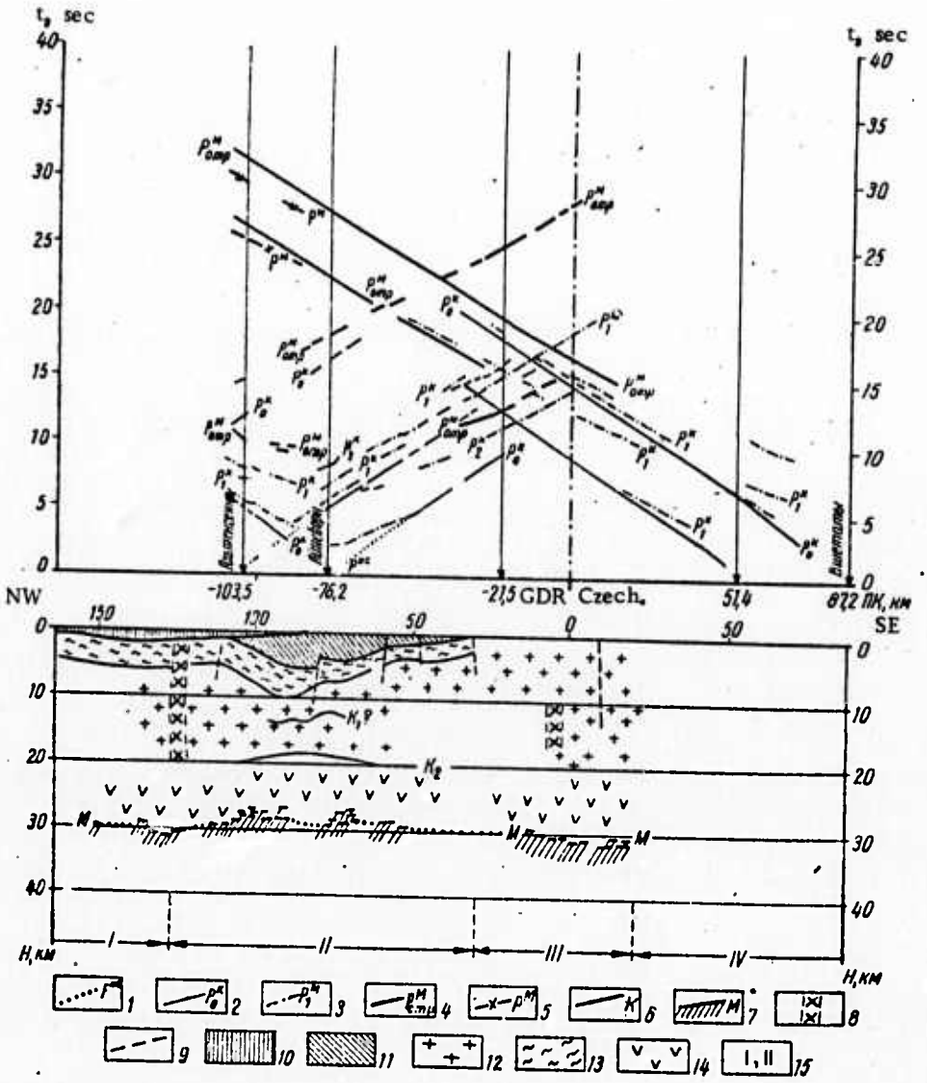

Fig. 13. System of Time-Distance Curves and Seismogeological Section along Profile VI (German Democratic Republic).

Time-distance curves for waves from: 1- interfaces within the sedimentary cover; 2- basement surface; 3- interfaces within the consolidated crust; 4- Moho discontinuity, reflected; 5- Moho discontinuity, refracted. Interfaces: 6- interfaces within the consolidated crust; 7- Moho discontinuity; 8- abyssal faults; 9- faults from geological data; 10- Mesozoic complex; 11- Paleozoic complex; 12- granitic layer; 13- crystalline schists; 14- basaltic layer; 15- tectonic blocks and regions: I - central German crystalline trough, II- Thuringian depression, III- Erz Gebirge (Krusne Mountains) IV - Donpov Mountains.

Polish People's Republic

Uchman, J.

Crustal studies in Poland were conducted along international profile V and profiles A, B and C (see Fig. 14).

Fig. 14. Location of DSS Profiles in Poland

1- flysch; 2- molasse; 3- carboniferous formation; 4- granitoids; 5- domes; 6- tectonic sutures; 7- general trend of the folded regions; 8- disjunctive dislocations (a-established, b- assumed) 9- gently sloping overthrusts and nappes; 10- steep overthrust; 11- foredeeps; 12- arbitrary boundaries; 13- DSS profiles; 14- shot points.

Profile A runs submeridionally from the Bay of Gdansk to the Czechoslovakian border, crossing the boundary of the East European platform.

Profile B runs sublatitudinally from the south end of profile A to profile V crossing Upper Silesia.

Profile C runs in a southwesterly direction crossing the boundary of the East European platform and Swietokrzyzckie Mountains.

Profile V runs meridionally, crossing the Carpathians and the Swietokrzyzckie Mountains.

Seismic observations were performed using continuous (profile C and northeastern part of profile A), piece-wise continuous (southwestern part of profile A) and discrete (profile A and B in 1960-64) observation systems.

The seismic instruments used prior to 1964 included SS-26-D, SS-24-P and SS-30/60 seismic recording systems and seismometers having natural a frequency of 30 Hz. Since 1965, SS-30/60-CMRW and SYE-S-33 seismic systems and seismometers having natural a frequency of 10Hz were used. In 1969, during work on international profile V, Poisk units and seismometers having a natural frequency of 2.6 Hz were used.

Explosive charges ranging in weight from 0.5 to 3.0 tons were detonated in the Bay of Gdansk and small lakes, while grouped charges up to 1-2 tons were detonated in 30-40-m-deep holes. Single charges within the groups did not exceed 100 kg.

The wave field recorded during deep crustal studies (sedimentary cover was studied separately) is characterized by the following wave groups: P^K - associated with the basement surface and interfaces within the consolidated crust and P^M - associated with the Moho discontinuity.

Results for profile A indicate that the crustal thickness in the northern part of the profile is 48 km. In the Torun area, the Moho discontinuity is displaced by 6 km at an abyssal fault. In the southern part of the profile, the following crustal thicknesses are observed: 28 km (Radyn area); 26 km and 34 km.

The crustal thickness determined for profile B from refraction and reflection data is: 27 and 32 km at the Okhoets shot point; 35 and 36.8 km at the Radgoshch shot point.

Along profile C, a crustal thickness of 48 km is observed in the marginal part of the East European platform.

On the northern part of profile V, near profile B, the crustal thickness is 40 km, while to the south it is 48-50 km thick.

Socialist Republic of Rumania

Constantinescu, P., and I. Cornea

Crustal studies in Rumania were conducted along international profiles II and XI (see Fig. 1).

Within Rumania, profile II crosses northern, central and southern Dobruja. Profile XI crosses the Cis-Carpathian foredeep on the southeast, the eastern Carpathians, the Transylvanian depression, the Bihar Mountains, and the Pannonian depression on the northwest.

Field work was performed by the technique of continuous profiling along profile II, piece-wise profiling along profile XI and point seismic soundings in the northwestern part of the region studied. The observation system consisted of shot points spaced 10-15 and 40-50 on profile II. Shot points were spaced 40 km apart on profile XI.

The instruments used consisted of SS-30/60-CMRW and Poisk-I-48-CMRW seismic systems and SPEN-1 seismometers set 100 m apart.

The crust along the Rumanian sector of international profile II is divided into two blocks: the southern block with a thickness of 30-35 km, and the northern, with a thickness of 40-45 km (see Fig. 15). The thickness of the granitic and basaltic layers increases by 7 km in the northern block.

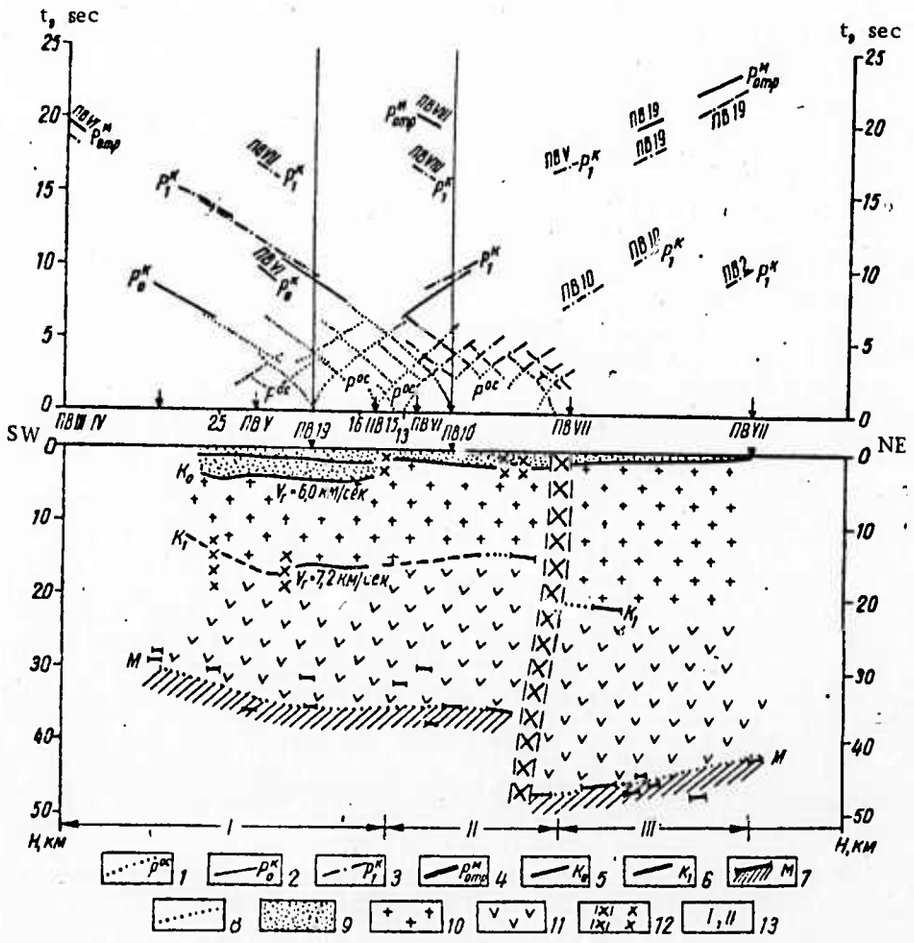

Fig. 15. System of Time-Distance Curves and Seismogeological Section along International Profile II.

1-4- Time-distance curve for waves from: 1- interfaces within the sedimentary cover; 2- crystalline basement surface; 3- basaltic layer surface; 4- Moho discontinuity, wide-angle reflections; Interfaces: 5- crystalline basement surface; 6- Conrad discontinuity; 7- Moho discontinuity; 8- assumed interface; 9- sedimentary layer; 10- granitic layer; 11- basaltic layer; 12a- abyssal faults; 12b- disjunctive dislocation; 13- tectonic blocks and regions: I- Misian plate, II- extension of the Central Dobruja, II- Northern Dobruja uplift.

Based on point seismic soundings, the crustal thickness in the Pannonian depression is 25-31 km and in the Eastern Carpathians, 45-54 km (Vrancea area).

Ukrainian Soviet Socialist Republic

Sollogub, V. B., and A. V. Chekunov

International and national DSS profiles in the Ukraine cross all principal tectonic structures and the abyssal fault zones separating them (see Fig. 1).

International profile II crosses the Dobruja folded system, the Peri-Dobruja foredeep, and the marginal parts of the East European platform.

International profile III crosses the Trans-Carpathian trough, the Carpathian folded system, the Cis-Carpathian foredeep, the Volynia-Podolia plate, the Ukrainian shield, and Dnepr-Donets aulacogene.

International profile VIII crosses the Ukrainian shield along the line Taganrog-Kirovograd.

International profile I extends submeridionally (850 km) crossing the Voronezh massif on the north, the Dnepr-Donets aulacogene, the Ukrainian shield, the Peri-Black Sea-Kuban trough, the Scythian plate, the Crimean Mountains, and the Black Sea depression in the south.

National profile 10, and its extension of international profile IX, crosses the Donbass folded system, the Peri-Azov massif, the Scythian plate, the Indol-Kuban trough, the eastern pericline of the Crimean Mountains, and the Black Sea depression.

National profile 17, 140-km long, extends along the Trans-Carpathian trough. The following wave groups were identified: $P^{oc}_{1,2,3}$ - associated with interfaces within the sedimentary layer; $P^{K}_{0,1,2,3}$ - associated with the basement surface and interfaces within the consolidated crust; and P^{M} and P^{M}_{refl} - associated with the Moho discontinuity and interfaces within the crust-mantle transition zone.

These wave groups include head waves, continuously refracted phases, reflected (at subcritical and wide angles), diffracted, etc. Some of these are illustrated in seismograms given in the chapter.

Detailed velocity distributions in the Ukraine were derived from data on reflected and continuously refracted waves. The velocity distribution in Trans-Carpathia was determined by a method based on the use of combined reflection and refraction data, which provides reliable identification of low velocity zones within the crust.

The velocity characteristics of the major geological structures in the Ukraine are described below.

Ukrainian shield and its flanks. The velocity in the sedimentary cover varies from 1.0-5.8 km/sec. The horizontal gradient is usually considerable. In the uppermost part of the granitic layer, the velocity monotonically increases from 5.8-6.0 km/sec near the surface to 6.2-6.3 km/sec in the 3-10 km depth range. The Korosten Pluton and the Belozerskiy ferriferous region, where the velocity sharply increases to 6.5-6.7 km/sec near the surface, are exceptions. The effective velocity in the lower crust increases slowly from 6.1 to 6.3 km/sec in the 8-30 km depth range. This fact, together with other indications, allows the assumption of a low-velocity zone within the granitic layer. The velocity below this layer is determined nonuniquely. The effective velocity increases from 6.3 to 6.7 km/sec in the 30-50 km depth range. The velocity within the 2-5-km-thick transition zone between the crust and the upper mantle increases from 6.8-7.0 to 8.0-8.2 km/sec.

Dnepr-Donets aulacogene. The velocity increases from 3.5 to 5.5 km/sec in the sedimentary layer, from 6.0 to 6.4 km/sec in the granitic layer, and from 6.8 to 7.6 km/sec in the basaltic layer. The crust and the upper mantle are separated by a 10-km-thick transition zone.

Carpathians. In the uppermost part of the crust (4-6 km), the velocity increases from 2.5 to 5.4 km/sec. A very pronounced horizontal velocity gradient is observed (four blocks with different velocity distribtuion are identified). The velocity in the basement complex is 5.8-6.0 km/sec, 6.6 km/sec in the upper basaltic layer, and 7.3-7.4 km/sec in its lower part.

Trans-Carpathian trough. The sedimentary cover is characterized by a velocity increasing with depth from 1.7-4.0 km/sec to 4.8-5.0 km/sec. A general increase of the velocity from the northwest to the southeast is observed. The folded basement surface is characterized by a velocity of 5.3-5.5 km/sec, which increases with depth to 6.0-6.1 km/sec. Below the folded basement lies the metamorphosed basement with a velocity of 6.1-6.5 km/sec. Within this complex, in the Chop-Mukachevskaya depression, a low velocity zone (6.0-6.1 km/sec) is observed. The adjacent layer has a velocity of about 6.4 km/sec, which is underlain by the Conrad discontinuity. Immediately above the Moho discontinuity, another low velocity zone (6.4 km/sec) is observed.

Detailed DSS studies reveal that in the Ukraine, the crust has a complex layered structure and is divided into blocks by numerous abyssal faults. A conditionally identified Conrad discontinuity is not locally observed or is diffused in the granitic-basaltic mixture. The characteristics of the boundary between the crust and the upper mantle vary widely over the region, i.e., from a sharp seismic interface to a very complex transition zone, 5 km or more thick. Sometimes, two Moho discontinuities are observed. The description of the crustal sections along international and national profiles is given below.

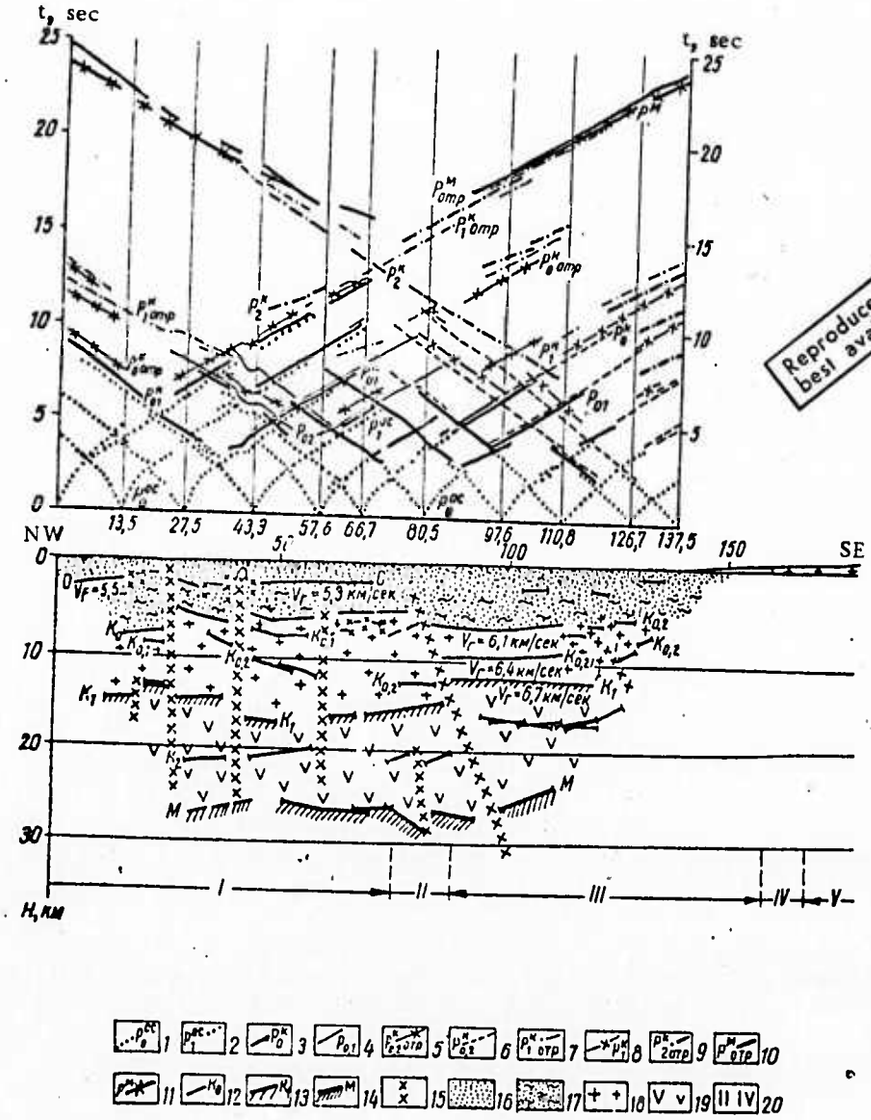

Fig. 16. System of Time-Distance Curves and Seismogeological Crustal Section along Profile 17 (Trans-Carpathian Trough).

Time-distance curves for waves from: 1- interfaces within the sedimentary layer; 2- Mesozoic-Paleogene basement surface; 3- crystalline basement surface; 4- top of the waveguide within the granitic layer; 5- interfaces within the waveguide, reflected; 6- interfaces within the gravitic layer in the Solotvinskaya depression, refracted; 7- basaltic layer surface; reflected; 8- basaltic layer surface, refracted; 9- top of the waveguide within the lower crust, reflected; 10- M discontinuity, wide-angle reflections; 11- M discontinuity, refracted: Interfaces: 12- crystalline basement surface; 13- Conrad discontinuity; 14- Moho discontinuity; 15- abyssal faults; 16- sedimentary layer; 17- Mesozoic-Paleogene folded basement; 18- granitic layer; 19- basaltic layer; 20- tectonic zones and blocks: I- Chop-Mukachevo depression, II- Vygorlat-Gutinskiy volcanic ridge, III-Solotvinskaya depression; IV- Marmaroshskaya zone of the Carpathians, V- Rakhovskiy crystalline massif.

The crustal thickness in the Trans-Carpathian trough (see profile 17, Fig. 16) varies from 24-29 km. The crust is broken by fault zones, some of them not penetrating the entire crust. Two low-velocity zones are observed in the consolidated crust: one between interface K_0 and $K_{0,1}$ with a velocity of 6.0-6.1 km/sec, and the other between interfaces K_2 and M, with a velocity of 6.4 km/sec.

The crystalline basement (Paleozoic) surface (K_0) with V_r = 6.1-6.5 km/sec occurs in the depth range from 4.5 to 8 km, forming an anliclinal bend.

The surface of the Baykalian folded complex ($K_{0,2}$) occurs at depths from 6.5 to 14 km. The Conrad discontinuity (K_1) occurs at depths from 8.0 to 17 km. The thickness of the granitic layer varies from 3-6 to 8-12 km.

The earth's crust along profile III (see Fig. 17) is characterized by the absence of continuous seismic interfaces and a velocity monotonically increasing with depth.

In the eastern Carpathians, all interfaces occur conformally, dipping from the Trans-Carpathian trough toward the Cis-Carpathian foredeep.

The metamorphosed basement surface (K_0), with V_r = 5.8-6.6 km/sec, occurs at a depth of 10-15 km, and is displaced by numerous faults.

The Conrad discontinuity (K_1) lies at depths of 18-23 km and in the Cis-Carpathian foredeep, it is displaced to a depth of 30-32 km.

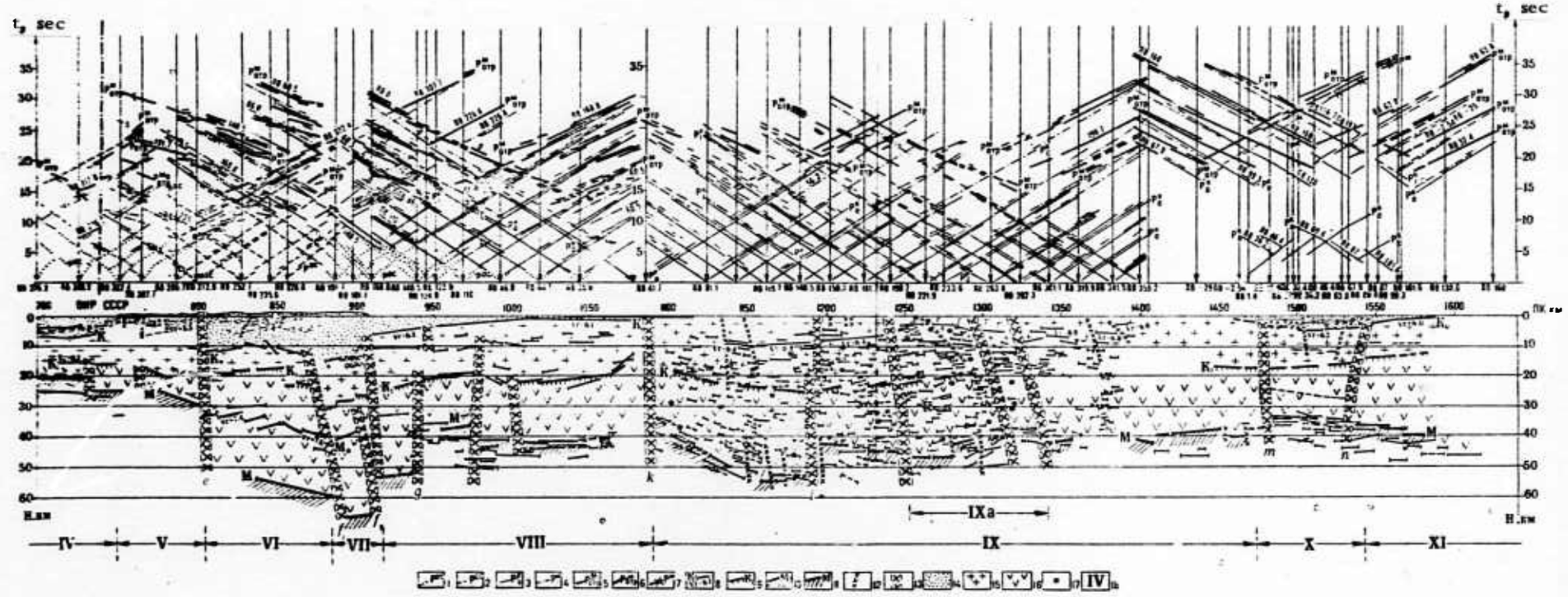

Fig. 17. System of Time-Distance Curves and Crustal Seismological Section along International Profile III within USSR Territory (Beregovo-Shepetovka-Gomel').

Time-distance curves for waves from: 1- interfaces within the sedimentary layer; 2- continuously refracted through the Mesozoic-Paleogene folded complex of the Carpathians; 3- crystalline basement surface; 4- basaltic layer surface; 5- M_0 discontinuity, reflected; 6- Moho discontinuity, reflected; 6- Moho discontinuity, refracted; Interfaces: 8- crystalline basement surface; 9- Conrad discontinuity; 10- M_0; 11- Moho discontinuity; 12- faults; 13- abyssal faults; 14- sedimentary layer; 15- granitic layer; 16- basaltic layer; 17- diffraction points; 18- tectonic zones and blocks; IV- Pannonian depression, V- Trans - Carpathian trough, VI- Carpathians, VII- Cis-Carpathian foredeep; VIII- Volynia-Podolia plate; IX- Ukrainian shield, IX_a- Korosten Pluton, X- Denepr-Donets aulacogene, XI- Voronezh massif.

The Moho discontinuity is clearly identified at depths from 53-65 km, with the maximum depth found in the Cis-Carpathian foredeep. Thus, the Carpathian "root" is asymmetric and displaced towards the northeast, submerging partly beneath the adjacent plate (Volynia-Podolia). Farther along the profile, all interfaces rise toward the Ukrainian shield.

Thus, in the Volynia-Podolia plate, the Conrad and Moho discontinuities rise step-wise from 30 to 15 km and from 65 to 40 km, respectively.

Within the western margin of the Ukrainian shield there is an anomalous zone where the intensively fractured Conrad and Moho discontinuities form sharp anticlinal bends. East of this zone, they descend and the crustal thickness increases to 50-54 km, such a thick crust is considered to be uncharacteristic of Pre-Riphean platforms.

Within the Korosten Pluton the Conrad discontinuity is not identified reliably, while the Moho discontinuity rises to 40 km. The crust within the limits of the Korostin Pluton has a distinct block-layered structure (see Fig. 18) with interstratified acid and basic rocks.

The crustal thickness in the Dnepr-Donets aulacogene decreases to 34-35 km. The Conrad discontinuity, at depths of 12-17 km, forms a downwarp.

Over the entire profile VIII (see Fig. 19) the consolidated ancient basement is exposed. Nearly over the entire profile, the Conrad discontinuity is a distinct seismic interface. Its depth changes from 10-15 km in the west, to 18-22 km in the east. The Moho discontinuity depth varies over a wide range from 30 to 55-60 km. The crust is divided into blocks by numerous abyssal fault zones, such as the very extensive Kirovograd, Krivoy Rog-Kremenchug, Orekhovo-Pavlograd zones.

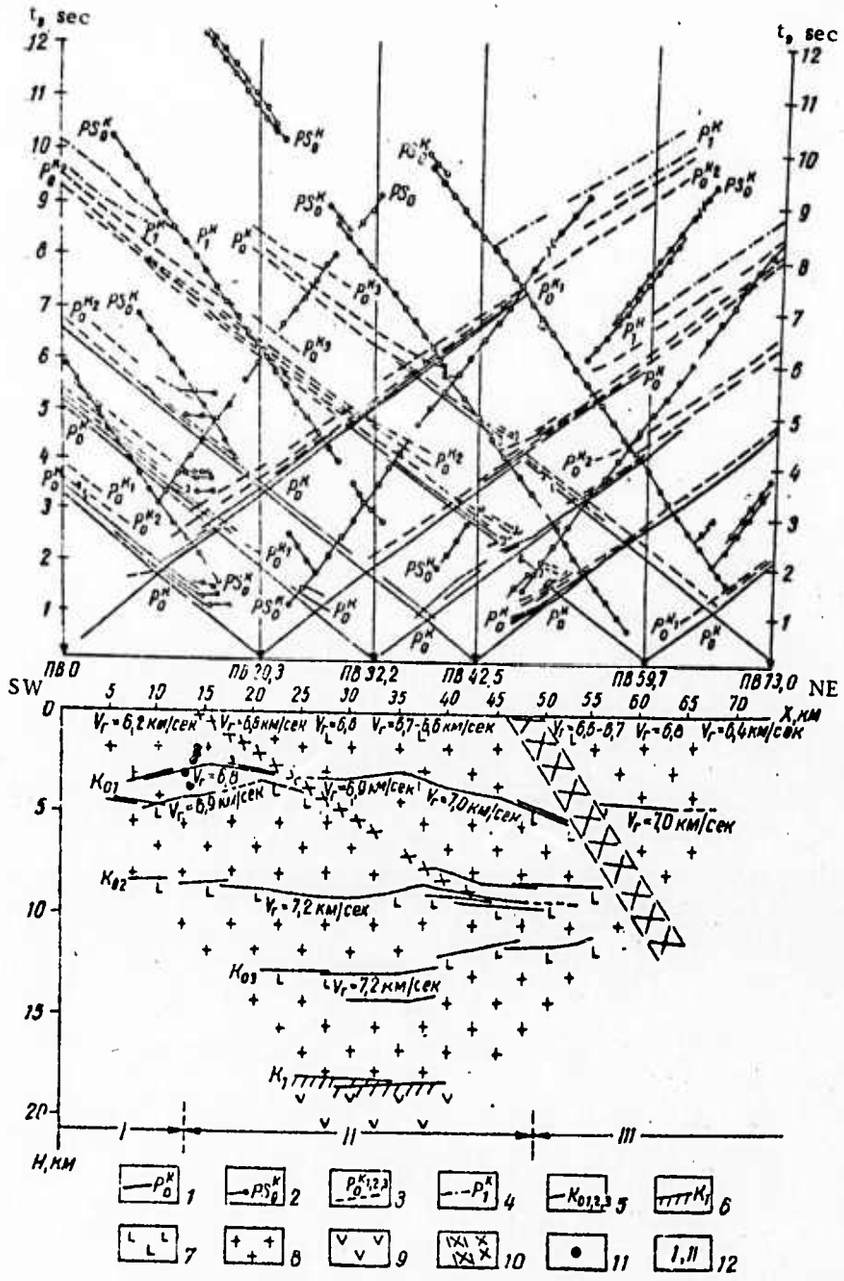

Fig. 18. System of Time-Distance Curves and Crustal Seismogeological Section along Detailed Profile 13 in the Region of the Korosten Pluton (Ukrainian Shield).

Time-distance curves for waves from: 1- crystalline basement surface, direct; 2- crystalline basement surface, converted; 3- interfaces within the granitic layer; 4- basaltic layer surface; Interfaces: 5- interfaces within the consolidated crust; 6- Conrad discontinuity; 7- gabbro-labradorites; 8- granitic layer; 9- basaltic layer; 10- faults; 11- diffraction points; 12- tectonic blocks; I- Korosten granites, II- Volynia gabbro-labradorite massif, III- Chepovichskiy gabbro-labradorite massif.

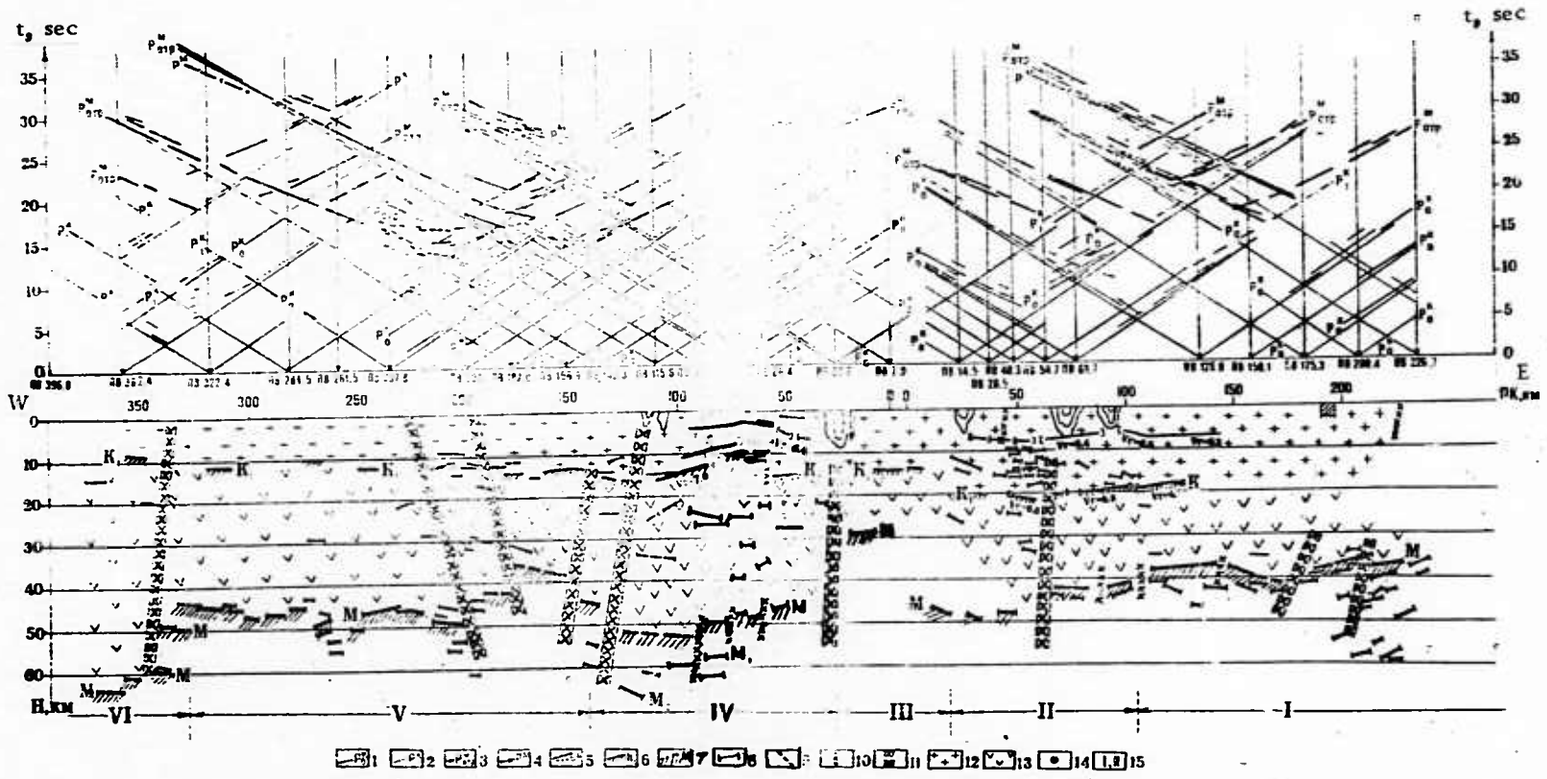

Fig. 19. System of Time-Distance Curves and Crustal Seismogelogical Section along Profile VIII (Uman'-Kirovograd-Taganrog).

1-4 Time-distance curves for waves from: 1- crystalline basement surface; 2- basaltic layer surface; 3- M discontinuity, reflected; 4- M discontinuity, refracted; Interfaces: 5- refraction surfaces within the granitic layer; 6- Conrad discontinuity; 7- M discontinuity; 8- reflection surfaces within the consolidated crust; 9- faults from geological data; 10- disjunctive dislocations; 11- abyssal faults; 12- granitic layer; 13- basaltic layer; 14- diffraction points; 15- tectonic zones and blocks: I- Peri-Azov massif, II- Orekhovo-Pavlograd Lower-Proterozoic geosynclinal system; III- Zaporozh'ye median massif, IV- Krivoy Rog - Kremenchug Lower-Proterozoic geosynclinal system; V- Kirovograd protoplatform block, VI- Odessa-Tal'nov Lower-Proterozoic geosynclinal system.

The crystalline basement surface along profile I (see Fig. 20) occurs at depths of 10-12 km in the Dnepr-Donets aulacogene whereas, in the adjacent Ukrainian shield, the basement is exposed. South of the Ukrainian shield, it gradually subsides, up to the Saythian plate where it abruptly subsides and younger (Cimmerian) folded basement underlies the sedimentary formations. In the junction zone between the ancient East European platform and the young Scythian plate, a suture graben is found where the sedimentary layer reaches a depth of several kilometers. In the Crimean Mountains, the basement of the Scythian plate becomes an outcrop. However, the thickness of the sedimentary complex in the Black Sea depression amounts to 10-14 km.

The Conrad discontinuity is downwarped in the Dnepr-Donets aulacogene. It lies at depths of 25-27 km, rising both toward the Ukrainian shield and the Voronezh massif. In the Ukrainian shield, the Conrad discontinuity locally looses the characteristics of distinct seismic interfaces. In the Crimean Mountains, the Conrad discontinuity rises to 8-10 km, and with a downwarped Moho discontinuity, a very thick (40 km) basaltic layer is formed. In the Black Sea basin, it lies at depths of 15-20 km, directly underlying the sedimentary cover in the deep-water section of the basin.

The Moho discontinuity is uplifted in the Dnepr-Donets aulacogene (40 km), while it subsides in the Ukrainian shield (45-50 km) and is uplifted in the Scythian plate. In the Crimean Mountains, the Moho occurs at a depth of 50 km. To the contrary, the crust in the Black Sea basin is very thin, locally only 20 km or less. In the central part of this basin, the crust consists only of the sedimentary and basaltic layers (suboceanic type).

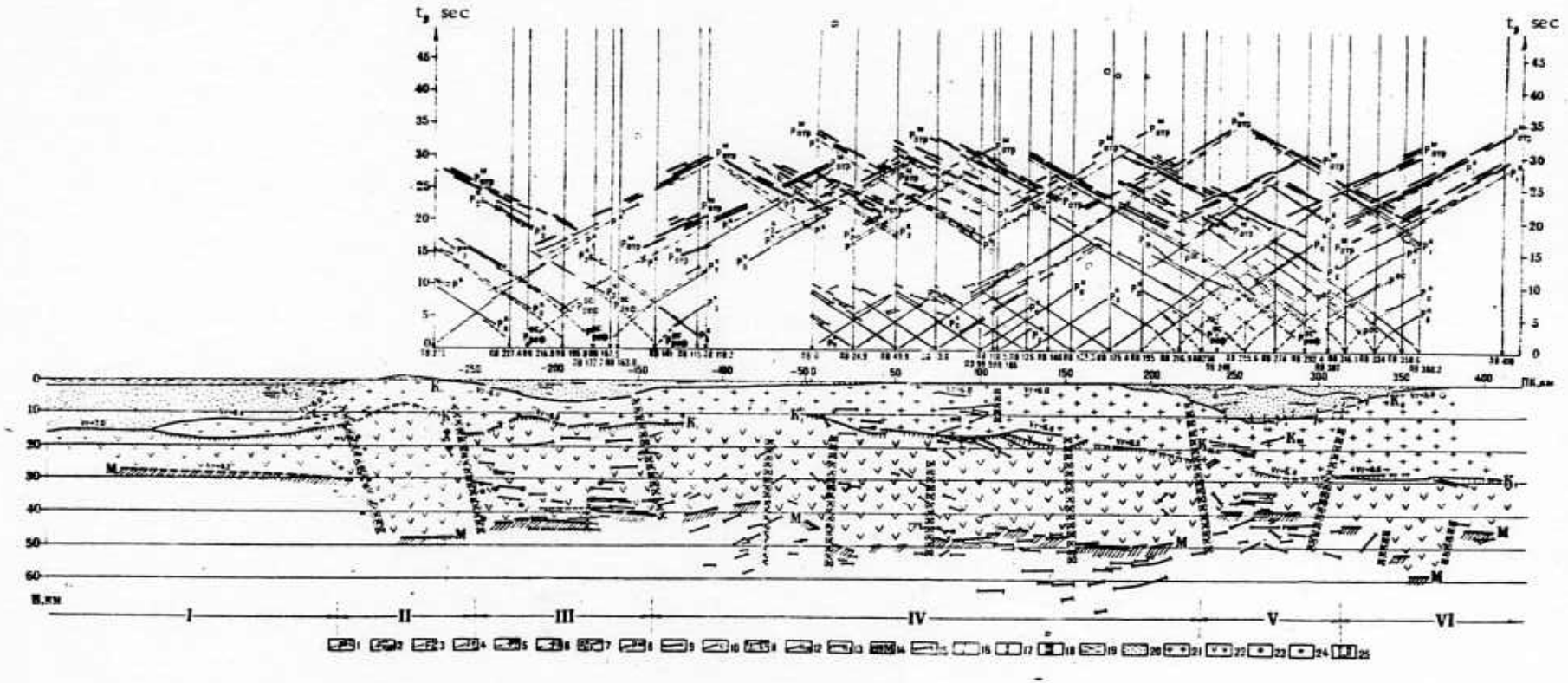

Fig. 20. System of Time-Distance Curves and Crustal Seismogeological Section along Profile I (Black Sea - Voronezh Massif).

Time-distance curves for waves from: 1- interfaces within the sedimentary layer; 2- sedimentary layer, continuously refracted; 3- crystalline basement surface; 4- interfaces within the granitic layer in the Dnepr-Donets aulacogene, reflected; 5- basaltic layer surface; 6- continuous reflection surfaces within the basaltic layer; 7- M discontinuity, reflected; 8- M discontinuity, refracted; 9- local reflection surfaces; Interfaces: 10- interfaces within the sedimentary layer; 11- crystalline basement surface; 12- interfaces within the basement of the Dnepr-Donets aulacogene; 13- Conrad discontinuity; 14- M discontinuity; 15- reflection surfaces; 16- faults from geological data; 17- disjunctive dislocations; 18- abyssal faults; 19- water; 20- sedimentary layer; 21- granitic layer; 22- basaltic layer; 23- diffraction points; 24- earthquake foci; 25- tectonic zones; I- Black Sea basin; II- Crimean Mountains; III- Scythian plate; IV- Ukrainian shield; V- Dnepr-Donets aulacogene; VI- Voronezh massif.

The crust along profile I is divided into blocks by a number of abyssal fault zones, their planes dipping northward. The most prominent of these are: between the Black Sea basin and the Crimean Mountains; the Crimean Mountains and Scythian plate; the Scythian plate and East European platform, as well as the faults bordering the Dnepr-Donets aulacogene and intersecting the Ukrainian shield.

The crystalline basement surface (see profile 10-IX, Fig. 21) in the Donbass folded system lies at depths of 15-17 km. Southward, the crystalline basement crops out forming the Peri-Azov massif of the Ukrainian shield. With the transition to the Scythian plate, the basement changes its age and submerges into the North Azov depression and Indol-Kuban trough. The thickness of the sedimentary layer in the Indol-Kuban trough reaches 15 km. In the Black Sea basin, the sedimentary layer is about 10 km thick, and in the deep-water section of the basin, it lies directly on the basaltic layer.

The Conrad discontinuity, downwarped in the Donbass region (about 30 km), rises toward the Voronezh massif, as well as toward the Ukrainian shield (10-12 km), where it forms a sharp anticlinal bend. In the Scythian plate (Azov swell), it lies at a depth of 25-27 km, rising toward the Black Sea basin, where it reaches a depth of 10 km.

The Moho discontinuity forms a very complex saddle-like structure at 40-45 km in the Donbass. However, along the entire 500-km-long sector between the Voronezh massif and the Azov swell, it forms a plateau-like structure at a depth of about 40 km. In the Black Sea its depth decreases rapidly up to 18-20 km in the deep-water section.

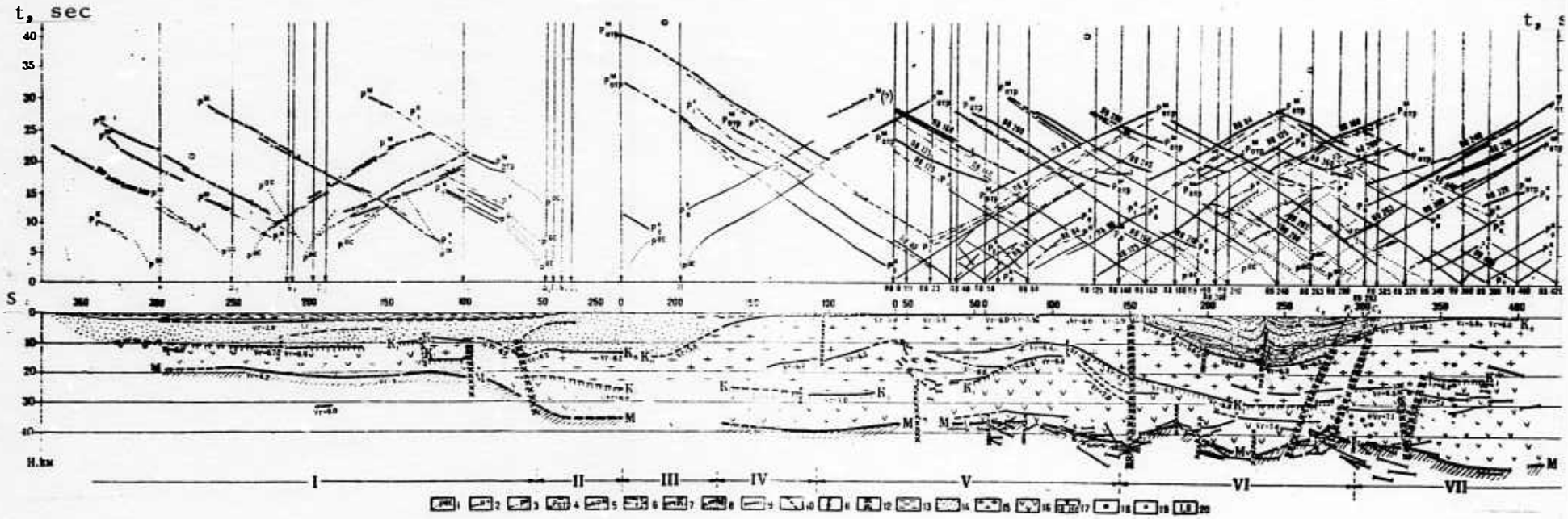

Fig. 21. System of Time-Distance Curves and Seismogeological Section along Profile 10-IX (Sinop-Nogaysk-Svatovo).

Time-distance curves for waves from: 1- interfaces within the sedimentary layer; 2- crystalline basement surface; 3- basaltic layer surface; 4- M discontinuity, wide-angle reflections; 5- M discontinuity, refracted; Interfaces: 6- crystalline basement surface; 7- Conrad discontinuity; 8- Moho discontinuity; 9- reflection surfaces; 10- faults from geological data; 11- disjunctive dislocation; 12- abyssal faults; 13- water; 14- sedimentary layer; 15- granitic layer; 16- basaltic layer; 17- shot points; 18- diffraction points; 19- depths determined from t_o at shot point; 20- tectonic zones: I- Black Sea basin; II- eastern plunge of the Crimean Mountains; III- Indol-Kuban foredeep; IV- Scythian plate; V- Peri-Azov massif of the Ukrainian shield; VI- Donbass; VII- Voronezh massif.

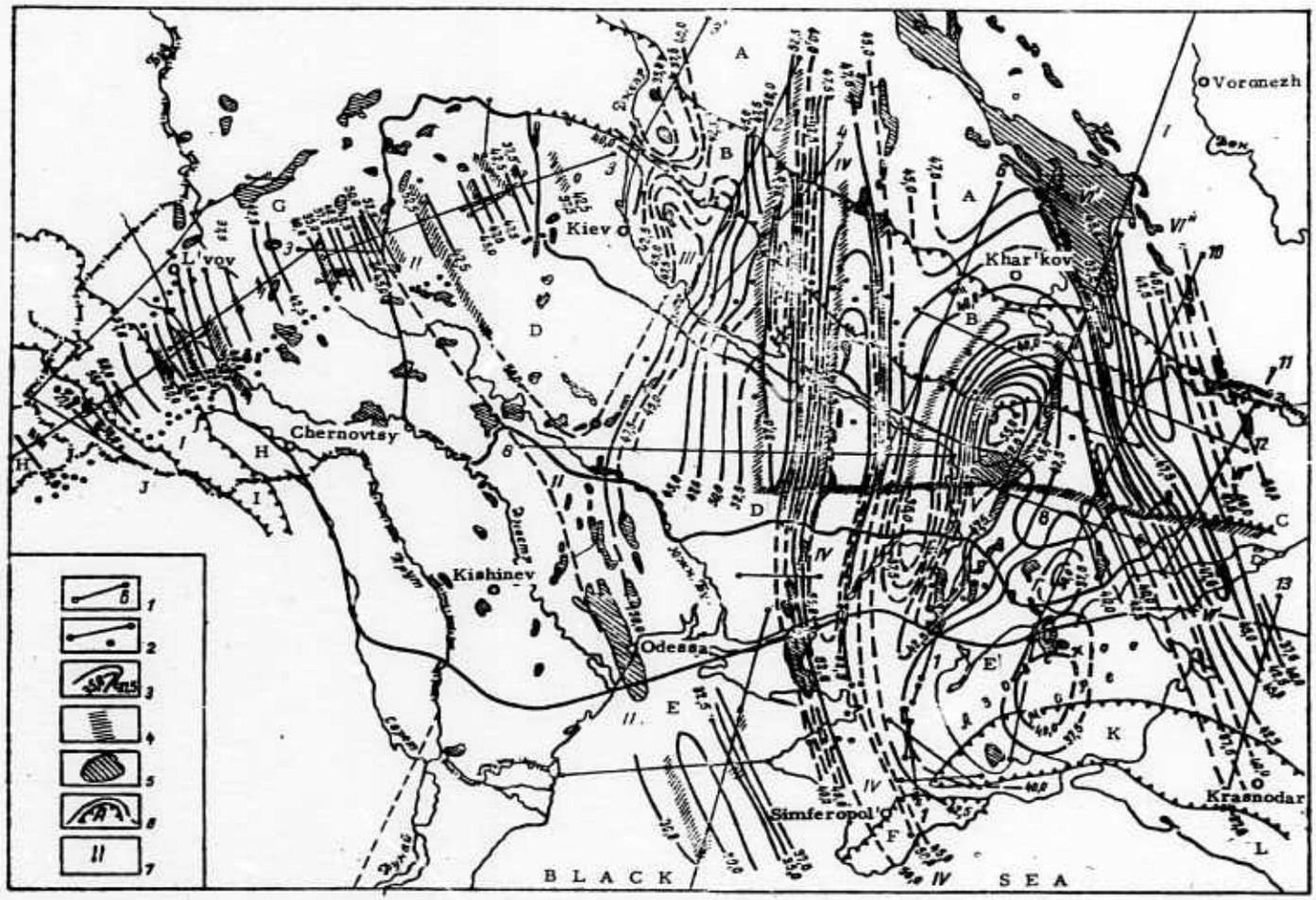

Fig. 22. Map of the Moho Discontinuity Relief in the Ukraine (after V. B. Sollogub).

1- DSS profiles; 2- points where the crustal thickness is determined; 3- depth isolines for the Moho discontinuity; 4- major abyssal faults from DSS data, 5- intense magnetic anomalies; 6- geological provinces; A- Voronezh massif; B- Dnepr-Donets aulacogene; C- Donbass; D- Ukrainian shield; E- Peri-Black Sea depression; F- Crimean Mountains; G- Volynia-Podolia plate; H- Cis-carpathian foredeep; I- Carpathian Mountains; J- Trans-Carpathian trough; K- Indol-Kuban foredeep; L- Caucasus; 7- zones of thickenned crust: I- Carpathian, II- Shepetovka-Odessa, III- Odessa-Tal'nov; IV- Krivoy Rog- Kremenchug; V- Orekhovo-Pavlograd; VI- Kursk-Adygey.

The crust along profile 10-IX, similar to [illegible]r profiles in the Ukraine, is intersected by numerous abyssal faults. A map showing the Moho discontinuity relief in the Ukraine is given in Figure 22.

Conclusions

1. The deep structure of the crust in the Ukraine was formed mainly in the Lower-Proterozoic. The observed "roots" beneath the Alpine Carpathian system and the Crimean Mountains were also formed in the Lower Proterozoic. In the process of the denudation of ancient mountains, the Moho discontinuity was smoothed, but not to such an extent as was previously accepted. The main Lower-Proterozoic crustal structures are preserved.

The structures of the Moho discontinuity may comform or not conform to young surface structures (Carpathians and Crimean Mountains, respectively).

2. The theory of isostasy should be reconsidered.

3. The previously established correlation between crustal thickness and gravity data can be applied only locally. A tentative analysis showed that only an insignificant portion of Δg is due to deep structures.

4. Information on the Moho discontinuity permits the refining of some concepts of the surface tectonics.

5. Abyssal and surface fault zones are closely associated.

6. The structure of the Moho discontinuity is very complex, and this is reflected in the shallow structures.

B. Recent Selections

Barinova, T. Ya. Reflection and refraction of plane compressional and SH waves in imperfectly elastic media. IN: AN TadSSR. Izvestiya. Otdeleniye fiziko-matematicheskikh i geologo-khimicheskikh nauk, no. 1, 1973, 27-34.

Chesnokov, Ye. M. Elastic anisotropy of multicomponent structural models of the upper mantle. IN: AN SSSR. Izvestiya. Fizika Zemli, no. 5, 1973, 28-38.

Davydova, N. I., et al. Models of the crust and Mohorovicic discontinuity. IN: AN UkrSSR. Geofizicheskiy sbornik, no. 51, 1973, 49-65.

Gel'fand, I. M., et al. Attempt to apply the high seismicity criteria of Central Asia to Anatolia and adjacent regions. IN: AN SSSR. Doklady, v. 210, no. 2, 1973, 327-330.

Khalevin, N. I., et al. Azimuth observations in deep seismic sounding in the Urals. IN: AN SSSR. Izvestiya. Fizika Zemli, no. 5, 1973, 87-94.

Kondorskaya, N. V., et al. Time-distance curves for seismic waves from Far East earthquakes. IN: AN SSSR. Izvestiya. Fizika Zemli, no. 5, 1973, 11-27.

Krauklis, P. V., and N. V. Tsepelev. Near-surface waves in a nonhomogeneous medium with an arbitrary smooth boundary. IN: AN SSSR. Izvestiya. Fizika Zemli, no. 5, 1973, 3-10.

Lurmanashvili, O. V. Regular variations in the time of occurrence of earthquakes in certain seismically active areas. IN: AN GruzSSR. Soobshcheniya, v. 70, no. 1, 1973, 69-72.

Mamadaliyev, Yu. A. Study of the seismicity parameters of the Dushanbe - Vakhsh region of Tadzhikistan. Gerlands beitrage fur geophysik, v. 82, no. 1,1973, 43-65.

Mostovoy, S. V. Construction of a filter to remove compressional and shear wave fluxes from a seismic record. IN: AN UkrRSR. Dopovidi. Seriya B. Heolohiya, heofizyka, khimiya ta biolohiya, no. 5, 1973, 412-414.

Nikolayev, A. V., and A. G. Aver'yanov. Study of compressional-wave amplitudes in a plane model of a medium with random velocity fluctuations. IN: AN SSSR. Izvestiya. Fizika Zemli, no. 5, 1973, 95-101.

Savarenskiy, Ye. F., et al. Shear waves from the Sarykamysh earthquake and its focal mechanism. IN: AN Gruz SSR. Soobshcheniya, v. 70, no. 2, 1973, 321-324.

TASS. Ground water as an earthquake precursor. Kazakhstanskaya pravda, 14 June 1973, p. 4, cols. 1-3.

Tigranyan, G. A. Multichannel telemetering system for studying earthquake prediction problems. IN: AN ArmSSR. Izvestiya. Seriya tekhnicheskikh nauk, no. 6, 1972, 19-23.

Urazayev, B. M., et al. The Alma-Ata Central Seismological Observatory. IN: AN KazSSR. Vestnik, no. 5, 1973, 3-12.

Vaniyek, L., et al. Use of schlieren photography to study elastic waves passing through an area of stress concentrations. IN: AN SSSR. Doklady, v. 210, no. 2, 1973, 324-326.

Verbitskiy, T. Z. Evaluation of rock relief coefficient from elastic-wave propagation velocities. IN: AN UkrRSR. Dopovidi. Seriya B. Heolohiya, heofizyzka, khimiya ta biolohiya, no. 5, 1973, 409-412.

Wagner, C., and W. Ullmann. Method for verification of Birch-Murnaghan's equation of state by use of seismic values (in English). Gerlands beitrage fur geophysik, v. 82, no. 1, 1973, 66-72.

Monographs

Polikarpova, L. A. Statisticheskoye issledovaniye dinamicheskikh kharakteristik seysmicheskikh zapisey (Statistical study of the dynamic characteristics of seismic recordings). Moskva, Izd-vo Nauka, 1973, 74 p.

Nikolayev, A. V. Seysmika neodnorodnykh i mutnykh sred (Seismicity of nonhomogeneous and turbid media). Moskva, Izd-vo Nauka, 1973, 173 p.

Savarenskiy, Ye. F. Seysmicheskiye volny (Seismic waves). Moskva, Izd-vo Nedra, 1972, 291 p.

4. Particle Beams

A. Abstracts

Iremashvili, D. V., S. V. Kuril'nikov, N. I. Leont'yev, and T. A. Osepashvili. Heavy-current plasma electron gun with a 50 ka current pulse. ZhETF P, v. 17, no. 1, 1973, 11-13.

An improved electron gun with a plasma cathode is introduced. Improvement over a previously described Soviet gun was accomplished in the electron flow transmission efficiency and stability, by introducing a set of spark sources uniformly distributed over the anode and oriented normal to the generatrix of the anode aperture. The experimental arrangement (Fig. 1)

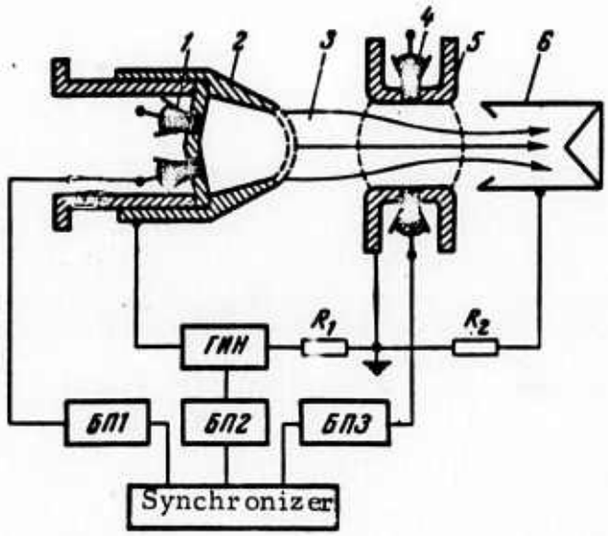

Fig. 1. Experimental electron gun arrangement:
1 - cathodic spark sources, 2 - cathode, 3 - 1-2cm. long acceleration gap, 4 - anodic spark sources, 5 - anode, 6 - Faraday cylinder; БП1, БП2, and БП3 - power supply units, ГИН - pulse voltage generator.

shows how the anode spark sources generate plasma synchronously with the cathodic plasma. The pulse generator delivers up to 100 kV pulses to the gun electrodes with a (0.5-1.5) μsec. time lag. Current pulses of maximum amplitude are delivered to the Faraday cylinder by varying cathodic (I_c) and anodic (I_a) firing currents and anodic voltage pulse delay (τ_3).

The oscilloscope traces show that, at $I_a = I_c = 700$ A and $\tau_3 =$ 0.8 μsec , current delivered to the Faraday cylinder is 52 kA for a 58 kA total current, i.e., 90% of the total current. Such a high electron beam transmission efficiency is due to the space charge compensation by dense anodic plasma and self-compression of heavy-current beam. An experimental source of bremsstrahlung x-ray pulses based on the described gun has produced pulses of $\sim 10^9$ r/sec radiation power, ~100 r/pulse radiation dose, and 15-25 keV energy.

Khirseli, Ye. M. Stability of a magnetically-active plasma with relativistic electron beam, located in a high-frequency electric field.
ZhTF, no. 1, 1973, 26-29.

Instability conditions are formulated for an electron plasma-relativistic electron beam system in a uniform magnetic field B_o and a h.f alternating electric field E(t). The electron beam propagates through the plasma with directional velocity V_o comparable to sound velocity C, and parallel to B_o and E(t). In addition, the frequency ω_o of E(t) is assumed to be well above all characteristic frequencies of the system. General formulas for instability increments γ and conditions of plasma oscillation instability in the presence of B_o and boundaries of instability regions in the absence or in the presence of B_o, are derived from the dispersion equation of potential

oscillations. It is shown that in the presence of both B_o and E(t), narrowing of the instability region leads to stabilization of oscillations with the transverse wave vector component $k_\perp \neq 0$. Cases are examined of hydrodynamic (cyclotron) and kinetic instabilities. In both cases, conditions are derived from the cited dispersion equation, under which instability may develop in a magnetically-active electron plasma. The corresponding γ values are formulated. In the case of cyclotron instability, oscillation instability regions are defined in terms of frequencies by means of the γ formula. In the case of kinetic instability, the γ formula shows that γ can change sign from plus to minus, if $k_\parallel v_o > \omega$ and electron beam emission exceeds wave damping by the particles. It is noted that γ decreases in the presence of a h.f. electric field.

In all cases studied, the increment of γ is reduced in the presence of the h.f. electric field, thus in this sense the electric field has a stabilizing effect on plasma oscillations and contributes to a narrowing of instability regions. The latter effect is of special importance with respect to achievement of high currents.

Belan, N. V., N. A. Mashtylev, and B. I. Panachevnyy. Transient processes in the inductive energy storage of a plasma injector. ZhTF, no. 1, 1973, 83-86.

This is a theoretical and experimental study of the charging-discharging processes in an inductive energy storage (IES), with charge circuit switching by moving discharge (plasma). Processes in the pulsed plasma injector with the IES are described, using an approximation for the motion of the plasma center of inertia, by a set of equations in dimensionless variables. An analytical solution of the set is given for the particular case

in which the plasma motion effects and inductance of the switching device with an d.c. external power supply can be neglected. A graphical presentation of the solution shows that charging current increases during IES charging, starts to decrease when discharge circuit is switched on, and continues to decrease exponentially after the charge circuit is switched off. The measurements of current i in an experimental IES confirmed the cited theoretical conclusions. In qualitative agreement with the theory, the experimental i(t) curves show that i in the IES increases with increase in time lag from 1 to 5 msec, or in short-circuit current from 0.24 to 1.68 kA.

Panasyuk, V. S., A. A. Sokolov, and V. M. Stepanov. Design principles and possible application of accelerators with a superstrong magnetic field, generated by an explosion. Atomnaya energiya, v. 33, no. 5, 1972, 907-912.

This paper discusses the principles of generating superstrong magnetic fields in accelerators by means of explosion generators. Two methods are considered: 1) induction acceleration and 2) high-frequency acceleration. The accelerators considered are of a cyclic as well as direct action type. The high frequency method of acceleration was experimentally verified in the model shown in Fig. 1. Parameters of the model were:

1. Kinetic electron energy at a finite radius R_K = 2 Mev
2. Maximum induction of the magnetic field at winding centre = 4.8 kg(force)
3. Acceleration cycle duration = 2 μsec
4. Accelerating electric field intensity = 500 v/cm
5. Wavelength of accelerating field = 11 cm.

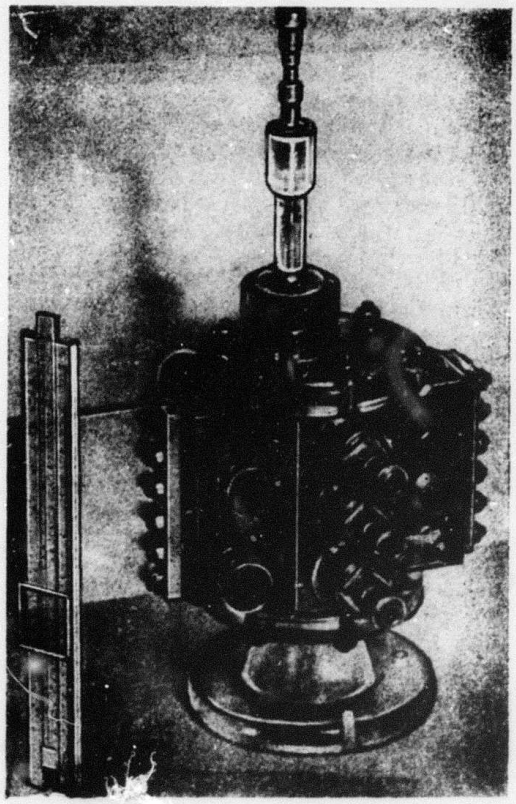

Fig. 1. Accelerator model without power supply and pump.

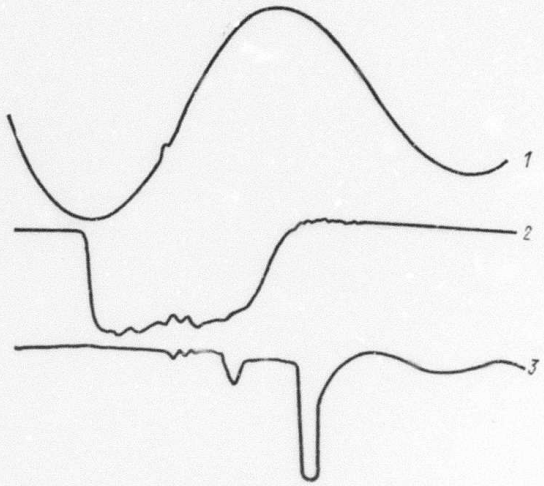

Fig. 2. Waveform oscillograms.
1 - pulsed magnetic field;
2 - high-frequency pulsed voltage curve; 3 - pulsed bremsstrahlung.

Fig. 2 shows typical waveforms. Possible applications are outlined of cyclic accelerators with a superstrong magnetic field.

Mamedov, M. A., and A. M. Fedorchenko. Kinetic theory of spatial instability in a radially confined plasma-electron flow system with a preset radially inhomogeneous plasma configuration. UFZh, no. 11, 1972, 1885-1892.

The increment Im y of spatial instability (amplification factor) in a plasma-electron beam system was computed with allowance for the electron-plasma particle collisions, thermal dispersion of the plasma and beam electrons, and finite cross-sectional dimensions of the system. The existing kinetic theories of plasma-beam spatial instability fail to take into account the cited factors, and hence are incorrect. In the present study, interaction is analyzed of an electron beam with a radially inhomogeneous plasma confined in a tube with internal radius a by a strong magnetic field in the direction of beam propagation. A Maxwellian velocity distribution is assumed for beam electrons. Radial distribution of plasma electrons is described by the parameter $\varkappa$, a characteristic of the radial decrease in electron density.

A radially confined electron plasma is then described by a known linearized equation. Applying successive approximations to this equation, the authors derive an equation for electric field in the system. Integration of the latter with respect to frequency x gives a dispersion equation for the system. Finally, an asymptotic formula for Im y is obtained by solving the dispersion equation. The Im y(x) plots computed from this formula illustrate the effects of low heat rates U_T and V_T of the beam and plasma electrons, respectively (Fig. 1), the effective collision frequency ν (Fig. 2), and the parameter $\varkappa$ (Fig. 3).

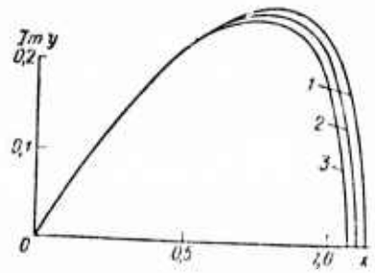

Fig. 1. Im y versus x plot at σ^2 = 0.03, q^2 = 0.21, σ^2 = 8.4, ν = 0.01 and $\varkappa$ = 0.3, ξ^2 = 8 (1), 13 (2), and 17 (3), ξ_1^2 = 13 (1), 15 (2), and 21 (3).

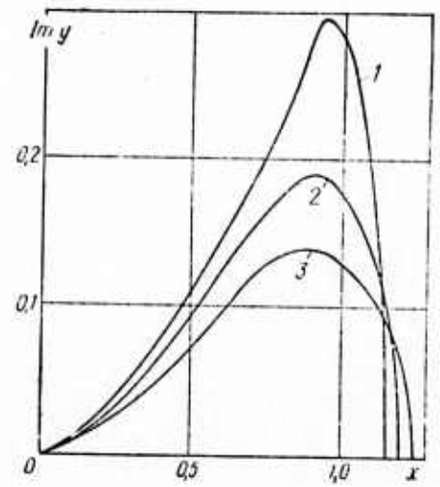

Fig. 2. Im y versus x plot at σ^2 = 0.04, q^2 = 0.12, ξ^2 = 10, ξ_1^2 = 12, δ^2 = 20, and $\varkappa$ = 0.4, γ = 0.1(1), 0.2 (2), and 0.3 (3).

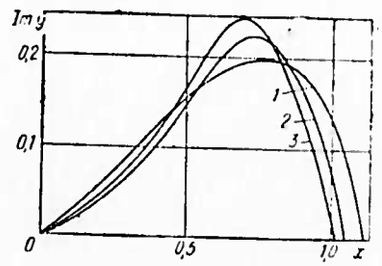

Fig. 3. Im y versus x plot at σ^2 = 0.02, q^2 = 0.23, ξ^2 = 16, ξ_1^2 = 18, δ^2 = 11, ν = 0.03, $\varkappa$ = 0.9 (1), 0.6 (2), and 0.3 (3).

The quantities y, x, q, δ, γ, ξ, ξ_1, and σ in Fig. 1-3 are given by the formulas

$$y = \frac{kv_0}{\omega_0}, \quad x = \frac{\omega}{\omega_0}, \quad \gamma = \frac{\nu}{\omega_0}, \quad \delta = \frac{\omega_H}{\omega_0}, \quad q = \mu_{01}v_0/a\omega_0, \quad \xi = \frac{v_\tau}{v_0}, \quad \xi_1 = \frac{u_\tau}{v_0}. \tag{1}$$

and $\sigma = \omega_b/\omega_o$, where V_o is the mean propagation velocity of electron beam, ω_o, ω_b, ω, and ω_H are the Langmuir frequencies of plasma electrons, beam electrons, electromagnetic waves, and magnetic field, respectively, and μ_{01} is the first root of the $J_o(Ta)$ function in the dispersion equation. Figs. 1 and 2 show that Im y decreases to zero at a sufficiently high x, contrary to the existing theory which predicts that Im $y \to \infty$ at $\omega \to \omega_o$.

Vasilevskiy, M. A., I. M. Royfe, and Ye. V. Seredenko. Dynamic stabilization of a toroidal discharge in a longitudinal magnetic field. ZhTF, no. 11, 1972, 2320-2325.

A combined quasidirect and hf-toroidal discharge in hydrogen in a longitudinal magnetic field H_z was studied in a "Toloskop" device, in both unstable and stabilized regimes. The plasma characteristics were measured, principally by magnetic probes. The oscilloscope traces of quasidirect current instabilities, the instability increment γ and wave number k determined from the scope traces led to the conclusion, in agreement with the theory, that a Kruskal-Shafranov screw-type current instability was occurring. The transition to a stable regime, which was observed at a sufficiently high h-f field, was interpreted in terms of dynamic stabilization theory applied to h-f radial oscillations of a plasma column at frequency ω. It is shown that the dynamic stabilization criterion for an ideal MHD plasma model coincides with the experimental criterion for H_z at frequency ω. The experimental stability limits also coincide well with theory over a fairly wide range of plasma fields and intensities.

Krivoruchko, S. M., and Ye. A. Kornilov. Excitation and interaction of low-frequency oscillations during beam instability. Fiz. plazmy i probl. upravl. termoyader. Sinteza. Resp. mezhved. sb., no. 3, 1972, 208-213. (RZhF, 11/72, no. 11G247). (Translation).

The excitation mechanism is investigated of low-frequency (plasma) oscillations. It is established through the use of multifrequency electron beam modulation that low frequency oscillations are a direct

result of the beam instability. They are generated by nonlinear interactions of low-frequency oscillations, or because of inhomogeneity and the nonequilibrium state of the plasma, produced by low-frequency fields. The use of multifrequency e-beam modulation makes it possible to control beam instability by the oscillation spectrum and to solve the problem of effective energy transfer from the beam to electrons and ions in the plasma.

Lutsenko, Ye. I., Ya. B. Faynberg, V. A. Vasil'chuk, and N. P. Shepelev. Interaction of an intensive electron beam with homogeneous and inhomogeneous plasma. Fiz. plazmy i probl. upravl. termoyader. sinteza. Resp. mezhved. sb., no. 3, 1972, 5-15. (RZhF, 11/72, no. 11G249). (Translation)

The problem of intensive electron beam generation in plasma at densities of 10^{11}-10^{13} /cm^3 was investigated by accelerating electrons in plasma with an external electric field of 500-1000 v/cm and duration of 0.5 μsec, produced by an induction accelerator. A beam was generated with currents above 1 ka and energy close to the applied voltage, at beam particle densities $n_1 \cong 10^{11}$/cm^3. The beam originates in the cathode layer of the plasma with thickness less than 2 cm, where the total applied voltage is redistributed. During beam passage through the plasma nearly 1/3 of the beam current is lost due to beam instability development with frequency ω_{pe}, and electron energy spectrum is broadened. Elimination of the instability is achieved by using an axially-inhomogeneous plasma.

Aseyev, G. G., G. G. Kuznetsova, N. S. Repalov, B. G. Safronov, and N. A. Khizhnyak. Parametric instability of an electron beam in a space-periodic electric field. Fiz. plazmy i probl. upravl. termoyader. sinteza. Resp. mezhved. sb., no. 3, 1972, 202-208. (RZhF, 11/72, no. 11G248). (Translation).

Parametric instability is experimentally investigated of an electron beam during its transit through space-periodic electric fields, and a discussion is given on the dependence of the h-f radiation level of the beam on accelerating voltage, start-up currents, and levels of external electric field. Theoretical and experimental values for the case of resonance at the second harmonic of plasma beam frequency are in good agreement. The results obtained are analysed.

Kiyashko, S. V., M. I. Rabinovich and V. P. Reutov. Explosive instability and generation of solitons in an active medium. ZhTF, no. 12, 1972, 2458-2465.

The interaction of electromagnetic waves is investigated in a nonlinear medium, in which the imaginary part of the dielectric constant is proportional to the field (quadratic non-linearity). Two cases are discussed: 1) when the medium is conservative and possesses a sufficiently strong dispersion $\beta >> \alpha, \nu$ (where β, α, ν are dispersion, nonlinearity and dissipation respectively), and 2) when the dispersion is absent, $\beta = 0$. The conditions for explosive instability in these media are

discussed. Characteristics are studied of the instability and its mechanism is theoretically determined. The authors note that in a weak dispersive medium, isolated pulses (solitons) and periodic pulse sequences (cnoidal waves) are generated owing to explosive instability. Forms of the nonlinear waves and the effect of the source on maintaining a nonequilibrium state of medium are approximately determined.

An experiment was conducted on a transmission line with tunneling to demonstrate the possibility of explosive instability. The model of such a transmission line is shown in Fig. 1. Parameters of the

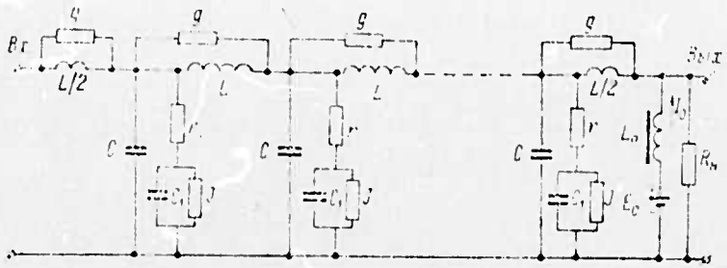

Fig. 1. 26 sections of LC-circuit loaded with tunnel diodes.

LC circuit were: L = 0.61 μh, C = 150 pf, r = 15 ohm, C_L = 10 pf. Linear damping at f = 10 MHz was $\sim 10^{-4}$. Investigations were conducted for double- and triple-wave processes and results were plotted in 3 graphs.

The authors refer in a concluding footnote to a related work on explosive instability of a beam-plasma system, presented by Homan at the 10th International Conference on Phenomena of Ionizing Gases, Oxford, 1971.

Tonkonogov, M. P., Z. S. Grinshpun, and Yu. D. Il'yushenkov. On the theory of shock waves generated in solids during pulsed arc discharges. EOM, no. 6, 1972, 37-43.

Parameters are theoretically determined of the discharge channel and shock waves generated in solids during pulsed electric breakdown, in accordance with a given energy law in the discharge channel. The discharge channel was assumed to be an approximate plasma cylinder, characterized by an ion temperature $T_i = T$. Expressions are derived for temperature and pressure in the discharge channel, channel widening rate and the density at the shock wave front. Expressions are also derived for radial and tangential stresses σ_r and σ_φ respectively due to shock waves, which are correlated with the discharge circuit parameters. The authors observe that if σ_r and σ_φ are known at any point in space, it is possible to estimate the degree of destruction to solids.

Val'dner, O. A. Progress in developing linear electron accelerators at Moscow Engineering Physics Institute. IVUZ Fiz, no. 12, 1972, 14-22.

This article gives a general review of progress in developing linear electron accelerators at Moscow Engineering Physics Institute. The main uses of the accelerators are: 1) to study propagation and diffraction of e-m waves in periodic waveguide structures; 2) to study the interaction of charged particle beams with e-m fields; and 3) for design studies in constructing linear accelerators as the main ionizing sources for laboratory radiation devices.

Development of the accelerators generally was done in the following sequence: 1) The particle dynamics were investigated in the acceleration process for working out schemes in engineering calculations; 2) Relationships were established between the phase velocity and voltage of accelerating waves and the geometrical dimensions of the iris waveguide. The most difficult part in this area is to obtain quantitative relationships with sufficiently high accuracy; 3) Stability conditions were studied for an h-f waveguide iris generator forming a complex high-frequency system in the linear accelerator; 4) Technological problems on manufacturing of accelerator subassemblies and structural elements based on designs of the prototype series were worked out; 5) The accuracy of the obtained results was verified on experimental models (at low as well as high power levels) of accelerating waveguides.

Descriptions are given of the application of linear accelerators in various field such as medicine, food industry, etc., and their advantages over other types of accelerators (cyclotron, betatron) are briefly outlined. Figures 1 and 2 show photographs of two installed linear accelerators.

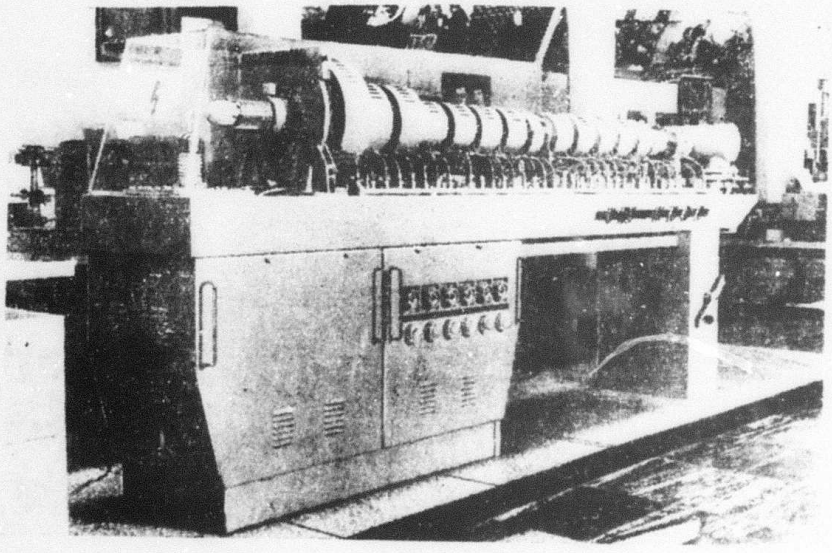

Fig. 1. U-27 high power accelerator with beam power = 5 kw, operating from a 10-centimeter magnetron.

Fig. 2. Compact U-30 accelerator with control panel, operating from 3 cm magnetron.

B. Recent Selections

Abu-Asali, Ye., B. A. Al'terkop, and A. A. Rukhadze. Nonlinear oscillations of an unstable plasma. ZhETF, v. 64, no. 5, 1973, 1621-1626.

Aleksandrov, A. F., V. V. Zosimov, A. A. Rukhadze, V. I. Savoskin and I. B. Timofeyev. Investigating equilibrium and stability of pinched discharges in an optically dense plasma. ZhETF, v. 64, no. 5, 1973, 1568-1580.

Bomko, V. A., A. P. Klyucharev, and B. I. Rudyak. Izucheniye kharakteristik lineynogo uskoritelya, rabotayushchego v rezhime transformirovannogo tipa volny. (Studying the characteristics of a linear accelerator, operating in wave transformation regime). Khar'kov, 1972, 17 p. (KL Dop vyp, 4/73, no. 7826).

Datlov, J., L. Kryska, and V. N. Budnikov. Microwave heating of electrons of a dense plasma column at frequencies higher than electron cyclotron frequency. Part 1. Czech. J. Phys., v. 23, 1973, 436-442.

Demutskiy, V. P., and R. V. Polovin. Influence of temperature effects and particle capture by plasma waves on dispersion properties of nonlinear waves. UFZh, no. 5, 1973, 819-823.

Efendiyev, A. Z., and N. A. Akopdzhanov. Studying the effect of a transverse magnetic field on breakdown formation time. IVUZ Fiz, no. 5, 1973, 69-74.

Fursey, G. N., N. V. Yegorov, S. P. Manokhin, and M. K. El'Nimr. Relaxation effects during field emission from silicon. FTT, no. 5, 1973, 1360-1363.

Grigoryeva, L. I., B. I. Smerdov, S. A. Sapogov, and V. V. Chechkin. Observing the growth of a high-frequency field in the resonance layer of an inhomogeneous plasma. ZhETF P, v. 17, no. 10, 1973, 541-544.

Krasovitskiy, V. B. A nonlinear theory of beam-plasma instability. ZhETF, v. 64, no. 5, 1973, 1597-1605.

Levin, V. M. Svin'in, A. Gal'chuk, A. Stepanov, A. Solnyshkov, and G. Tarvid. Accelerators for the national economy. VDNKh, no. 9, 1973, 34-35.

Strashko, A. P., Ye. I. Lutsenko, N. A. Levanyuk, V. G. Korzh, and V. V. Kuz'menko. Excitation of an open resonator by initial emission of a heavy-current discharge. UFZh, no. 5, 1973, 866-868.

Vakhrushin, Yu. P., and I. M. Matora. Linear induction accelerators - new powerful relativistic electron beam generators. UFN, v. 110, no. 1, 1973, 117-137.

Vekhov, A. A., F. A. Nikolayev, and V. B. Rozanov. Investigating heavy-current pulsed discharge emission in metal vapors in the vacuum UV region. ZhETF P, v. 17, no. 10, 1973, 570-573.

Vlasenko, S. M., L. N. Kazanskiy, A. A. Kolomenskiy, et al. Elektronnyy sil'notochnyy uskoritel' "IMPUL'S". (A heavy-current electron accelerator - IMPUL'S). Moskva, 1972, 38 p. (KL Dop vyp, 4/73, no. 7946)

5. Material Science

A. Abstracts

Al'tshuler, L. V., Ye. A. Dynin, and V. A. Svidinskiy. Gas dynamic methods of low temperature compression of solid hydrogen. ZhETF P, v. 17, no. 1, 1973, 20-22.

Different dynamic methods of molecular hydrogen metallization by low-temperature compression are discussed. A cylindrical system of noninstantaneous compression loading generates pressures over 600 kbar at a low temperature and under conditions of total isentropicity. In the system described (Fig. 1) the first step of the process consists of isentropic

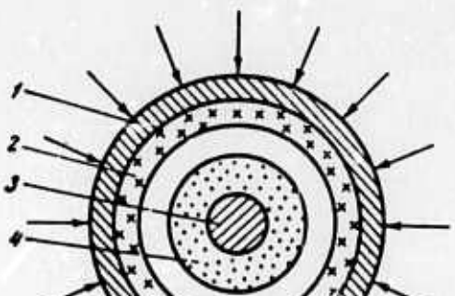

Fig. 1. Cylindrical system of low-temperature compression: 1- metallic shell accelerated by explosion products; 2- light-weight layer; 3- cooling copper rod; 4- solid hydrogen layer at liquid He temperature.

compression by gas stream dispersion towards the center. Pressure subsequently increases due to convergence of the cylindrical shell. Quasi-isentropic compression of the layer of investigated material is achieved by shock wave propagation through the layer; the final pressure in the layer is the result of a multiple circulation of shock waves. At

equal pressures, the entropy increment in such a system is estimated to decrease by a factor not less than $4/(3m^2+1)$, where m is the ratio of dynamic rigidities of the cylindrical element to shock compression systems.

A numerical solution to the problem of solid hydrogen compression between two copper plates converging at a 2 km/sec velocity gave 8, 32, 64, and 125 kbar for the amplitudes of the consecutive shock waves in hydrogen and 1,180 kbar for the end-pressure. At the end of compression, the fraction of thermal pressure does not exceed 4% of the end pressure. A multi-layer system, with a successively and rapidly decreasing amplitude of shock waves, would be even closer to an isentropic process. The methods discussed are cited as simpler and more convenient for electric conductivity measurement than magnetic compression. The latter advantage is particularly important in determination of hydrogen metallization pressure.

Vereshchagin, L. F., Ye. N. Yakovlev, G. N. Stepanov, K. Kh. Bibayev, and B. V. Vinogradov. Pressure of 2.5 megabar between anvils made of black diamond. ZhTF, no. 12, 1972, 2621-2622.

Results of testing modified Bridgman anvils are given. The principal modification was the substitution of black diamond (carbonado) type material for carboloy or similar tungsten carbide base materials used in Bridgman anvils. Carbonado-type diamonds were synthesized in 1969 by Vereshchagin et al. (DAN SSSR, v. 185, no. 3, 1969, 555). The

experimental apparatus consisted of a plane and a cone-shaped anvil supported by a steel mandrel (Fig. 1). The vertex angle of the cone is

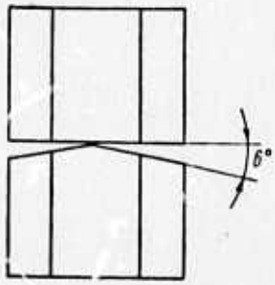

Fig. 1. Experimental anvils made of carbonado.

168°, with the vertex somewhat blunted. Force F exerted on the area S of the plane diamond surface was measured. The area S was determined from the cone imprint on a film deposited on the plane anvil. The sharpest imprint was obtained on a nitrocellulose lacquer film. The area-averaged contact stress was calculated as $P = F/S$. The tabulated test data show that a 2.5×10^6 kg/cm^2 maximum P was achieved for the first time; the maximum P obtained previously with the Bridgman anvils was 5×10^5 kg/cm^2. Achievement of pressures up to 2.5 Mbar in static experiments thus offers an enlarged means for physical investigations and synthesis of new materials.

Gorskiy, V. V., and Yu. V. Polezhayev.
Surface heat and mass transfer of glass-graphite materials in a high temperature gas flow. MZhiG, no. 6, 1972, 71-87.

The theory on ablation of glass-graphite-reinforced phenolic resins in a hypersonic air flow is expanded to the range of high ablation rates, designated as G_w. In this case, the effect of chemical composition of the

gaseous boundary layer on heat- and mass-transfer becomes significant. Therefore the summary thermal effect ΔQ_Σ of physicochemical conversions and the summary G_w are analyzed with respect to interaction of the vaporized glass molecules (SiO_2) with the combustion products (CO_2 and CO) of coke, which is the secondary product of the resin thermal decomposition.

The quasistationary ablation regime is described in terms of glass vaporization by means of a nonequilibrium sublimation equation. A thermodynamic analysis of chemical reactions in the gaseous boundary layer led to identification of three different SiO_2 vaporization regimes which correspond to different gas compositions of the boundary layer. In the first ablation stage, at a relatively low G_w, SiO_2, SiO and CO_2 are the main components of the gaseous phase. At a moderate G_w, only SiO, CO_2 and CO are considered. At high G_w gas phase composition is reduced to SiO, CO, and Si. The approximate critical ablation rates $G_w'^{(1)}$ and $G_w'^{(2)}$ at the first-to-second and second-to-third regime transitions are formulated and their limiting values for $\xi = p_{co}/p_{co2} = 0$ and 1 are evaluated for laminar and turbulent flows. The characteristic $G_w^{(1)}$ and $G_w^{(2)}$ values are indicated in Fig. 1. The tabulated data show only a weak dependence of

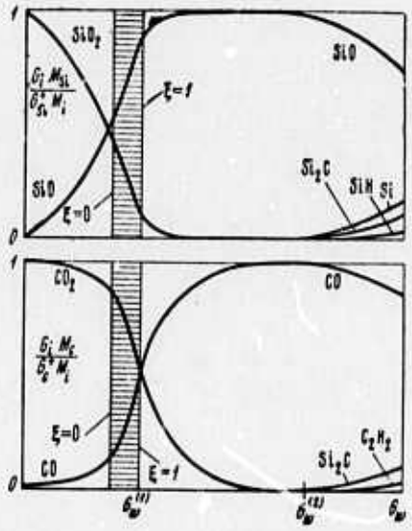

Fig. 1. Relative composition of ablation products vs. G_w.

the mean $G'^{(1)}_{w,\,m}$ but a very strong dependence of $G'^{(2)}_{w}$ on the flow regime. The surface temperature T_w dependence of G_w (Fig. 2) is shown to be

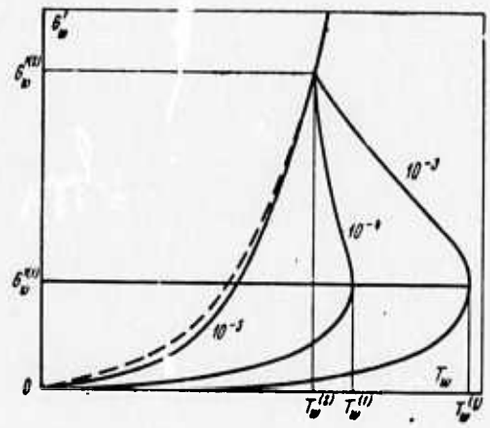

Fig. 2. Ablation rate G'_w versus surface temperature T_w. Figures on the curves indicate the parameter $p_e/(\alpha/Cp)_o$, where p_e is the pressure on the outer boundary of the gas layer and $(\alpha/Cp)_o$ is the coefficient of heat transfer at the nondestructive surface.

indeterminate at $p_e/(\alpha/Cp)_o > 0.5 \times 10^4$ sec., i.e., in the second ablation stage, when SiO_2 vaporization is intensified due to the presence of free C in the surface layer. The thermal effect ΔQ_Σ is formulated as the sum of heat quantities absorbed by the material components conversion into a reference group of compounds and subsequent formation of the components in excess over the case of a nondestructive surface.

Typical G'_w (ΔQ_Σ) plots show that at a low G'_∞, C burnup leads to a significant decrease in ΔQ_Σ in relation to SiO_2 glass. In the second ablation stage, ΔQ_Σ increases due to a decrease in p_{CO_2} w and pH_2O, w and termination of SiO_2 dissociation. In the third regime, ΔQ_Σ increases even more due to partial dissociation of SiO and minimum C oxidation. The ΔQ_Σ increase in the case of SiO, CO, and C_2H_2 components in the gas phase is due to the excess C conversion to C_2H_2 which is less effective than C to CO conversion. Numerical calculations of the main ablation characteristics of the glass-graphite material and fused quartz are illustrated for supersonic air flow around a specimen with 0.015 m radius of curvature.

Suris, A. L. Liquid evaporation in high temperature gas flow. I-FZh, v. 24, no. 1, 1973, 161-162.

This is a theoretical study on evaporation of liquid solutions in high-temperature gas flow. A single drop evaporation, with allowance for time-dependence of solution density γ_p, is described by the equation

$$\frac{dg}{d\tau} = -\frac{(P+Fg)}{(u+hg)\beta}\left(g+\frac{\gamma_{ж}}{\gamma_p}-1\right)^{1/3} \quad (1),$$

where $\gamma_{ж}$ is the solvent density and g is the ratio of weight flow rates in the random and initial cross-sections of the apparatus. Expression for u, β, P, F, and h are given. Solution of (1) with the initial condition g(0) = 1 is formulated. A formula for the gas flow cooling rate is derived by differentiating the expression for temperature T of the vapor-gas mixture, with allowance for solution of Eq. (1).

Zverev, A. F., A. I. Kovalev, and A. V. Logunov. High-temperature thermophysical properties of nickel. I-FZh, v. 24, no. 1, 1973, 164.

Thermal conductivity λ, volume resistivity ρ, Lorenz number L, total emissivity ϵ, and spectral emissivity ϵ_λ (λ = 0.65 μ) of pure nickel were determined in the 20 to 1,400° C range. Measurements in the 1000-1400° C range were done by electrical heating of nickel rod specimens with parabolic temperature distribution in the central part. Reliability of the data was confirmed by convergence of λ values obtained by two different methods with different apparatus. The tabulated data give smoothed

values of ρ in the 20-1400° C range, λ and L in the 200-1400° C range and ϵ and ϵ_λ in the 1,000-1400° C range. The maximum error of measurement was 5.5 and 9% for λ, 1.5 and 2% for ρ in the 200-900° C and 1000-1400° C ranges, respectively, and 10 and 11% for ϵ and ϵ_λ, respectively.

Kul'gavchuk, V. M., and A. A. Zakrevskiy. Method of determining mechanical properties of materials at high temperatures from heating by a pulsed electric current. IN: Sbornik. Svoystva materialov pri povyshennoy temperature i apparatura dlya ikh ispytaniya. Moskva, 1972, 45-55. (RZhMekh, 1/73, no. 1V1046) (Translation).

Mechanical characteristics of materials at a high temperature were studied by applying short electric pulses to excite longitudinal oscillations in a rod of the material and measuring its oscillation parameters. A schematic of the experimental apparatus is given. The experimental dynamic elasticity modulus data at different rod temperatures are given for 1Kh18N9T steel, titanium, tantalum, and graphite. In addition, stresses generated by rapid heating and coefficient of thermal expansion were determined for a graphite rod.

Babadzhanov, P. B., and V. S. Getman. Ablation of large meteor particles. DAN TadSSR, v. 15, no. 11, 1972, 19-22.

Changes in the ratio Λ/Q of the heat transfer coefficient to the specific energy of ablation during the flight of a meteor were studied to

clarify the mechanism of meteoroid ablation in the atmosphere. The Λ/Q ratio was calculated for 346 points on the trajectory of 140 meteors which were photographically recorded in Dushanbe during 1960-1966. Calculations were based on theoretical physics of meteors, with the necessary data partly provided by direct observations and partly taken from literature. The Λ/Q versus altitude H plots thus calculated for different meteors (Figs. 1, 2 and 3) show that Λ/Q decreases with

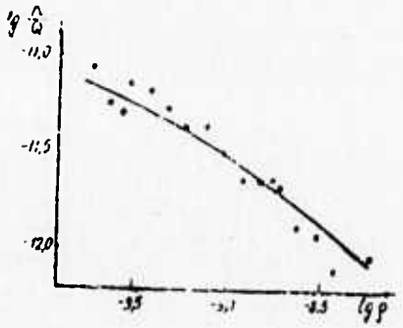

Fig. 1

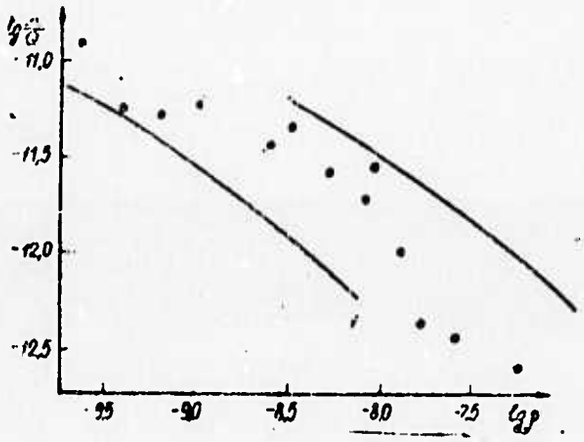

Fig. 2

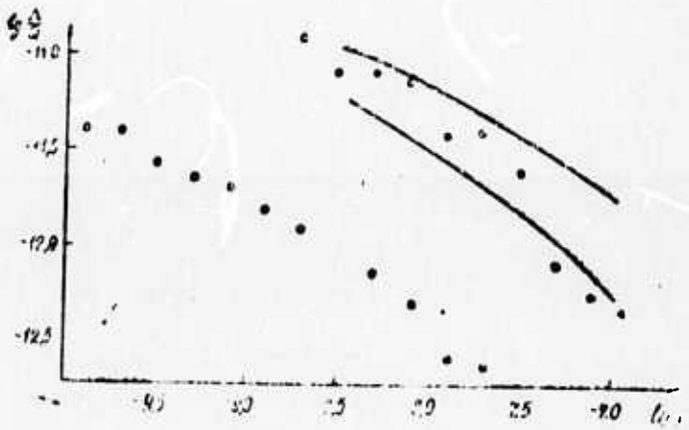

Fig. 3

The plots of averaged log Λ/Q versus log ρ, where ρ is the atmospheric density, for: Fig. 1- Perseids with velocity V_{av} = 60 km/sec; fig. 2- sporadic meteors with V_{av} = 30-60 km/sec; fig. 3- upper data-sporadic meteors with V_{av} = 20-30 km/sec, lower data- Taurids with V_{av} = 32 km/sec. Solid lines are theoretical curves.

increase in ρ. Theoretical curves were calculated on assumptions of the predominant vaporization mechanism of ablation and the barrier effect of the vaporized molecules, which is responsible for a decrease in Λ. Figures 1-3 show that, despite the assumption of a constant Q, the theoretical curves agree quite well with the experimental data. It is concluded that basically the rate of ablation of large, nearly spherical meteor particles is determined by Λ. Calculations indicate that, in agreement with the vaporization mechanism, Λ fluctuates within a range of 0.02 to 1 at H = 70-110 km. The abnormal H and Λ/Q magnitude observed for Taurids may be explained by the extremely high vaporization rate of meteoroids in the Taurid shower.

Lebedev, P. D., D. P. Lebedev and Ye. K. Zlobin. Heat-shielding properties of anisotropic insulation. I-FZh. v. 24, no. 1, 1973, 84-90.

In a heat-shield analysis it is stressed that experimental results obtained by the authors (I-FZh, v. 21, no. 15, 1971) for screen-vacuum insulation show the anisotropy in heat conduction in both longitudinal and transversal directions of its layers, and that in estimating the heat-shielding properties, this anisotropy must be taken into account. The case of stationary heat conduction through a plane layer of an anisotropic screen-vacuum insulation system in the presence of heat exchange at its faces is then analyzed. The calculation scheme for heat exchange shown in Fig. 1 represents the cross-section of a plane infinite layer of an anisotropic

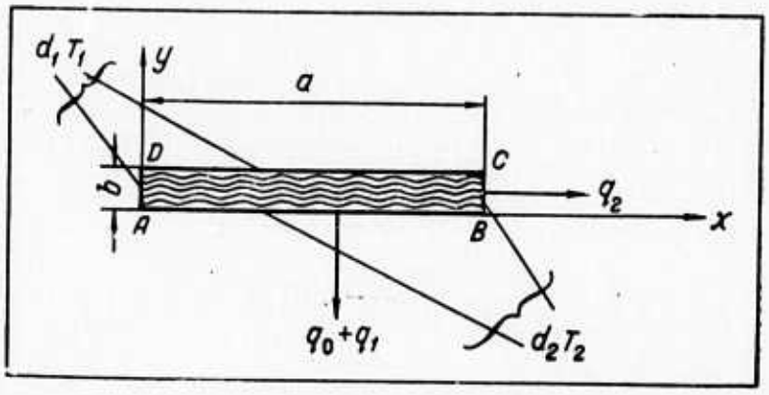

Fig. 1. Heat transfer model for layered insulation.

insulation. Heat exchange at its faces is defined by boundary conditions of the third kind. The corresponding heat conduction equation with boundary conditions are written and the solution of this third boundary-value problem, i.e. the harmonic function $f(\xi, \eta)$, is sought in the form of infinite trigonometric sums with unknown coefficients. The unknown coefficients are obtained from the boundary conditions using expansions in eigenfunctions of the Sturm-Liouville boundary value problem. Expressions for the total heat flux Q_o on a unit width strip for a uniform temperature field, additional heat flux Q_1 stipulated by the heat exchange on the faces and total heat flux Q_2 on the unit width strip of the face $x = a$, are derived. Dependences of heat exchange through the insulation on the heat parameters are analysed on the basis of the derived expressions and represented in graphs. The results obtained verify that additional heat fluxes through the faces of anisotropic insulation can decrease by several times the effectiveness of its application.

Pankratov, B. M., O. M. Alifanov, A. I. Ivanov and A. D. Markin. Study of heat-shielding materials in a nonstationary regime. I-FZh, v. 24, no. 1, 1973, 75-83.

Theoretical and experimental methods for analysing heat-shield materials are investigated. Stationary heating and ablation of heat-proof coatings of bodies in a high-temperature gas flow are first considered. The nonstationary boundary layer equation was solved by the finite difference method using implicit computation. Calculations made for a wide range of flow parameters and trajectory characteristics indicate that mass forces and nonstationary conditions of braking temperature have the most significant effect on the ablation of material and temperature profiles. Calculation results for one point of a trajectory are presented in two graphs. In the first, the effect of the nonstationary conditions for gas flow on the temperature profile of a heated body is presented. The second graph shows the variation in maximum temperature profile deviations along the trajectory.

In the second section, the ablation and heating of coking heat-proof materials was analyzed using a mathematical model of the process in the form of a system of partial differential equations, constructed under certain simplifying conditions imposed upon the physico-chemical processes taking place in the coking heat-proof materials. Numerical solution of this system makes it possible to obtain the non-stationary temperature field in the material. For the experimental study of transient heating and of heat-proof coatings it is necessary to determine boundary conditions on the surface of a body. The only way to determine the thermal boundary conditions under nonstationary heat exchange is to solve the inverse heat conduction problem.

In the third part of the article a numerical method for solving the nonlinear inverse heat conduction problem in a homogeneous plate is proposed. For the solution of this problem the implicit finite-difference approximation scheme of a quasilinear heat-conduction equation must be used.

Apshteyn, E. Z. Solution to equations for liquid films and emergence of a maximum temperature in a glassy solid from high power external radiation. DAN SSSR, v. 208, no. 1, 1973, 60-62.

The author notes that failure of glassy coatings in a high-temperature gas flow is a function of the ability of the material to transmit the radiation. The solution of liquid film equations is analysed for the case when the external radiation penetrating the body from the shock layer is substantially higher than the radiation in the coating material. A system of dimensionless equations describing the flow of a liquid film in the vicinity of a critical point of a glassy body, taking radiation into account, is used; these were derived earlier by the author (Mekh. zhidkosti i gaza, no. 1, 1970). By neglecting the internal radiation of the body, and after certain transformations, the system of equations takes the form

$$\varphi'' = -(\tau_0 + \eta)\exp(-1/\theta),$$
$$\theta' = h - (\theta - \theta_\tau)d, \quad h' = -\varkappa j, \quad j' = -\varkappa h. \tag{1}$$

The following boundary conditions are used:

$$\varphi'(\infty) = 0, \quad \varphi(\infty) = d, \quad \theta(0) = \theta_0,$$
$$h(0) = h_{\text{пл}}(1 - r), \quad h(\infty) = 0. \tag{2}$$

Here φ = stream function for liquid film; θ = dimensionless temperature; h = dimensionless flow; j- radiation energy density, $x = \sqrt{x_A(X_A + X_S)}$; X_A, X_S - dimensionless absorption and scattering coefficients respectively; τ_o - dimensionless friction of the coating surface, η - the coordinate in the direction of a body, d = dimensionless complete ablation; θ_o = temperature on the surface of the body, θ_T = temperature inside the body; h_{nd} = radiation flow from the shock layer; and r = effective reflection coefficient. The last two equations of set (1) are radiation transfer equations for the absorption and scattering media. By approximating θ in the form $1/\theta \approx 1/\theta_o + m_1\eta + m_2\eta^2$, Eq. (1) can be integrated. The final analytical solution is written in the form

$$d = \alpha_1 + \{\exp(z^2)[1 - \Phi(z)](1 + 2z^2) - 2z/\sqrt{\pi} + 2\tau_0\sqrt{m_2}(1/\sqrt{\pi} - z\exp(z^2)[1 - \Phi(z)])\}\exp(-1/\theta_0)\sqrt{\pi}/4m^2,$$
$$\left(z = m_1/(2\sqrt{m_2}),\quad \Phi(z) = \frac{2}{\sqrt{\pi}}\int_0^z \exp(-t^2)\,dt\right); \qquad (3)$$

where α_1 is dimensionless ablation in the gas phase. The solution is obtained for a homogeneous material with dimensionless temperature at infinity equal to θ_T. In the case of a composite material, the solution has the same form except that instead of θ_T, the value θ_T* applies, which is determined from the boundary conditions. Conditions for the maximum temperature inside the coating are also derived.

Khrabrov, V. I. Magnetic reversal hysteresis of orthoferrite crystals. FTT, v. 15, no. 1, 1973, 148-154.

Domain structure rearrangements in magnetic fields to 300 oe were studied in 2-3 mm single crystals of $SmFeO_3$ and $YFeO_3$. The powder

diagram method was used to reveal location, dimensional variations, and stability of the remanent domain structures (RDS) as functions of the applied magnetic field H_m. Demagnetized crystals exhibited a multi-domain structure. In an applied field H_m, the RDS in the form of small more or less stable regions of magnetic reversal were observed at crystal defects. Magnetic reversal begins in a field H_S, first by discontinuous growth of one RDS, followed by a smooth shift of domain boundaries, when the field is decreased. Some RDS disappear progressively and irreversibly when H_m is increased. The more stable RDS remained, hence the field H_S shifted toward even more negative values until magnetization of the entire crystal was reversed in one step. RDS over 10μ in size remained until the H_m fields attained ~100-150 oe.

The observed phenomena and the fact that the RDS boundaries are irregular indicate that RDS stability depends on the strength of domain boundary attachment to crystal defects. The RDS behavior and the $H_S(H_m)$ dependence are discussed in terms of the critical field H_o. Local H_o values which are necessary for irreversible shift of domain boundaries are different in real crystals, in which defects are not always uniformly distributed. Consequently the RDS must disappear selectively, depending on the H_o value of each. This in turn hinders the magnetic reversal process and leads to discontinuity of $H_S(H_m)$ dependence. Analysis of the $H_S(H_m)$ curves of orthoferrites shows that the dependence in the form

$$H_s = 2NI_s - H_m. \qquad (1),$$

where N is the demagnitization factor and I_s is saturation magnetization, is observed at initial H_m only. The $|H_S|$ increase slows down when H_m is increased. Since $(NI_s)_{max} = 100$ oe in orthoferrites, the critical fields H_o^+ and H_o^- corresponding to disappearance and growth of an RDS must be asymmetric. The crystal size D dependence of H_o may result

from nonuniform defect distribution. In the case of defects localized within the crystal bulk $H_o \sim D^{-2}$. In the case of defects localized in a surface layer, $H_o \sim D^{-1}$, which dependence explains the experimentally observed increase in coercive force of ferromagnetics with decrease in their D. The cited cases of H_o (D) dependence may be the cause of high local H_o values near the crystal edges, protrusions on the crystal faces, etc., i.e., in the regions of small local D. Thus additional prerequisites exist in the cited regions for stable RDS formation during magnetization.

Grigor'yev, V. N., B. N. Yesel'son, V. A. Mikheyev, and Yu. Ye. Shul'man. Quantum diffusion of He^3 impurities in solid He^4. ZhETF P, v. 17, no. 1, 1973, 25-28.

The diffusion coefficient D of He^3 impurity in He^4 at 0.4-1.4°K was determined experimentally to establish the correlation between this characteristic of He^3 behavior and the quantum nature of solid He. A spin echo method was used in conjunction with an NMR apparatus described earlier by the authors (ZhETF, v. 64, no. 2, 1973). The experimental temperature dependence of D (Fig. 1) shows that, in contrast to high-temperature data, collisions between the impurity quasiparticles have a predominant effect on diffusion processes at T < 1.1° K. The effect of quasiparticles is described by an interpolation formula in terms of relaxation times of quasiparticle scattering on each other and on phonons. In the plateau region of the Fig. 1 curves, the scattering on phonons can be neglected, hence the interpolation formula can be given in the simplified form

$$D \sim \frac{J_{34} a^2}{\hbar x} \qquad (1)$$

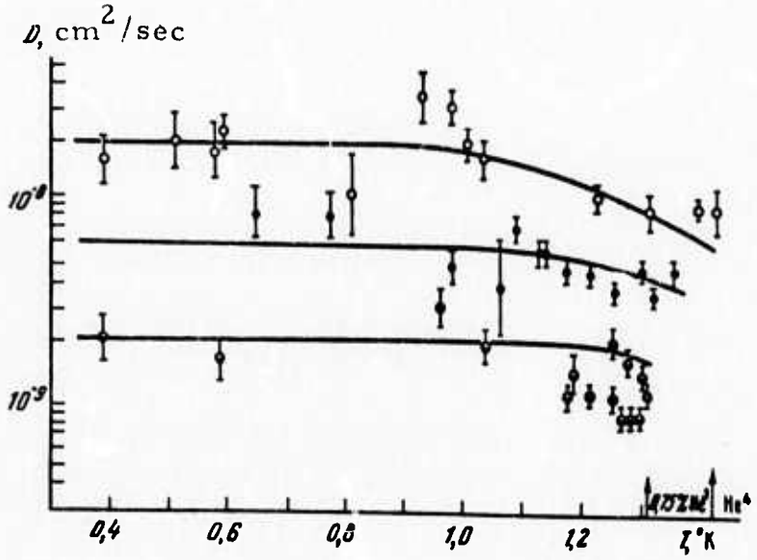

Fig. 1. He^3 diffusion coefficient vs. temperature at 0.092 (Φ), and 0.75% (Φ) He^3 concentrations. Solid curves correspond to the equation $D^{-1} = 6.25 \times 10^{10} X + 4.6 \times 10^6 T^9$. Arrows on the T axis identify the b.c.c-h.c.p. transition boundaries.

where J_{34} is the exchange integral or energy gap between quasiparticles, a is the distance between the two nearest neighbors, and x is He^3 concentration. The rectilinear experimental x dependence of D at $T < 1.2^\circ$ K is described, in agreement with (1), by the equation $D = 1.6 \times 10^{-11} x^{-1}$ cm^2/sec. The order of magnitude of J_{34} calculated from (1) coincided with that obtained independently by treatment of the experimental data according to the complete interpolation formula for D, with allowance for quasiparticle scattering on phonons. This coincidence, and the experimental x dependence of D, confirm the quantum nature of He^3 diffusion in the h.c.p. phase of solid He. D measurements in the b.c.c. phase also confirm earlier authors' data on the wide difference in D between the b.c.c. and h.c.p. phases (ZhETF, v. 64, no. 2, 1973). The small increase detected in D with a decrease in x of He^3 is tentatively attributed to the existence of quantum diffusion.

Aleshin, V. I., and Ye. V. Kuvshinskiy. Retarding of cracks in PMMA. FTT, no. 1, 1973, 266-268.

Results are given of microscopic observations of crack propagation in PMMA (plexiglas) plates under different shear loads. Load magnitude was selected such that the crack growth rate V was below a limiting value V_{lim}. Initially, the log V versus log t plots at a specific fracture work W in the 50-96.4 j/m^2 range are spread over two orders of magnitude range of V, and then converge to a limit V. Simultaneously with the arrest of the shear crack growth, growth is observed of the main "check" in front of the shear crack and secondary "checks" parallel to it. Width of the main "check", size and number of the secondary "checks", and the "checking" area increase with increased. W. Hence convergence of the log V-log t curves at $V < V_{lim}$ cannot be interpreted as the end of the load dependence of the fracturing process, since the material volume involved in the process continues to increase with increase in W. Deceleration of the crack propagation is explained by growth of "checks" at a rate higher than their rate of conversion to the shear crack. A similar crack deceleration process was observed earlier in nonpolymeric materials (crystals), e.g., on account of dislocations.

Guz', I. S., V. M. Finkel', and G. A. Chervov. Results from a study of Rayleigh pulse interaction with edge cracks. ZhPMTF, no. 6, 1972, 145-151.

Rayleigh pulse interaction with stationary edge cracks was studied by the dynamic photoelasticity technique in plexiglass specimens of three different geometrics. The purpose was to investigate crack propagation under transient loading (microcharge explosion) which generates Rayleigh waves on the free surfaces and edges of a crack. Various specimen geometries were selected to obtain different crack orientation versus

wave propagation direction. Thus Rayleigh wave propagation at 1200 m/sec towards the crack tip was recorded on one of its edges in directions along the crack or normal to the half-space, and on both edges simultaneously. Theoretical distribution of the maximum tangential stress for a Rayleigh pulse and Heaviside load was calculated and the dynamic stress field was plotted. Comparison between the theoretical stress field and the field calculated from the experimental data for the real load shows that the recorded stress distribution is typical for the Rayleigh pulse. It is thus shown that Rayleigh waves are one of the energy supply sources to the crack tip. This conclusion helps explain the fact that the critical rate of fracture does not exceed the Rayleigh wave propagation rate.

Korsunskaya, I. A., D. S. Kamenetskaya, and I. L. Aptekar'. Properties of liquid carbon in relation to melting characteristics of graphite and diamond at high pressures. FMiM, v. 34, no. 5, 1972, 942-949.

Phase equilibria for carbon at high pressures are analyzed theoretically, using either a formalistic approach with allowance for different compressibility β of the liquid and solid phases, or Kittel's two-level model of liquid carbon. The latter is equivalent to the pseudobinary solutions model and is based on assumption of different energy levels in liquid under low and high pressures. The graphite melting curves calculated for p up to 130 kbar by both cited methods practically coincide with the experimental curve of Bundy (J. Chem. Phys, v. 38, 1963, 618). The diamond melting curve calculated for p to 200 kbar on the basis of Kittel's model closely follows the experimental curve, in contrast to the curve calculated with allowance for β of the C phases.

It is concluded that the pseudobinary model of liquid C fits the experimental data better than the formalistic approach. The pseudobinary model explains many experimental facts associated with the effect of high pressure on liquid C. High pressure ($p > 110$ kbar) causes metallization of the liquid, which corresponds to the lower energy level. It follows from this model that $\beta(P)$ of liquid carbon is complex, with a maximum coinciding with the peak of the graphite melting curve.

Mirsalimov, V. M. Effect of plastic deformation on crack propagation. Problemy prochnosti, no. 1, 1973, 63-65.

Brittle crack propagation is analyzed to determine the effect of plastic deformation on crack propagation rate in an elastoplastic body. The solution to the cited problem is based on the Broberg formula for an ideal elastic body with allowance for inertial terms in the first approximation only. A more rigorous equation for crack propagation rate dy/dx in an ideally elastic body was obtained by substituting an exact dynamic condition on the stress field around a growing crack, in place of the Griffith-Irwin condition. The corresponding formula for dy/dx in the elastoplastic body was derived from the Broberg formula by imposing a supplemental condition on the stress field around a dynamic crack. Energy γ_* of formation of a new unit surface was assumed to be independent of the crack length y. The dy/dx versus y plots calculated from both formulas are practically identical. The effect of plasticity is shown to give a smoother rise in dy/dx and a slower crack branching rate. In practice, however, the effects of γ_* unaccounted for in the study may be more significant.

Kartashov, E. M. Determining kinetics of crack propagation in brittle solids from fracturing in a surface-active medium. FKhMM, no. 6, 1972, 38-44.

Brittle fracture of solids, e.g. inorganic glass, in a surface-active medium, such as water, is examined theoretically. The study is based on the fluctuation theory of strength, with allowance for surface diffusion of the medium molecules towards the tip of a pre-existing microcrack. Crack propagation is analyzed from the edge of a 1 cm wide thin band subjected to uniaxial tension. The crack propagates owing to thermal fluctuations and tensile stress, by way of successive breaking of inter-atomic bonds ahead of the growing crack. Analytical formulas are derived for the mean crack propagation rate v (t) as a function of relative concentration $C_F(t)/CO$ of the medium at the tip; the crack length l(t); and lifetime τ, i.e. time in which l of a crack propagating at the rate V(t) attains critical value l_k. The formula for τ accounts for velocity distribution of medium molecules. An example of calculation of τ, V, and l versus t and stress σ is given for inorganic glass in a moist atmosphere. The theoretical log τ(sec) versus σ plot agrees with the experiment. The derived formulas can be used to study time dependence of strength of metals, plastics, polymer fibers, and other materials.

New polymeric semiconductors. Soviet Science Review, September 1972, 263.

New polymer-based semiconductor devices, such as tensile and compressive strain gauges and thermoresistors, have been developed at a lower cost and for a much wider operational range than

the conventional devices. The polymeric materials for the new devices were selected from more than 200 semiconducting polymers synthesized by chemists and electronic engineers at the Moscow Institute of the Petrochemical and Gas Industry under the direction of Professor J. Paushkin. The strain gauge described has a directional sensitivity of 200-250, is reliable to 400° C, insensitive to radiation, and chemically inert. It can be attached like a plaster onto the surface to be monitored and even can be pressed into a grooved surface. Its production cost is 1% of that of a comparable germanium gauge. Polymer thermoresistors can be used at temperatures in the -269 to +500° C range to stabilize voltages up to 100 V. They are also suitable for IR and UHF radiation measurements. About half a million of these units were produced in a few days under lab conditions, which is equivalent to the annual output of a medium size plant for silicon thermoresistors.

Kandyba, V. V., V. Ye. Finkel'shteyn, G. L. Iosel'son, and G. P. Pushkarev. Obtaining and measuring high temperatures. IN: Sbornik. Ukr. resp. nauch-tekhn. konf. posvyashch. 50-letiyu metrol. sluzhby USSR, 1972. Kharkov, 1972, 235-237. (RZh Metrolog, 2/73, no. 2.32.1011)

Specifications are briefly given for a line of standard pyrometers developed at KhGNIIM for laboratory use. The instruments described range from photoelectric spectropyrometers for the 3000-4000° C range, up to avalanche-transit diode radiators for the 50,000° C range.

Shevchenko, A. V., L. M. Lopato, K. G. Akinin, A. Ye. Kushchevskiy, and S. T. Baskakov. High-temperature material. Author's certificate, USSR, no. 364577, published March 27, 1971.

An Author's Certificate is awarded for a high-temperature material used for heat insulation comprised of hafnium dioxide and yttrium oxide. It has a high heat-resistance and great adherence to a substrate. The composition of the material is as follows:

	Mol. %
Hafnium dioxide	85-90
Yttrium oxide	10-15

Arakelyan, G. Long-lasting, economical (new refractory materials). Pravda, 14 March 1973, p. 2.

New highly refractory materials have been developed at the Yerevan Institute for Stone and Silicates. Based on clays of the Tumanyanovsk region, the materials feature unusually high resistance to heat and acids.

B. Recent Selections

i. Crack Propagation

Bobrinskiy, A. P.,and A. M. Vasnin. Breaking strength characteristics of a zirconium alloy with 2.5% niobium. IN: Sbornik. Konstruktivn. prochnosti staley i splavov i metody yeye otsenki. Moskva, 1972, 171-175. (RZh Metallurgiya, 5/73, no. 5I440)

Kolomytsev, P. T., Ye. G. Ivanov, P. D. Kalafirov, and S. A. Strekopytov. Device for investigating plasticity of diffusion layers deposited on heat resistant alloys. ZL, no. 5, 1973, 618-619.

Neshpor, G. S., P. G. Miklyayev, V. G. Kudryashov and A. G. Rakhshtadt. Determining failure viscosity of structural materials. ZL, no. 5, 1973, 595-598.

Vladimirov, V. I., and Sh. Kh. Khannanov. Origin of cracks in opposed dislocation clusters. Problemy prochnosti, no. 5, 1973, 62-66.

Vylezhnev, V. P., V. I. Sarrak, and R. I. Entin. Effect of steel structures on crack propagation resistance. IN: Sbornik. Probl. metalloved i fiz. met., no. 1, Moskva, Metallurgiya, 1972, 190-198. (RZh Metallurgiya, 5/73, no. 5I448)

ii. High Pressure Research

Al'tshuler, L. V., M. A. Podurets, G. V. Simakov, and R. F. Trunin. Highly-compacted forms of fluorite and rutile. FTT, no. 5, 1973, 1436-1440.

Amirkhanov, Kh. I., Ya. B. Magomeddov, and S. N. Emirov. Effect of hydrostatic pressure on thermal conductivity of tellurium. FTT, no. 5, 1973, 1512-1515.

Banik, I., and J. Zamecnik. Dependence of V-A characteristics of amorphous semiconducting $Ge_{15}Te_{81}S_2As_2$ on hydrostatic pressure. Czech. J. phys., v. 23, 1973, 479-483.

Baskakov, V. Ya., and V. K. Semenchenko. Study of cholesteryl valerate under pressure. ZhETF P, v. 17, no. 10, 1973, 580-583.

Brazhnev, V. V., Z. M. Gelunova, and L. I. Gerasimenko. Fine structure of Armco iron, treated by shock wave pressures up to 1.2 megabar. IN: Trudy Volgogradskogo politekhnicheskogo instituta, no. 4, 1972, 92-99. (RZh Metallurgiya, 5/73, no. 5I62).

Gorbachev, S. V. Gazy pod vysokim davleniyem. Posobiye po kursu fiz. khimii. (Gases under high pressure. Textbook on physical chemistry.) Moskva, 1971, 44 p. (LC-VKP)

Kirshenina, I. I., V. S. Mikhaylov, and L. N. Fedotov. Change in the structures and electrical properties of titanium, zirconium and their alloys from high pressures. IN: Sbornik. Pretsizionnyye splavy, no. 1, Moskva, izd-vo Metallurgiya, 1972, 151-161. (RZh Metallurgiya, 5/73, no. 5I305)

Leonidova, G. G., and I. N. Polandov. Conductivity of ammonia near the triple point. ZhFKh, no. 5, 1973, 1261.

Omel'chenko, A. V., and E. I. Estrin. Effect of pressure on the kinetics of polymorphic transitions. IN: Sbornik. Probl. metalloved. i. fiz. met., no. 1. Moskva, Metallurgiya, 1972, 5-14. (RZh Metallurgiya, 5/73, no. 5I178).

Polyakova, I. I. Phase state of the surface layer (up to 0.10 mm) of cobalt during high-speed impact. IN: Trudy Volgogradskogo politekhnicheskogo instituta, no. 4, 1972, 168-173. (RZh Metallurgiya, 5/73, no. 5I280).

Prozorov, L. V., et al. Pressovaniye metallov zhidkost'yu vysokogo davleniya. (Compression of metals by high pressure liquid). Moskva, Mashinostroyeniye, 1972, 152 p. (LC-VKP)

Shashkov, D. P. Effect of pressure on the brittleness of chromium. FMiM, no. 4, 1973, 837-838.

Sirenko, A. F., G. P. Klinishev, V. N. Zubov, and Vu Tkhe Khoy. Effect of hydrostatic pressure on the kinetics of copper recrystallization. FMiM, no. 4, 1973, 767-772.

Tambovtseva, L. N., and D. P. Cheprasov. Structural changes in hardened steel from oblique and plane shock waves. IN: Trudy Volgogradskogo politekhnicheskogo instituta, no. 4, 1972, 146-154. (RZh Metallurgiya, 5/73, no. 5I256)

Yershova, T. P., and T. S. Lesikhina. Thermodynamic calculation and experimental study of T-P-C diagrams of a Bi-Cd system at pressures up to 25 kbar. IN: Sbornik. Prob. metalloved. i fiz. met., no. 1. Moskva, Metallurgiya, 1972, 14-24. (RZhMetallurgiya, 5/73, no. 5I16).

Zasavitskiy, I. I., A. I. Likhter, E. G. Pel', and A. P. Shotov. Ustanovka dlya opticheskikh issledovaniy poluprovodnikov v usloviyakh gidrostaticheskogo davleniya do 5 kbar pri 77° K. (Device for optical investigation of semiconductors in conditions of hydrostatic pressures up to 5 kbar at 77° K.) Moskva, 1972, 12 p. (KL Dop vyp, 4/73, no. 8349).

Zaytsev, V. I., Ye. A. Pavlovskaya, and B. P. Filatov. Effect of hydrostatic pressure on substructural developments during fcc-polycrystal deformations. UFZh, no. 5, 1973, 854-858.

iii. High Temperature Research

Bondarenko, V. P., V. V. Kandyba, Ye. N. Fomichev, N. P. Slyusar, A. D. Krivorotenko, and A. A. Kalashnik. Measuring enthalpy, heat and melting point of materials in the condensed phase at high temperatures. Metrologiya, no. 5, 1973, 3-8.

Dugladze, G. M., G. Sh. Darsavelidze, and G. V. Tsagareyshvili. High-temperature internal friction in boron fibers. AN Gruz SSR. Soobshcheniya, v. 70, no. 1, 1973, 141-144.

Grigor'yev, Yu. M., Yu. A. Gal'chenko, and A. G. Merzhanov. Investigating the kinetics of high temperature interaction of aluminum with oxygen by a combustion method. FGiV, no. 2, 1973, 191-199.

Ignatova, T. S., L. V. Uzberg, V. A. Perepelitsyn, and G. V. Gauer. Investigating formation conditions of ZrO_2 solid solution in MgO. NM, v. 9, no. 5, 805-808.

Kashcheyev, V. N. Ferromagnetizm pri vysokikh temperaturakh. (Ferromagnetism at high temperatures). Riga, Izd-vo zinatne, 1972, 162 p. (UFN, v. 110, no. 1, 1973, p. 162)

Lavrenko, V. A., L. A. Glebov, and Ye. S. Lugovskaya. High-temperature oxidation of chromium boride in oxygen. Zashchita metallov, no. 3, 1973, 291-293.

Logachev, Yu. A., and L. N. Vasil'yev. Temperature dependence of phonon thermal conductivity of Ge, Si, and $A^{III}B^{V}$ compounds at high temperatures. FTT, no. 5, 1973, 1612-1614.

Lyutyy, Ye. M. Effect of preload stress values on long-term strength of 1Kh18N9T steel at high temperatures. Problemy prochnosti no. 5, 1973, 76-78.

Nekrasov, K. D., et al. Tyazhelyy beton v usloviyakh povyshennykh temperatur. (Heavy concrete under elevated temperature conditions). Moskva, Stroyizdat, 1972, 128 p. (LC-VKP)

Okrainets, P. N., and V. K. Pishchak. Characteristics of high-temperature creep of metals with an fcc-lattice. IAN Met, no. 3, 1973, 151-156.

Poloskin, Yu. V., and N. L. Makarovskiy. Effect of temperature on the effectiveness of hardening heat-resistant alloy part, MiTOM, no. 5, 1973, 56-59.

Samsonov, G. V., T. V. Dubovik, T. V. Andreyeva, and V. M. Sleptsov. Baked electric insulation material based on boron nitride. Author's certificate USSR, no. 377308, published November 29, 1971. (Otkr izobr, 18/73, p. 18)

Samsonov, G. V., T. V. Dubovik, T. V. Andreyeva, and V. M. Sleptsov. Baked high-temperature material based on boron nitride. Author's certificate USSR, no. 377309, published November 29, 1971. (Otkr izobr, 18/73, p. 18)

Tarasov, V. D., V. Ya. Chekhovskoy, E. E. Shpil'rayn, D. N. Kagan, and L. S. Barkhatov. High-temperature heaters for type TVV-2 and TVV-4 ovens. ZL, no. 5, 1973, 623-625.

Teplofizicheskiye svoystva i gazodinamika vysokotemperaturnykh sred. (Thermophysical properties and gas dynamics of high-temperature media). Moskva, Izd-vo nauka, 1972, 169 p. (RBL, 1/73, no. 983)

Teplofizicheskiye svoystva tverdykh tel. Materialy III Vsesoyuz. teplofiz. konf. po svoystvam veshchestv pri vysokikh temperaturakh. Baku, 1968 g. (Thermophysical properties of solids. Materials of 3rd All-Union thermophysical conference on properties of substances at high temperatures. Baku. 1968). Kiyev, Izd-vo Naukova dumka, 1971, 219 p. (LC-VKP)

Teplofizika i teplotekhnika, vyp. 22. (Thermal physics and thermal engineering, no. 22.) Kiyev, Naukova dumka, 1972, 151 p. (RBL, 1/73, no. 984)

Tkachenko, I. G., and Ye. K. Fen'. Electrophysical properties of hot-pressed niobium pentoxide. Poroshkovaya metallurgiya, no. 5, 1973, 78-81.

Turayev, U., and A. A. Vertman. Magnetic susceptibility of transition metals at high temperatures and in the liquid state. Report 1. Magnetic susceptibility of iron, nickel and cobalt. IAN Tadzh. Fiz-mat. i geol.-khim nauk, no. 1, 1973, 50-55.

Yelyutin, V. P., and Yu. A. Pavlov. Vysokotemperaturnyye materialy. Chast' 1. (High-temperature materials. Part 1). Moskva, Izd-vo energiya, 1972, 120 p. (UFN, v. 110, no. 1, 1973, p. 164).

iv. Miscellaneous Material Properties

Belova, V. M., V. I. Nikolayev, and V. M. Stuchebnikov. Magnetocaloric effect in a superparamagnet. ZhETF P, v. 64, no. 5, 1973, 1746-1749.

Berlin, A. M., V. V. Korshak, Ye. S. Krongauz, R. L. Nikitina, and N. M. Kofman. Synthesis of new polyquinoxalines. DAN SSSR, v. 209, no. 6, 1973, 1333-1336.

Chechik, A. I., P. M. Shvarev, I. O. Yelin, A. S. Perevertov, V. N. Tsvetkov, M. D. Frenkel' and M. S. Akutin. Structural-mechanical investigation of metholon polymer. Plasticheskiye massy, no. 5, 1973, 55-56.

Chistyakov, I. G., L. K. Vistin', L. T. Kantardzhyan, and R. V. Khalatyan. Properties of liquid crystals and their practical application. Promyshlennost' Armenii, no. 4, 1973, 20-22.

Dergunov, N. N., V. I. Frolov, N. Ye. Ripp, V. P. Sosedov and V. N. Barabanov. Reinforcing carbon fibers during conditioning. DAN SSSR, v. 210, no. 1, 1973, 70-71.

Dorofeyev, S. P., P. A. Okunev, and O. G. Tarakanov. Thermogravimetric analysis of acrylonitrile copolymers. IVUZ Khim, no. 5, 1973, 771-773.

Gringauz, G. D., and V. B. Lamper. Methods of determining lower-boundary spread of endurance of duralumin specimens. ZL, no. 5, 1973, 605-609.

Iordanskiy, S. V., O. V. Lokutsiyevskiy, Ye. B. Vul, L. A. Sidorovich, and A. M. Finkel'shteyn. Structural instability of metallic hydrogen with respect to small changes from electron-electron interactions. ZhETF P, v. 17, no. 9, 1973, 530-534.

Kabilov, Z. A., T. M. Muinov, and Sh. Tuychiyev. Mass-spectrometric study of imidization and thermal destruction of poly (pyromellitimide). DAN TadSSR, v. 16, no. 4, 1973, 20-24.

Kipnis, A. Ya. Karbonil'naya metallurgiya. (Carbonyl metallurgy). Moskva, Izd-vo znaniye, 1973, 64 p. (LC-VKP)

Korshak, V. V., A. D. Markov, and A. A. Izyneyev. A method of obtaining sulfone-containing poly (heteroarylenes). Author's certificate, USSR, no. 377322, published May 18, 1971. (Otkr izobr, 18/73, p. 42).

Korshak, V. V., S. V. Vinogradova, V. A. Pankratov, and A. A. Mayorova. Copolymerization of tetracarboxylic dianhydrides with aryldicyanates. Vysokomolekulyarnyye soyedineniya, Kratkiye soobshcheniya, no. 5, 1973, 319.

Nayda, Yu. I., O. S. Nichiporenko, and A. B. Medvedovskiy. Aerodynamic characteristics of nozzles for spraying metallic melts. Poroshkovaya metallurgiya, no. 5, 1973, 94-100.

Poltavtsev, Yu. G., V. P. Zakharov, I. M. Protas, T. V. Remizovich, and V. N. Chugayev. Investigating the molecular composition of vapors and condensate structures during vaporization of various arsenic chalcogenides by laser radiation. UFZh, no. 5, 1973, 752-755.

Shur, Ye. A. Seminar-conference on structural strength of steel and alloys, and methods of their estimation. MiTOM, no. 5, 1973, 77-78.

Sukhushin, Yu. N., Yu. A. Zakharov, and F. I. Ivanov. Decomposition of metal azides in a strong magnetic field. Topography and microscopic decomposition laws of PbN_6, AgN_3 and TlN_3 single crystals. KhVE, v. 7, no. 3, 1973, 261-268.

Turyanitsa, I. D., and B. M. Koperles. Investigating the glass formation region in an Sb-S-I system. NM, no. 5, 1973, 851-852.

Vashchuk, V. Ya., V. G. Nosenko, and N. K. Moshchinskaya. Synthesis and investigation of the properties of polyarylates of aromatic bicyclic dicarboxylic acids and phenolphthalein. IN: Sbornik. Voprosy khimii i khimicheskoy tekhnologii, no. 28, 1973, 15-21.

Yermolenko, A. S., A. V. Korolev, and Ya. S. Shur. $SmCo_5$ single crystals with 32 million gauss x oersted magnetic energy. ZhETF P, v. 17, no. 9, 1973, 499-501.

Zmiy, V. I., A. S. Seryugina, N. V. Kovtun, and Yu. T. Kondratov. The kinetics of siliconizing hafnium in a diffusion regime. NM, no. 5, 1973, 788-790.

v. Superconductivity

Abdullayev, A., N. A. Vitovskiy, Ye. D. Krymova, T. V. Mashovets, S. M. Ryvkin, and A. Ya. Shik. Temperature dependence of the surface layer resistance of indium antimonide in the transition region to superconductivity. FTP, no. 5, 1973, 925-927.

Andreyev, A. F., and V. Bestgen. Fluctuation theory of the two-dimensional mixed state of first order superconductors. ZhETF, v. 64, no. 5, 1973, 1865-1880.

Baramidze, G. A. Eddy oscillation spectra in a pure superconductor. AN GruzSSR, Soobshcheniya, v. 70, no. 1, 1973, 57-60.

Bobrov, V. S., and E. Yu. Gutmanas. Kinetics of plastic deformation at superconducting transitions. Phys. status solidi (b)., v. 54, no. 2, 1972, 413-424. (RZh Metallurgiya, 5/73, no. 5I404)

Druinskiy, Ye. I., and I. I. Fal'ko. Weakening effect in pure double-band superconductors. FMiM, no. 4, 1973, 681-686.

Galayko, V. P. High-frequency current conditions in small superconductors. ZhETF, v. 64, no. 5, 1973, 1824-1838.

Ganzhula, N. N., V. I. Latysheva, V. M. Pan and K. V. Chuistov. Investigating the segregation process in superconducting niobium-aluminum alloys. Metallofizika. Resp. mezhved. sb., no. 36, 1971, 107-111. (RZh Metallurgiya, 5/73, no. 5I228)

Golub, A. A. Excitation of acoustic oscillations in superconducting plates. FTT, no. 5, 1973, 1468-1472.

Gor'kov, L. P. Role of linear chains in forming properties of superconductors with an A-15 structure. ZhETF P, v. 17, no. 9, 1973, 525-529.

Izyumov, Yu. A. Temperature of the superconducting transition in compounds with a β-tungsten structure. FMiM, no. 4, 1973, 687-698.

Khromova, L. I., S. M. Khromov, L. N. Fedotov, V. A. Suvorov, V. I. Krasnykh, and A. I. Il'ichev. Critical current of a superconducting type 70B strip with electrolytic copper coating. IN: Sbornik. Pretsizionnyye splavy, no. 1. Moskva, Metallurgiya, 1972, 100-103. (RZh Metallurgiya, 5/73, no. 5I293)

Nikulin, Ye. I., N. V. Volkenshteyn, and V. Ye. Startsev. Superconductivity of lutetium. ZhETF P, v. 17, no. 9, 1973, 470-472.

Osipova, S. G., A. K. Shtol'ts, and P. V. Gel'd. Intersolubility of lower chromium and vanadium germanides. NM, no. 5, 1973, 860-861.

Palistrant, M. Ye. Effect of pressure and paramagnetic impurities on superconducting properties of metals. TMF, v. 15, no. 2, 1973, 280-287.

Pan, V. M. Relationship of turbulent and filamentary models for nonideal superconductors of the second type. IN: Metallofizika. Resp. mezhved. sb., no. 36, 1971, 98-104. (RZh Metallurgiya, 5/73, no. 5I303.)

Pan, V. M., V. I. Latysheva, and A. I. Sudovtsov. Causes of variations in critical temperatures of Nb_3Al and $Nb_3Al_xGe_{1-x}$ superconducting compounds. IN: ibid., 104-107. (RZh Metallurgiya, 5/73, no. 5I312).

Petrosyan, V. I., V. N. Molin, P. A. Skripkina. Energy gap formation during semimetal - semiconductor quantum dimensional transition in Bi films. FTP, no. 5, 1973, 993-997.

Rabin'kin, A. G., V. N. Galev, and V. N. Laukhin. Effect of uniform high pressures and residual stresses on superconductivity of $V_3(Si_{1-x}Ge_x)$ alloy system. ZhETF, v. 64, no. 5, 1973, 1724-1733.

Rassman, C., and L. Illgen. Relation between structure and critical current density in superconducting titanium-niobium binary alloys. Neue Hutte, v. 17, no. 9, 1972, 321-328. (RZh Metallurgiya, 5/73, no. 5I309).

Rassman, G., and L. Illgen. Relation between structure and critical current density in superconducting titanium-niobium alloys with α-stabilizer admixtures. ibid., 547-553. (RZh Metallurgiya, 5/73, no. 5I306).

Savitskiy, Ye. M., A. V. Revyakin, Yu. V. Yefimov, B. D. Glyuzitskiy, and V. N. Sumarokov. Ultra-high-speed hardening of niobium and vanadium. DAN SSSR, v. 210, no. 2, 1973, 405-407.

Sverkhprovodimost'. (Superconductivity). Kharkov, 1970, 198 p. (LC-VKP)

Sverkhprovodyashchiye splavy i soyedineniya. Trudy VI Vsesoyuz. soveshch. po probleme sverkhprovodyashchikh materialov. (Superconducting alloys and compounds. Proceedings of the 6th All-Union conference on the problem of superconducting materials). Moskva, Izd-vo nauka, 1972, 204 p. (LC-VKP)

Urushadze, G. I. Tunneling of electron pairs in an acoustic field in superconductors. ZhETF, v. 64, no. 5, 1973, 1881-1886.

Venikov, V. A., E. N. Zuyev, and V. S. Okolotin. Sverkhprovodniki v energetike. (Superconductors in power engineering). Moskva, Izd-vo energiya, 1972, 120 p. (UFN, v. 110, no. 1, 1973, 164)

Veselovskiy, A. S., V. F. Verob'yev, et al. A 100 kw alternator with superconducting inductor. Elektrichestvo, no. 5, 1973, 28-32.

Vitovskiy, N. A., G. A. Vikhliy, T. V. Mashovets, and S. M. Ryvkin. Formation conditions and the nature of surface superconductivity of indium antimonide. FTP, no. 5, 1973, 868-873.

Volkov, A. F. Critical current in narrow superconducting bridges. FTT, v. 15, no. 5, 1973, 1364-1368.

Yeru, I. I., S. A. Peskovatskiy, and A. V. Poladich. Nonthermal break in the V-A characteristics of a thin superconducting film. FTT, no. 5, 1973, 1599-1601.

Zelechower, M. On a Josephson tunneling effect in superconductivity. Acta physica polonica, v. A43, no. 5, 1973, 733-735.

Zenkevich, V. B., Ye. Ya. Kazovskiy, and M. G. Kremlev, et al. Sverkhprovodniki v sudovoy tekhnike. (Superconductors in marine technology). Leningrad, Sudostroyeniye, 1971, 256 p. (LC-VKP)

vi. Epitaxial Films

Distler, G. I., and Ye. I. Tokmakova. Epitaxial growth of AgCl on thermoelectret films of poly (vinylchloride), duplicating the electrical properties of an NaCl surface. Kristall, no. 3, 1973, 614-617.

D'yachkova, N. N., L. A. Ivanyutin, A. Yu. Malinin, D. Nishanov, and A. G. Sabinin. Se migration from $AsCl_3$ in a GaAs epitaxial layer. NM, no. 5, 1973, 775-778.

Gorodnichiy, O. P., Ye. P. Seitov, and A. G. Shavrin. Transverse reluctance of n-GaAs epitaxial layers. FTP, no. 5, 1973, 1015-1017.

Kesamanli, F. P., T. D. Raskevich, and A. M. Tuzovskiy. Determining epitaxial n^+ n film thickness in silicon. Tsvetnyye metally, no. 5, 1973, 90-91.

Khitova, L. N., V. B. Lazarova, and N. G. Ryabtsev. Studying the kinetics of GaAs epitaxy in a GaAs-I_2-He flow system. NM, no. 5, 1973, 779-783.

Lavrent'yeva, L. G., M. D. Vilisova, Yu. G. Katayev, Yu. M. Rumyantsev, and A. D. Shumkov. Investigating transition layers in epitaxial gallium arsenide. Effect of the substrate treatment method on distribution of electrons and impurities. IVUZ Fiz, no. 5, 1973, 138-139.

Lyutovich, A. S., O. A. Mamanov, V. V. Kharchenko, and V. P. Pashkudenko. Effect of substrate temperature and partial pressure of PCl_3 on phosphorus capture by silicon epitaxial layers during the growth process. IAN Uzb, no. 2, 1973, 60-62.

Problemy epitaksii poluprovodnikovykh plenok. (Problems on epitaxy of semiconductor films). Novosibirsk, Izd-vo nauka, Sib. otd-niye, 1972, 226 p. (LC-VKP)

Rogulin, V. Yu., and A. A. Shlenskiy. Photoluminescence characteristics of n-$Al_xGa_{1-x}As$ epitaxial layers doped with Te. FTP, no. 5, 1973, 988-990.

Shachnev, V. I. Obtaining alloyed autoepitaxial layers of silicon. NM, no. 5, 1973, 855-857.

Yemel'yanenko, O. V., T. S. Lagunova, R. K. Radu, G. N. Talalakin, and A. A. Telegin. Electrical properties of epitaxial gallium arsenide, tin-doped. FTP, no. 5, 1973, 979-980.

vii. Magnetic Bubble Materials

Sigal, M. A. Resonance absorption in uniaxial crystals with cylindrical (bubble) domain structures. ZhETF P, v. 17, no. 10, 1973, 563-566.

Yakovlev, Yu. M., V. S. Filonich, M. M. Klyuchnikov, and Yu. L. Sapozhnikov. Cylindrical magnetic domains in noncubic single crystals of bismuth-calcium-vanadium ferrogarnets. FTT, no. 5, 1973, 1607-1609.

6. Energy Technology

The articles listed below were collected during the first half of 1973, and are offered as a sample of the type of material available rather than a comprehensive list.

A. Recent Selections

i. MHD

Abkhazi, V. V., A. I. Malykhin, and I. V. Rybin. Nadezhnost' zhidkometallicheskikh induktsionnykh MGD mashin (Reliability of liquid metal induction MHD machines). Moskva, Izd-vo energiya, 1972, 104 p. (LC-VKP)

Abramovich, G. N., D. S. Kovner, A. Ya. Kolpakov, and V. G. Lushchik. Effect of the magnetic field on turbulent flow with shear. Magnitnaya gidrodinamika, no. 1, 1973, 19-25.

Alferov, V. I., L. M. Dmitriyev, and G. N. Dudin. Numerical experiment to study separation of a laminar boundary layer in an MHD channel. TVT, no. 3, 1973, 568-574.

Andreyev, P. A., and I. V. Ioffe. Acoustoelectric effect in hydrodynamics. ZhTF, no. 4, 1973, 849-850.

Bakanov, Yu. A., L. M. Dronnik, M. N. Levin, V. K. Makarevich, L. M. Reshet'ko, V. Ye. Strizhak, I. M. Tolmach, S. R. Troitskiy, and Ye. I. Yantovskiy. An experimental study of the liquid metal induction pump regime. Magnitnaya gidrodinamika, no. 1, 1973, 153-155.

Baranov, V. Yu., D. D. Malyuta, and F. R. Ulinich. Current flow through a boundary layer. TVT, no. 3, 1973, 457-467.

Bashkatov, V. Scientific talent serves the nation (review of Soviet MHD developments). Vechernyaya Moskva, 23 December 1972, p. 2, cols. 3-7.

Bertinov, A. I., L. K. Kovalev, S. M. -A. Koneyev, and V. N. Poltavets. A laminar striated conducting fluid flow in annular channels at large MHD interaction parameters. Magnitnaya gidrodinamika, no. 1, 1973, 79-94.

Bibik, Ye. Ye., B. Ya. Matygullin, Yu. L. Raykher, and M. I. Shliomis. Magnetostatic properties of magnetite colloids. Magnitnaya gidrodinamika, no. 1, 1973, 68-72.

Bondarenko, N. F., Ye. Z. Gak, and G. N. Komarov. Kinetic phenomena in electrolytes of capillary-pore systems under magnetohydrodynamic pressure. Part IV. ZhTF, no. 3, 1973, 684-686.

Buznikov, A. Ye., V. Ye. Vanin, and V. V. Kirillov. Experimental study on nonequilibrium characteristics of an MHD generator. TVT, no. 3, 1973, 622-631.

Chugayevskiy, Yu. V. Nonlinear theory of magnetogravitational (MGR) oscillations and waves. IN: Sb. 7-ye Soveshchaniye po magnitnoy gidrodinamike, Riga, Izd-vo zinatne, v. 3, 1972, 165-166. (RZhF, 11/72, no. 11G32)

Dekhtyarev, V. L., V. N. Khalaydzhi, Yu. V. Smolkin, and I. Z. Kopp. Thermodynamic cycles in an atomic plant using MHD generators. TVT, no. 2, 1973, 385-389.

Electrodeless MHD generator. Jugend und Technik, no. 4, 1973, 337.

Garib, M., and T. P. Kravchuk. A relaxation method for plasma diagnostics. IN: Trudy Un-ta im. Patrisa Lumumby, v. 62, 1972, 48-55. (RZh Elektrotekh, 6/73, no. 6F14)

German, V. O., Yu. P. Kukota, G. A. Lyubimov, B. V. Parfenov, I. S. Poltavtseva, V. M. Sleptsov and G. M. Shchegolev. Operational study of a porous-electrode MHD converter using argon flow with added potassium. TVT, no. 3, 1973, 632-638.

Golovanivskiy, K. S. Resonance diagnostics of pulsed plasma flow in a magnetic field. IN: Trudy Un-ta im. Patrisa Lumumby, v. 62, 1972, 34-47. (RZh Elektrotekh. 6/73, no. 6F16)

Gorbachev, L. P., and Yu. N. Savchenko. Magnetoacoustic signal generation by means of the acoustic wave pulse in an anisotropic conducting medium. Magnitnaya gidrodinamika, no. 1, 1973, 85-89.

Ignatova, T. S., and L. V. Uzberg. Use of periclase materials in MHD generators. IN: Tr. Vostochnogo instituta ogneuporov, no. 13, 1972, 53-73. (RZhKh, 5/73, no. 5M63)

Isers, A. B., and I. Ye. Tarapov. Motion of a magnetizing liquid between parallel planes. Magnitnaya gidrodinamika, no. 1, 1973, 73-78.

Khait, V. D. Superheat instability in the flow of an incompressible conducting medium, in terms of an internal boundary problem. TVT, no. 3, 1973, 468-474.

Kirillov, V. Kh. Electric field in a rectangular MHD channel with Hall effect. PMM, v. 37, 1973, 459-468.

Korotkov, B. A. A method for studying the combined operation of a Faraday MHD generator with an inverter. IAN Energ, no. 3, 1973, 56-61.

Krylova, L. M. Analyzing the electrical efficiency of an induction MHD generator at low magnetic Reynolds numbers. TVT, no. 2, 1973, 396-400.

Lebedev, V. V. Organizing economical computer calculation of optimized parameters of an MHD generator. IN: Nauchn. trudy Mosk. inzh. - ekon. institut, no. 57, 1972, 161-166. (RZh Elektrotekh, 6/73, no. 6F8)

Legeyda, V. I. A study of one problem of flow past bodies in MHD. Magnitnaya gidrodinamika, no. 1, 1973, 145-148.

Makarov, A. M., L. K. Martinson, V. R. Romanovskiy, and S. L. Simkhovich. Electrodynamic visco-plastic fluid flow. Magnitnaya gidrodinamika, no. 1, 1973, 56-60.

Medin, S. A., and N. L. Farber. Distribution of potential and magnetic field in the optimum plane of an MHD generator. TVT, no. 2, 1973, 390-395.

Medin, S. A., and I. M. Rutkevich. Electric field in a channel cross-section of a Hall MHD generator. ZhPMTF, no. 1, 1973, 3-10.

Merkulov, V. I. The motion of a sphere in a conducting fluid in the presence of crossed electric and magnetic fields. Magnitnaya gidrodinamika, no. 1, 1972, 38-42.

Merkulov, V. I., V. F. Tkachenko, and V. I. Yatsenko. Periodic conducting fluid flow in a travelling magnetic field. Magnitnaya gidrodinamika, no. 1, 1973, 43-48.

Motornenko, A. P., Ye. V. Belousov, and A. G. Boyev. MHD generator with a nonequilibrium plasma, generated by SHF ionization. UFZh, no. 6, 1973, 1007-1011.

Mozgovoy, Ye. N., E. Ya. Blum, and A. O. Tsebers. Ferromagnetic fluid flow in a magnetic field. Magnitnaya gidrodinamika, no. 1, 1973, 61-67.

Nemets, I. I., A. I. Nestertsov, G. V. Kukolev, A. I. Rekov, R. Ya. Drozdov, B. M. Barykin, D. A. Vysotskiy, and A. I. Romanov. Study of the interaction of MgO with various Al-containing components. NM, no. 3, 1973, 443-447.

Pishchikov, V. I., G. G. Zezyul'kia, and K. K. Krutikov. Operating characteristics of an MHD generator inverter, for the case of zero and infinite smoothing reactance. Elektrichestvo, no. 1, 1973, 19-24. (RZh Elektrotekh, 5/73, no. 5F13)

Slavin, V. S., and V. S. Sokolov. Closed energy cycle with an MHD generator using the T-layer effect. IN: Sb. Aerofizicheskiye issledovaniya, Novosibirsk, 1972, 76-78. (RZhMekh, 5/73, no. 5B28)

Stefanov, B., and R. Yenikov. Magnetohydrodynamic instability in a direct-current plasmatron. TVT, no. 2, 1973, 401-404.

Strezh, P. Ye. Calculating the dielectric constant tensor of a nonuniform magnetoactive plasma by the T-matrix method. IN: Trudy Un-ta im. Patrisa Lumumby, v. 62, 1972, 77-83. (RZh Elektrotekh, 6/73, no. 6F14)

Tsinober, A. B., and P. G. Shtern. An experimental study of the pressure distribution in a constricted MHD flow past cylinders. Magnitnaya gidrodinamika, no. 1, 1973, 12-18.

Tul'vert, V. F. The application of a pulsation energy balance equation in the theory of MHD pipe and channel flows. Magnitnaya gidrodinamika, no. 1, 1973, 33-37.

Volkov, A. V. An experimental study of the effect of a magnetic field on the turbulence behind the grid. Magnitnaya gidrodinamika, no. 1, 1973, 26-32.

Yantovskiy, Ye. I., and I. M. Tolmach. Magnitogidrodinamicheskiye generatory (Magnetohydrodynamic generators). Moskva, Izd-vo nauka, 1972, 424 p. (LC-VKP)

ii. Fuel Cell

Burshteyn, R. Kh., A. G. Pshenichnikov, M. R. Tarasevich, Yu. A. Chizmadzhev, and Yu. G. Chirkov. Moisture exchange in a hydrogen-oxygen fuel cell with a capillary membrane. II. High moisture capacity electrodes. Elektrokhimiya, no. 1, 1973, 107-110.

Burshteyn, R. Kh., M. R. Tarasevich, V. S. Vilinskaya, F. Z. Sabirov, and A. M. Khutornoy. On the mechanism of promoting action of oxide electro-catalysts. Elektrokhimiya, no. 5, 1973, 725.

Chirkov, Yu. G., G. V. Shteynberg, A. P. Baranov, and V. S. Bagotskiy. Theory of the waterproof air electrode. I. Localization of the current generation region. Elektrokhimiya, no. 5, 1973, 655-659.

Chirkov, Yu. G., G. V. Shteynberg, A. P. Baranov, and V. S. Bagotskiy. Theory of the waterproof air electrode. II. Limiting currents; their dependence on oxygen partial pressure. Elektrokhimiya, no. 5, 1973, 659-662.

Druzhinin, N. G., V. A. Onishchuk, and Yu. A. Chuzmadzhev. Anomalous gas flow into a liquid through a porous hydrophobic membrane [in fuel cells]. Elektrokhimiya, no. 5, 1972, 686-690.

Ganin, Ye. A., and V. P. Postanogov. Stability of a three-phase interface in gas diffusion electrodes in fuel cells. IAN Energ, no. 6, 1972, 107-111.

Gurevich, I. G., and V. S. Bagotskiy. Differentiation between different modes of energy losses during operation of a porous liquid electrode. Elektrokhimiya, no. 12, 1972, 1833-1836.

Jandera, J., and K. Smrcek. Development of electrochemical power sources in Czechoslovakia. Techn. zpravy CKD, no. 3, 1972, 23-29. (RZhElektrotekh, 3/73, no. 3F97)

Krajcsovics, F., G. Gerzsenyi, and P. David. Development of high-temperature fuel cells in Hungary. Elektrotechnika, (Magyar), v. 65, no. 1-2, 1972, 28-33. (RZhElektrotekh, 2/73, no. 2F57).

Lidorenko, N. S., and V. A. Onishchuk. Some aspects of research on hydrogen-oxygen electrochemical power sources. Elektrokhimiya, no. 5, 1972, 676-681.

Mavrodin-Tarabic, M., I. Onaca, and I. Solacolu. Fuel cells with a liquid fuel as high-efficiency power sources. Optimum characteristics of fuel, oxidizers, and electrolytes. Electrotehnica, v. 20, no. 11, 1972, 430-433. (RZhKh, 13/73, no. 13L256)

Meyerovich, I. G., and G. F. Muchnik. Limiting effect of the thermal regime on fuel cell characteristics. I-FZh, v. 24, no. 6, 1973, 1010-1014.

Mokrousov, L. N., N. A. Urisson, and G. V. Shteynberg. Study of hydrophobic property of carbon materials by the charging curves method. Elektrokhimiya, no. 5, 1973, 683-686.

Muchnik, G.F., I. B. Rubashov, V. M. Vlasov et al. Study of active gas flow into electrolysis chambers of fuel cells. Elektrokhimiya, no. 5, 1972, 690-694.

Palanker, V. Sh. Kholodnoye goreniye (Cold combustion). Moskva, Izd-vo nauka, 1972, 112 p. (RZhElektrotekh, 2/73, no. 2F56 K)

Radovici, O., M. Mavrodin-Tarabic, I. Onaca, and I. Solacolu. Effect of a silver activated gas electrode structure on efficiency of fuel cells and air-metal type primary cells. Electrotehica, v. 20, no. 10, 1972, 383-389. (RZhElektrotekh, 6/73, no. 6F79)

Radyushkina, K. A., R. Kh. Burshteyn, B. D. Berezin, M. R. Tarasevich, and S. D. Levina. Oxygen reduction on carbon activated with iron and cobalt phthalocyanines. Elektrokhimiya, no. 3, 1973, 410-412.

Serebryakov, V. N., M. V. Mel'nikov, V. S. Ovchinnikov, and E. I. Grigorov. Analysis of external mass transfer and selection of transfer parameters in the reaction product vapors removal by convection, in a hydrogen-oxygen fuel cell with capillary membrane. I-FZh, v. 24, no. 1, 1973, 28-40.

Shapotkovskiy, N. V. Current-voltage characteristic of a hydrogen-oxygen fuel cell and its dependence on drying conditions. Elektrokhimiya, no. 5, 1972, 682-686.

Sosenkin, V. Ya., Yu. M. Vol'fkovich, and V. S. Bagotskiy. Experimental study of large scale macrokinetics in a hydrogen-oxygen fuel cell with capillary membrane. I. Effect of varying electrolyte content on cell operation. Elektrokhimiya, no. 4, 1973, 514-517.

Svata, M. A catalyst mixture for oxygen electrochemical reduction in fuel cells. Author's certificate, ChSSR no. 140063, published 15 February 1971. (RZhKh, 5/73, no. 5F82P)

Tarnowska-Tierling, A. Carbon oxygen electrode for low-temperature fuel cells. Zeszyty nauk. PSzczec., no. 129, 1972, 67-83. (RZhElektrotekh, 4/73, no. 4F36)

Tarnowska-Tierling, A. Fuel cell polarization in the light of an oxygen half-cell impedance study. Zeszyty nauk. PSzczec., no. 129, 1972, 85-94. (RZhElektrotekh, 4/73, no. 4F30)

Veles, R., M. Kren, I. Khadushfalvi, E. Kadar, Sh. Kultsshar, Ch. Demeter, and L. Chedreki. A production technique for the oxygen electrode of a low temperature fuel cell. Otkr izobr, no. 35, 1972, no. 359872.

Vol'fkovich, Yu. M., and V. S. Bagotskiy. Capillary equilibrium in an electrochemical cell with a porous electrolyte-containing membrane. II. Accounting for the electrolyte concentration gradient. Elektrokhimiya, no. 3, 1973, 362-365.

Vol'fkovich, Yu. M., V. Ye. Sosenkin, and V. S. Bagotskiy. Self-regulation of water drain in a hydrogen-oxygen fuel cell. II. Width of the self-regulation region. I-FZh, v. 23, no. 4, 1972, 618-626.

Volgin, M. A., A. L. Lvov, and V. A. Loskutkin. Electrochemical determination of the coefficient of molecular hydrogen diffusion in a carbonate melt. Elektrokhimiya, no. 3, 1973, 368-371.

Volod'kovskiy, V. Fuel cell power plants. Morskoy sbornik, no. 9, 1972, 86-91.

Wiesener, K. Sulfur dioxide oxidation on porous carbon electrodes in an acid electrolyte. Wiss. S. Techn. Univ. Dresden, v. 21, no. 3, 1972, 513-518. (RZhKh, 7/73, no. 7L285)

Wiesener, K. Theoretical feasibility of direct chemical to electrical energy conversion in technical redox processes. ibid., 507-511. (RZh Kh, 7/73, no. 7L291)

Yanakiyev, A. B., R. N. Kvachkov, and I. M. Geronov. New chemical power sources. Khimiya i industriya (NRB), v. 44, no. 4, 1972. (RzhElektrotekh, 2/73, no. 2F63)

iii. Solar

Agayev, G. B. Problem of solar-energy concentrator geometry. IN: Tr. Moskovskogo aviatsionnogo instituta, no. 229, 1971, 141-144. (LZhS, 6/73, no. 18460)

Akhmedov, A. R. First All-Union Scientific-Technical Conference on the Uses of Regenerative Energy Sources (Tashkent, 1972). Geliotekhnika, no. 1, 1973, 58-59.

Akramov, Kh. T., B. D. Yuldashev, and A. Saidkhanov. Electrical properties and photoconductivity of thin layers of CdS obtained in a hydrogen atmosphere. Geliotekhnika, no. 2, 1972, 3-5.

Arifov, U. A. Development of solar engineering in the USSR. Geliotekhnika, no. 6, 1972, 3-8.

Ashmarin, V. K., and A. S. Lisin. Problem of measuring surface leakage currents in a semiconductor photoconverter. Geliotekhnika, no. 4, 1972, 16-19.

Avesov, R. R., G. Ya. Umarov, M. Kim, and T. Ziyayev. Analysis of the thermal balance of a film-covered semicylindrical solar hothouse. Geliotekhnika, no. 2, 1973, 29-33.

Bayramov, R., and N. R. Korpeyev. Determination of the optimum design of solar water-purification units. IAN Turk, seriya fiz.-tekhn. kh. i geol. nauk, no. 6, 1972, 53-57.

Baum, V. A., A. Kakabayev, and O. Klyshchayeva. Temperature regime of coatings used as regenerators of solutions in solar refrigerating units. Geliotekhnika, no. 2, 1973, 34-37.

Belenov, A. T., O. Annayev, Ch. Agabayev, and Yu. N. Malevskiy. Mechanical characteristics of d.c. motors powered by solar thermoelectric generators of commensurate power. IN: Doklady 1-y Vsesoyuznoy nauchno-tekhnicheskoy konferentsii po vozobnovlyayem, istochn. energii, Moskva, Izd-vo energiya, no. 1, 1972, 27-33. (RZh Elektrotekhnika i energetika, 2/73, no. 2F33)

Dorokhina, T. P., A. K. Zaytseva, M. B. Kagan, A. A. Polisan, and B. A. Kholev. High-voltage gallium arsenide photo converters. Geliotekhnika, no. 2, 1973, 6-8.

Fayzullayev, A. On the determination of the initial tension of a solar-concentrator cover. Geliotekhnika, no. 1, 1973, 27-31.

Gavrilova, I. P. Comparison of the effectiveness of photocells with step-wise and exponential distribution of additives in the alloy layer. Geliotekhnika, no. 6, 1972, 23-28.

Gaziyev, U. Kh., M. M. Koltun, and V. S. Trukhov. Investigation of the thermal resistance of mirror reflecting surfaces with various protective coatings. Geliotekhnika, no. 1, 1973, 32-34.

Gaziyev, U. Kh, M. M. Koltun, and V. S. Trukhov. Formation of defects in reflective coatings under high temperatures. Geliotekhnika, no. 4, 1972, 53-55.

Grilikhes, V. A. Quality-control methods applied to the reflecting surfaces of solar-energy concentrators. Geliotekhnika, no. 4, 1972, 3-15.

Groshkova, G. N. Possible use of semiconductor photocells as ultraviolet receivers. Geliotekhnika, no. 1, 1973, 7-9.

Gurevich, A. M., and G. M. Pozin. Calculation of maximum temperature of caulking compounds used in hothouse enclosures, considering solar radiation. Geliotekhnika, no. 1, 1973, 35-43.

Kim, M., G. Ya. Umarov, and R. R. Avezov. Temperature conditions and the accumulation of heat in film-covered solar hothouses. Geliotekhnika, no. 1, 1973, 50-55.

Kolenko, Ye. A., and M. G. Verdiyev. Use of thermosiphons in thermoelectric instrument building. Geliotekhnika, no. 1, 1973, 10-12.

Kolomoyets, N. V., M. A. Markman, I. A. Sagaydachnyy, and L. M. Simanovskiy. Investigation of rated and actual parameters of room-temperature thermopiles. Geliotekhnika, no. 2, 1973, 9-14.

Kuchkarova, M. A., P. M. Tokhri, and M. Sadikov. Effect of concentrated solar light pulses on productivity of several blue-green algae. Geliotekhnika, no. 1, 1973, 47-49.

Landsman, A. P., D. S. Strebkov, V. A. Unishkov, and V. A. Shvarkova. Investigation of high-voltage photocells under low radiation intensities. Geliotekhnika, no. 1, 1973, 3-6.

Malevskiy, Yu. N., R. R. Aparisi, and Ya. G. Kolos. Solar energy unit. Author's certificate, USSR no. 330312, published 13 October 1972. (RZhElektrotekh, 5/73, no. 5F43 P)

Matveyev, V. M., and V. A. Grilikhes. Analysis of parameters of solar power installations with energy storage. Geliotekhnika, no. 2, 1973, 15-20.

Obshchiye i teoreticheskiye voprosy teploenergetiki. Gelio-energetika. T. 3. Teploobmen pri plenochnom kipenii v elementakh energeticheskikh apparatov (General and theoretical problems in thermal power engineering. Solar engineering. Vol. 3. Heat transfer during film boiling in the components of power units). Itogi nauki i tekhniki, VINITI AN SSSR, Moskva, 1972, 147 p. (RZhMekh, 12/72, no. 12B863 K)

Pul'manov, N. V., V. N. Potapov, and L. I. Prosmushkin. Independent photoelectric generators with solar cells in transparent gas-filled shells. IN: Doklady 1-y Vsesoyuznoy nauchno-tekhnikcheskoy konferentsii po vozobnovlyayem. istochn. energii, Moskva, Izd-vo Energiya, no.1, 1972, 7-12. (RZhElektrotekh, 2/73, no. 2F31)

Rabbimov, R. T., G. Ya. Umarov, and R. A. Zakhidov. On the use of corrugated glass in solar installations. Geliotekhnika, no. 2, 1973, 38-41.

Rodichev, B. Ya. Engineering and economic characteristics of photoelectric water pumping installations. Geliotekhnika, no. 2, 1973, 42-47.

Rzayev, P. F. Temperature determination in a solar hothouse. Geliotekhnika, no. 2, 1973, 48-52.

Saliyeva, R. B. Principles in designing storage units for solar installations. Geliotekhnika, no. 2, 1973, 53-59.

Savchenko, I. G., and B. V. Tarnizhevskiy. Determination of the optimum solar-radiation concentration level for solar batteries with different cooling methods. Geliotekhnika, no. 4, 1972, 20-23.

Shumov, Yu. S. Activity spectrum and quantum yield of the photovoltaic effect in porous phthalocyanine. ZhFKh no. 3, 1973, 718-720.

Tarnizhevskiy, B. V., B. Ya. Rodichev, G. B. Levitskiy, and R. S. Grigoryan. Sun-tracking solar power unit. Otkr izobr, no. 3, 1973, no. 362977.

Teplyakov, D. I. Concentrating capacity of solar engineering paraboloids in various spectral ranges. Geliotekhnika, no. 1, 1973, 20-26.

Teplyakov, D. I. Optical and energy aspects of radiation concentration in high-temperature solar installations. Geliotekhnika, no. 2, 1973, 21-28.

Tsvid, A. A. , and G. V. Davydyuk. Solar radiation flux magnitude on variously oriented vertical surfaces in the city of Khabarovsk. IN: Sb. Voprosy stroitel'stva na Dal'nem Vostoke, Vladivostok, 1972, 51-53. (RZhTeploenerg, 7/73, no. 7G98)

Umarov, G. Ya., and R. A. Zakhidov. Solar engineering research in Uzbekistan. Geliotekhnika, no. 6, 1972, 9-15.

Umarov, G. Ya., I. A. Tursunbayev, I. V. Borisov, V. S. Trukhov, Yu. Ye. Klyuchevskiy, and Ye. P. Orda. A dynamic converter modelled after the Stirling-cycle solar engine, and prospects for its use in self-contained solar power units. IN: Doklady 1-ye Vsesoyuznoy nauchno-tekhnicheskoy konferentsii po vozobnovlyayem. istochn. energii, Moskva, Izd-vo energiya, no. 1, 1972, 20-26. (RZhElektrotekh, 2/73, no. 2F32)

Usmanov, Yu. U., L. N. Teslenko, V. N. Yeliseyev, and G. Ya. Umarov. Some results of theoretical and experimental studies of the thermal state of a solar salt basin. Geliotekhnika, no. 2, 1973, 60-65.

Yakubov, Yu. N., G. Ya. Umarov, and K. B. Baybutayev. Calculation of solar radiation incident on an inclined, finned surface. Geliotekhnika, no. 4, 1972, 60-63.

Yeliseyev, V. N., Yu. U. Usmanov, and G. Ya. Umarov. On determining the efficiency of a solar salt pond. Geliotekhnika, no. 1, 1973, 44-46.

Yevdokimov, V. M., and A. F. Milovanov. Effect of the discontinuity of a fixed field on the receptivity effectiveness of a semiconductor photocell. Geliotekhnika, no. 4, 1972, 24-35.

Yevdokimov, V. M. Accounting for series and shunt resistance in the volt-ampere characteristic of a solar cell. Geliotekhnika, no. 6, 1972, 16-22.

iv. Thermionic

Atomic power without turbines [direct atomic to thermionic energy conversion]. Yunyy tekhnik, no. 8, 1971, 14-15.

Berzhatyy, V. I., V. P. Gritsayenko, A. S. Karnaukhov, V. P. Kiriyenko, V. A. Korolev, O. I. Lyubimtsev, V. A. Mayevskiy, M. V. Mal'nikov, and V. V. Sinyavskiy. Reactor tests of a single thermionic element with a tungsten emitter and an 0.3 mm gap. ZhTF, no. 11, 1972, 2439-2440.

Bito, J. Thermionic generators. Magyar tudomany akademia Muszaki tudomany oszt. kozlemenyek, v. 45, no. 3-4, 1972, 315-329. (RZhElektrotekh, 6/73, no. 6F22)

Broval'skiy, Yu. A., and V. V. Sinyavskiy. Multiparameter optimization of a thermionic generator element. ZhTF, no. 9, 1972, 1909-1914.

Kan, Kh. S., and B. S. Kul'varskaya. Carbide emitters with increased thermionic emission properties. ZhTF, no. 6, 1973, 1269-1274.

Kuznetsov, V. I., and A. Ya. Ender. Characteristics of electron oscillations in a Knudsen thermionic converter. ZhTF, no. 11, 1972, 2391-2397.

Morgulis, N. D., A. I. Kravchenko, and V. Ya. Chernyak. Characteristics of ionization-recombination processes in a plasma discharge diode. ZhTF, no. 11, 1972, 2385-2390.

Nevolin, V. K., V. P. Tsiberev, V. K. Tskhakaya, and V. I. Yarygin. Experimental study on the effect of magnetic pressure on a heavy-current thermionic converter. ZhTF, no. 6, 1973, 1298-1300.

Takibayev, Zh. S. Feasibility of developing a new type of thermionic converter. VAN KasZZR, no. 5, 1973, 28-31.

v. Thermoelectric

Belevtsev, A. T., B. N. Gorshkov, and R. V. Koval'skiy. Selecting the operating temperature of an organically fuelled thermoelectric generator. IAN Energ, no. 6, 1972, 101-106.

Cherkasskiy, A. Kh., and L. L. Silin. Termoelektricheskiye i fotoelektricheskiye generatory (Thermo- and photoelectrical generators). Moskva, 1972, 303 p. (LC-VKP)

Iordanishvili, Ye. K., N. F. Kartenko, A. G. Orlov, and A. D. Finogenov. Thermoelectric properties of gallium-nickel alloys under standard conditions. Geliotekhnika, no. 4, 1972, 36-42.

Kvasnikov, L. A., and G. G. D'yachuk. Maximum efficiency operation of a multistage thermoelectric generator, for the case of series connected stages. IAN Energ, no. 3, 1973, 62-72.

Malygin, Ye. A., M. P. Kozorezov, and A. M. Chernikov. Study on the technology of thermoelectric batteries. IN: Sb. Okhrana truda v razlichnykh otraslyakh narodnogo khozyaystva, Voronezh, Voronezhskiy universitet, 1972, 16-20. (RZhElektrotekh, 2/73, no. 3F23)

Malygin, Ye. A., and M. P. Kozorezov. Safety procedures in manufacturing thermoelectric devices based on bismuth chalcogenides. IN: ibid, 21-24. (RZhElektrotekh, 2/73, no. 2F24)

Nikitin, Ye. N., and V. I. Tarasov. A method for commutating thermoelements. Author's certificate, USSR no. 336739, published 20 June 1972. (RZhElektrotekh, 2/73, no. 2F26 P)

vi. Storage Batteries

Aleskovskiy, V. B. [New anode material for oxygen extraction from sea water]. IAN Kh, no. 5, 1973, 1194-1195.

Boldin, R. V., S. N. Sushentsova, and N. N. Milyutin. Cell wettability and electrolyte flow in hermetically sealed nicad batteries. IN: Sb. rabot po khimicheskim istochnikam toka, Vsesoyuznyy nauchno-issledovatel'skiy akkumulyatornyy institut, no. 7, 1972, 161-163. (RZhElektrotekh, 4/73, no. 4F103)

Budennyy, G. G., A. I. Idzikovskiy, S. A. Levitskiy, N. V. Mgeladze, M. S. Popov, and V. S. Pugachev. A device for controlling the operating mode of an electrochemical generator. Author's certificate, USSR no. 354498, published 24 October 1971. (RZhElektrotekh, 7/73, no. 7F55 P)

Dunayeva, T. I., G. P. Yereyskaya, and N. P. Gayvoronskaya. Study of a silver oxide electrode under conditions of continuous anode-cathode polarization in various modes. ZhPK, no. 4, 1973, 787-792.

Kedrinskiy, I. A. Thermodynamic fundamentals in direct conversion of chemical to electric energy. IN: Sb. Materialy Konferentsiya po itogam nauchno-issledovatel'skiy rabot, Sibirskiy tekhnologicheskiy institut, Neorganicheskaya i analiticheskaya khimiya, Krasnoyarsk, 1972, 173-184. (RZhKh, 5/73, no. 5L247)

Pozin, Yu. M., A. S. Miroshnichenko, and A. V. Nikol'skiy. Preparation method for the positive electrode of an alkaline hermetically sealed nicad battery. Author's certificate, USSR no. 339996, published 21 June 1972 . (RZhElektrotekh, 5/73, no. 5F117 P)

Sbornik rabot po khimicheskim istochnikam toka (Collection of articles on chemical sources of current). Leningrad, Izd-vo energiya, Leningradskoye otdeleniye, no. 7, 1972, 204 p. (KL, 8/73, no. 5546)

Surova, M. D., and S. I. Zhdanov. Electrical conductivity of lithium perchlorate solutions in γ-butyrolactone. Elektrokhimiya, no. 3, 1972, 350-352.

Tomitz, J. Sealed nicad storage batteries and the method of producing them. Author's certificate, GDR NO. 86869, published 5 January 1972. (RZhElektrotekh, 6/73, no. 6G129 P)

vii. Miscellaneous Energy Studies

Adrianov, V. N., and G. L. Polyak. Current status of and prospects for the expansion of research on radiative and complex heat transfer. Teploenergetika, no. 9, 1972, 6-9.

Kapitsa, P. Our home is the planet Earth [Comments on nuclear energy and ecology]. Pravda, 15 May 1973, p. 3.

Laser power plants. Moscow News, no. 5, 1973, p. 10.

Lidorenko, N. S. New methods for generating electrical energy. Elektrichestvo, no. 1, 1973, 1-5.

Makarov, A. A., G. Ye. Tkachenko, V. N. Khanayeva et al. Optimizatsiya i upravleniye v bol'shikh sistemakh energetiki (Optimization and control in large energy systems). Irkutsk, 1970, 143 p. (LC-VKP)

Optimizatsiya raspredeleniya elektroenergii (Optimization of electrical energy distribution). Tallin, 1972, 180 p. (LC-VKP)

Razevig, D. V. High tension power lines go underground [Comments on power transmission and generation systems]. Pravda Ukrainy, 18 April 1973, p. 3.

Semenov, N. Power engineering of the future. Nauka i zhizn', no. 11, 1972, 25-33.

Styrikovich, M. A. Are we threatened by an energy famine? Kazakhstanskaya pravda, 10 June 1973, p. 4, cols. 1-3.

Vorob'yev, O. S., V. B. Yeleiseyev, A. N. Yermilov, V. D. Zakharenko, I. V. Orfanov, and S. V. Ryabikov. Theoretical feasibility of [non-magnetic] conversion of the kinetic energy flux of an ionized gas into electricity. IAN Energ, no. 6, 1972, 96-100.

7. Miscellaneous Interest

A. Abstracts

Tolkachev, K. Rocket goes into antispace [field testing of production prototype of Soviet tunneling rocket]. Sotsialisticheskaya industriya, 25 July 1973, p. 4, cols. 1-5.

A production prototype of a previously described* Soviet tunneling rocket (see Fig. 1) has been field tested in an attempt to dig an

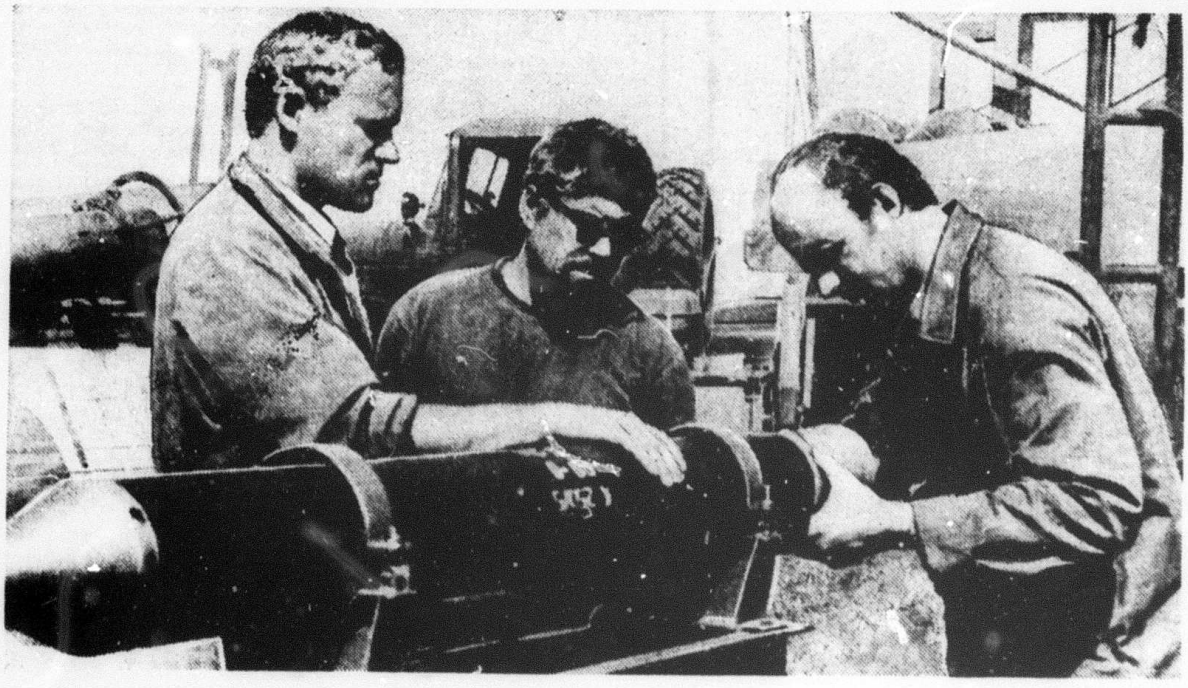

Fig. 1. Refueling the Tunneling Rocket

irrigation well for a Saratov Oblast collective farm.

---

* Stevovich, V. A. Soviet tunneling rockets. Informatics, May 1973, 7 p. (ARPA Order No. 1622-4).

After ignition of the test rocket, sod, loose soil, and other material formed a 40-meter-high column (see Fig. 2), followed

Fig. 2. Tunneling Rocket Ejecta Plume.

13 seconds later by the appearance of white steam. Within 18 seconds, the tunneling rocket had "drilled" a well 1 meter in diameter and 17 meters deep, penetrating three meters into a water-bearing layer. An estimated energy equivalent of 50,000 hp was developed during the eighteen seconds of drilling. After the rocket had been removed* from the well, observers representing the Central Geophysical Trust measured the well diameter and soil temperature at various depths.

---

* It is vaguely implied that the rocket was pulled out of the well by a steel cable, possibly attached prior to the drilling operation; this indicates that the previously reported "self-extraction" capabability either has not yet been achieved or simply was not used in this test.

The tunneling rocket is described as being only 1.5 m long, capable of carrying up to 200 kg of fuel, and fitted with a heat-resistant "nosecone". The refueling operation takes about 20 minutes, and it is mentioned that a single fueling provides the capability for drilling about 10 boreholes of the type described above at negligible cost.

The designer confirms that the principles for the tunneling rocket will be the same regardless of the drilling depth and type of soil. Basically, the drilling is accomplished by highly focused gas jets firing through several sets of nozzles in the head of the rocket. The tip (cutting) nozzles produce gas jets with temperatures of 1000-1500° C and a velocity of about 2000 meters per second, concentrating an enormous amount of energy on a small area and resulting in pulverization of the encountered ground.

Another set of back-angled nozzles firing almost tangentially from the base of the "nosecone" impart forward and rotary motion to the rocket. These side nozzles are used to widen the hole and, combining with the partially expended cutting gas, they also eject loose soil from the well at a rate of 2 tons per second [sic].

Presently, Tsiferov is working on a new rocket with an automatic combustion-chamber cooling and fuel-feed system, capable of operating in hard soil for about half an hour and independently returning to the surface for refueling. In addition, designers are working on a self-propelled transporter, which will also be used to launch the rocket. This system also envisages telescoping well casings to be used in conjunction with the rocket to sink a cased well in 20-30 seconds.

In a related parallel development, Doctor of Technical Sciences V. M. Senyukov has developed a pneumatic drilling tool based on

Tsiferov's principle, where compressed air is utilized instead of gas jets. Presently, this pneumatic rocket is being used in Chelyabinsk to drill boreholes 1.2 m in diameter at a speed of 2.5 meters per second in soft soils.

Sonic Sun? Komsomol'skaya pravda, 3 March 1973, p. 4.

Examination of recent sunspot photographs has revealed unusual waves with a length of 2500 km and propagation velocities ranging from 29,000 to 40,000 km/hr, appearing at 4.5 minute intervals. The constant velocity seems to leave little doubt that the waves are of sonic rather than magnetic origin.

Kachikov, S. "Ikhtiandr" goes on a search. Rabochaya gazeta, 26 July 1973, p. 4, cols. 7-8.

The Kherson Shipyard is completing construction of the 3870-ton (displacement) ship Ikhtiandr which will apparently replace the R/V Odissey as the URV Sever-2* support ship. In addition to its role as a URV tender, the Ikhtiandr will also be capable of fisheries-related research and reconnaissance. The ship is equipped with fish-finding sonar and underwater television cameras capable of horizontal and vertical search. A "hangar" on the deck (port side) will house the URV Sever-2. According to the Ikhtiandr's captain, V. A. Litun, the ship will soon undergo sea trials after which it will depart for Sevastopol' for outfitting. It is interesting to note that this ship bears the same name as an apparently discontinued Soviet man-in-the-sea program which advanced from a simple one-man cabin (1966) through a 30 m^3 three-room sealab (1967) to a diver life-support suit and system (1969-1970) with at least 38 hours endurance. No relationship between the two has yet been established.

---

* Recent Soviet activities in undersea research vehicle development. Selected Material from Soviet Technical Literature, May 1972, 148-150.

Dement'yev, V. V., and O. I. Yas'ko. Magnetogasdynamic effects in a high-intensity electric arc in hydrogen flow. I-FZh, v. 24, no. 1, 1973, 115-119.

The possibility of practical applications of an electric arc in heating hydrogen to high temperatures has prompted an experimental study of the field intensity E and specific heat flux q distributions over a water cooled diaphragm in an arc-discharge plasma. The experimental plasma generator with the diaphragms is described. Measurements were made in a 5-20 mm long narrow (d = 4 mm) water-cooled channel of a discharge chamber at 200-500 a. discharge currents and 1-2 g/sec hydrogen flow rates. The experimental E and q plots versus the diaphragm length ℓ_D show that a negative E and a minimum q = 0 appear simultaneously at I = 400-500 a and ℓ_D = 10-15 mm from the hydrogen inlet. The heat flux q may even decrease to below zero. Both E and q increase sharply at the diaphragm's end. The observed pattern of E and q variations along the diaphragm are tentatively explained by the same process. It is estimated that at a density of the order of 10^5 a/cm^2, E changes sign partly on account of interaction between radial current components in the region of sharp changes in arc diameter and the magnetic field of the axial component.

Kolerov, L. N., G. D. Petrov, and P. A. Samorskiy. Laser methods in heterogeneous plasma diagnostics. IN: Sb. Ukrainskaya respublikanskaya nauchno-tekhnicheskaya konferentsiya posvyashch. 50-letiyu metrologicheskoy sluzhbi UkrSSR, 1972, Khar'kov, 1972, 57 (RZhMetrolog, 2/73, no. 2.32.1007). (Translation).

A submillimeter wavelength interferometric apparatus is described for determining electron concentration in a carbon plasma under

atmospheric pressure. The method of Faraday rotation of the polarization plane is used. Scattering of a high-power laser beam by the particles is used to determine particle size spectrum and concentration of suspended particles. Experimental data are given. The average accuracy of measurements was about 25-30%.

Lomonosov, Yu. I., K. G. Novgorodov, O. G. Sorokhtin, and B. V. Shekhvatov. Side-looking sonar. Avtomatizatsiya nauchnykh issledovaniy morey i okeanov. Symposium. Part I. Sevastopol', 1972, 263-265. (RZh. Geofizika, no. 7, 1973, Abs. 7V73, 11).

A sonar developed in 1968 by the Institute of Oceanology of the USSR Academy of Sciences is described briefly. The operating principle of the instrument is based on the inclined sounding of the bottom by acoustic pulses. The ship-towed sonar transceiver system has a narrow directivity pattern in the horizontal plane, and it emits short acoustic pulses which are reflected from the bottom and returned to the antenna. By proper selection of the pulse repetition frequency, towing depth, and ship speed, a line scan is generated which plots the relief and sediment patterns of the bottom (Translation of abstract).

Inventory of Soviet Marine Research Vessels

The attached list of 291 Soviet vessels has been in compilation since 1965 from three basic sources: scientific and technical literature; newspapers; and the 1964-65 and 1970* Soviet Registers of Seagoing Ships. The ships listed apparently have all operated since the early to mid 1950's and by now, some probably have been retired from service.

As mentioned above, newspapers have been a primary source of information on the existence and activities of Soviet research ships. In some instances, journalistic liberty may have been taken in describing a ship of opportunity or a charter vessel as a research ship; however, in almost all cases this is very difficult to establish, since the Soviets have been somewhat reticent about providing a single, complete guide to their marine-research fleet. Monographs and review articles on research ships generally cover the well-known vessels and mention the existence of others. Rarely is a total number given, and the highest figure yet quoted is "more than 200."

The list is arranged alphabetically by the official or accepted name of the vessel (e.g. Kosmonavt Yuriy Gagarin). A cross-reference entry is also provided based on a vessel's popularly known name (e.g. Gagarin - see Kosmonavt Yuriy Gagarin or Lomonosov - see Mikhail Lomonosov). Additionally, in cases where more than one research vessel bears the same name, the name is multiply listed with a parenthetical indication of the number of such vessels. All of the vessels listed have been mentioned in Soviet open literature presently on file. The amount of information available on any one vessel may vary from complete descriptions of the vessel and its activities, to brief mention of its existence or participation in a research cruise.

---

* only Volume I, A-O of the 1970 Register is presently available in the U.S. Volume N - Ya has been published and should be available soon.

SOVIET OCEANOGRAPHIC, HYDROGRAPHIC, FISHERIES, GEOPHYSICAL, AND WEATHER RESEARCH VESSELS

A

A. I. Boykov
A. I. Voyeykov
A. Smirnov
Adasu (or Ada-Su)
Adler
Admiral Nakhimov
Akademik A. Kovalevskiy
Akademik Arkhangel'skiy
Akademik Berg
Akademik Derzhavin
Akademik Gamburtsev
Akademik Golitsyn
Adademik Gubkin
Akademik Knipovich (1)
Akademik Knipovich (2)
Akademik Korolev
Akademik Krylov
Akademik Kurchatov
Akademik Mir Kasimov
Akademik Oparin
Akademik S. A. Zernov
Akademik Sel'skiy
Akademik Shirshov
Akademik S. Vavilov
Akademik Vernadskiy
Aksay
Alazeya
Aleksandr Nevskiy
Aleksey Chirkov
Algama
Alma-Ata
Al'ba
Al'banov
(see Valerian Al'banov)
Al'batros
Ametist
Andoma
Andrey Vil'kitskiy
Andromeda
Antarktika
Argus
Arkhangel'sk
Arkhangel'skiy
(see Akademik Arkhangel'skiy)
Artem
Artemida
Atlantida
Aysberg (1)
Aysberg (2)
Azimut

B

Bakuvi
Balkhash
Bataysk

Baykal
Bellinsgauzen
(see Faddey Bellinsgauzen)
Belyana
Berg
(see Akademik Berg)
Beta
Bezhitsa
Biolog
Birokan
BMRT Atlant
BMRT Gizhiga
BMRT Salekhard
Boguchar
Boldyrev
(see Konstantin Boldyrev)
Bora
Boris Davydov
Borok
Borovichi
Boykov
(see A. I. Boykov)

C

Chatyr-Dag
Chelyuskin
(see Semen Chelyuskin)
Chernomor
Chirkov
(see Aleksey Chirkov)
Chumakov
(see Kapitan Chumakov)

D

Dal'nevostochnik
Danilevskiy
(see Nikolay Danilevskiy)
Davydov
(see Boris Davydov)
Derygin
(see Professor Deryugin)
Derzhavin
(see Akademik Derzhavin)
Dezhnev
(see Semen Dezhnev)
Diana
Dmitriy Mendeleyev
Dmitriy Ovtsyn
Dobrynin
(see Professor Dobrynin)
Dolinsk
Dzintaryura

E

8-449
Ekvator
Ernst Krenkel' (former Vikhr')

F

Faddey Bellinsgauzen
Farvater
Fedor Litke

Fiolent

Frit'of Nansen

G

G. U. Vereshchagin

Gamburtsev

(see Akademik Gamburtsev)

Gavriil Sarychev

Geliograf

Gemma

Gennadiy Nevel'skoy

Geofizik

Geolog

Georgiy Sedov (1)

Georgiy Sedov (2)

Gidrograf

Gidrolog

Godin

(see Yuriy Godin)

Golitsyn

(see Akademik Golitsyn)

Golovnin

(see Vasiliy Golovnin)

Gonets

Gorizont

Grad

Gromova

(see Ul'yanova Gromova)

Grot

Gubkin

(see Akademik Gubkin)

I

Ikhtiandr

Ikhtiolog

Iney

Ingur

Iskatel'

Issledovatel'

Izmiran

Izumrud (1)

Izumrud (2)

K

Kal'mar

Kamchadel

Kamenskoye

Kapitan Chumakov

Kashkarantsy

Kasimov

(see Akademik Mir Kasimov)

Kegostrov

Khariton Laptev

Kholmogory

Khronometr

Knipovich

(see Akademik Knipovich)

Komarov

(see Kosmonavt Vladimir Komarov

Konstantin Boldyrev

Korifeye

Korolev

(see Akademik Korolev)

L

M

Pelamida
Persey-2
Persey-3
Pervenets
Petr Lebedev
Petr Pakhtusov
Plastun
Poisk
Polyarnik
Polyarnyy
Polyus
Poryv
Poseydon
Povodets
Priboy
Professor Deryugin
Professor Dobrynin
Professor Mesyatsev (1)
(see NIS-5 Professor Mesyatsev)
Professor Mesyatsev (2)
Professor Rudovits
Professor Shorygin
Professor Soldatov
Professor Somov
Professor Vasnetsov
Professor Vize
Professor Zubov
Prometey

R

Radon
Raduga
Rif
Ristna
Rombak
Roslavl'
Rossiya
RS-105 Krasnograd
RS-300
RS-5216
RT-97 Sevastopol'
RT-98 Odessa
RTM Bakhchisaray
RTM Belogorsk
Rudovits
(see Professor Rudovits)

S

Sad-gorod
Sanzar
Sarychev
(see Gavriil Sarychev)
Sedov
(see Georgiy Sedov)
Sekstan
Semen Chelyuskin
Semen Dezhnev
Semga
Sergey Vavilov
(see Akademik S. Vavilov)
Seskar
Sevastopol'
(see RT-97 Sevastopol')

Vega (submarine)
Vereshchagin
(see G. U. Vereshchagin)
Vernadskiy
(see Akademik Vernadskiy)
Vernyy
Vest
Vikhr' (1)
Vikhr' (2) (now Ernst Krenkel')
Vil'kitskiy
(see Andrey Vil'kitskiy)
Vitr-1
Vityaz' (1)
Vityaz' (2)
Vize
(see Professor Vize)
Vladimir Komarov
(see Kosmonavt Vladimir Komarov)
Vladimir Obruchev
Vladimir Vorob'yev
Volna (1)
Volna (2)
Vorob'yev
(see Vladimir Vorob'yev)
Voskhod
Voyeykov
(see A. I. Voyeykov)

Y

Yaroslavets
Yastreb
Yu. M. Shokal'skiy
Yurate
Yuriy Godin

Z

Zarnitsa
Zarya
Zenit
Zernov
(see Akademik S. A. Zernov)
Zeya
Zhemchug
Zheleznyakov
Zhizdra
Zubov
(see Professor Zubov)
Zvezda
(see NIS-Zvezda)
Zuid
Zund

B. Recent Selections

Agranat, M. B., N. P. Novikov, V. P. Perminov, and P. A. Yampol'skiy. Improving the optical stability of liquids. ZhETF P, v. 17, no. 9, 1973, 501-504.

Ballisticheskaya raketa na tverdom toplive. (Solid-fuel ballistic rockets). Moskva, Voyenizdat, 1972, 511 p. (RBL, 1/73, no. 672)

Dolzhenkov, V. A. Priyemniki radiolokatsionnykh stantsiy s selektsiyey dvizhushchikhsya tseley. Ucheb. posobiye po II ch. kursa 'Radiopriyemnyye ustroystva'. (Radar receivers with moving target selection. Textbook for the course in radioreceiver equipment, part 2). Moskva, 1973, 96 p. (KL, 21/73, no. 16098).

Fridman, V. Ts., V. M. Malyshev, and V. V. Blinov. Sudovyye navigatsionnyye radiolokatsionyye stantsii "Kivach-1" and "Kivach-2". (Marine navigation radars Kivach-1 and Kivach-2). Moskva, Pishchevaya prom-st', 1971, 169 p. (LC-VKP)

Frolov, V. S. Elektronno-vychislitel'naya tekhnika v voyennom dele. (Electronic computer technology in military affairs). Moskva, Izd-vo DOSAAF, 1972, 126 p. (LC-VKP)

Gol'danskiy, V. I., and Yu. Kagan. O printsipial'noy vozmozhnosti osushchestvleniya yadernogo gamma-lazera (Preprint). [Possibility of obtaining nuclear gamma-laser. (Preprint)]. Chernogolovka, 1972 22 p. (KL, Dop. vyp, 4/73, no. 7841)

Grigor'yev, M. A., B. D. Zaytsev, G. I. Pylayeva, and V. N. Shevchik. Decay of linear elastic waves in topaz and ruby crystals. FTT, v. 15, no. 5, 1973, 1398-1400.

Ispiryan, K. A., and S. T. Kazandzhyan. Transient radiation and optical properties of materials in the vacuum UV range. FTT, no. 5, 1973, 1551-1555.

Issledovaniye istochnikov nizkotemperaturnoy plazmy. (Investigating sources of low-temperature plasma). Leningrad, 1971, 140 p. (LC-VKP)

Ivandikov, Ya. M. Optiko-elektronnyye pribory dlya oriyentatsii i navigatsii kosmicheskikh apparatov. (Optico-electronic device for orientation and navigation of space apparatus). Moskva, Mashinostroyeniye, 1971, 199 p. (LC-VKP)

Khalatnikov, I. M. Sound propagation in solutions of two superfluids. ZhETF P, v. 17, no. 9, 1973, 534-538.

Kogan, I. M. Blizhnyaya radiolokatsiya. (Teoret. osnovy). (Short-range radar. Theoretical principles). Moskva, Izd-vo "Sov. radio", 1973, 272 p. (KL, 22/73, no. 16809)

Kravets, A. N., V. P. Kuznetsov, and A. A. Kurmangaliyeva. Possibilities of using NaCl crystals as memory cells. IVUZ Fiz, no. 5, 1973, 140-142.

Lebedeva, Ye. A. SShA: gosudarstvennoye vozdeystiye na nauchno-tekhnicheskiy progress. (The USA: Government influence on progress in science and technology). Moskva, nauka, 1972, 215 p. (RBL, 1/73, no. 812)

Metodika i rezul'taty issledovaniy zemnoy kory ·khney mantii. (Methods and results of Earth crustal and upper n...tle studies). Moskva, nauka, 1972, 262 p. (LC-VKP)

The Vint 20- a unique torsatron with an extended magnetic axis. Atomnaya energiya, v. 34, no. 5, 1973, 415-416.

Rokityanskiy, I. I. Geofizicheskiye metody magnitovariatsionnogo zondirovaniya i profilirovaniya. (Geophysical methods of magnetic variational sounding and profiling). Kiyev, Naukova dumka, 1972, 226 p. (RBL, 1/73, no. 435)

Sagdeyev, R. Plasma research in space and in the laboratory. Soviet Science Review, November 1972, 362-368.

Shkadov, L. M., R. S. Bukhanova, V. F. Illarinov, and V. P. Plokhikh. Mekhanika optimal'nogo prostranstvennogo dvizheniya letatel'nykh apparatov v atmosfere. (Mechanics of optimum spatial motion of aircraft in the atmosphere). Moskva, Mashinostroyeniye, 1972, 240 p. (LC-VKP)

Vakman, D. Ye., and R. M. Sedletskiy. Voprosy sinteza radiolokatsionnykh signalov. (Problems on the synthesis of radar signals). Moskva, Sov. radio, 1973, 312 p. (LC-VKP)

Veselago, V. G., Yu. V. Korobkin, and Yu. S. Leonov. Effect of a magnetic field on light dispersion in liquid nematic crystals. ZhETF P, v. 17, no. 10, 1973, 552-554.

Yantovskiy, Ye. I., and I. M. Tolmach. Magnitogidrodinamicheskiye generatory. (MHD generators). Moskva, Izd-vo nauka, 1972, 424 p. (UFN, v. 110, no. 1, 1973, p. 164)

Yushchenkova, N. I., S. A. Senkovenko, and S. M. Chernin. Eksperimental'noye issledovaniye kolebatel'noy neravnovesnosti v sverkhzvukovoy struye CO_2. (Experimental investigation of the vibrational nonequilibrium state of a supersonic CO_2 jet). Moskva, 1972, 10 p. (KL Dop vyp, 4/73, no. 7950)

Zhukov, R. F., et al. Sistemy, pribory i ustroystva podvodnogo poiska. (Systems, instruments and devices used in underwater search). Moskva, Voyenizdat, 1972, 182 p. (RBL, 1/73, no. 1039)

SOURCE ABBREVIATIONS

AiT	-	Avtomatika i telemekhanika
APP	-	Acta physica polonica
DAN ArmSSR	-	Akademiya nauk Armyanskoy SSR. Doklady
DAN AzSSR	-	Akademiya nauk Azerbaydzhanskoy SSR. Doklady
DAN BSSR	-	Akademiya nauk Belorusskoy SSR. Doklady
DAN SSSR	-	Akademiya nauk SSSR. Doklady
DAN TadSSR	-	Akademiya nauk Tadzhikskoy SSR. Doklady
DAN UkrSSR	-	Akademiya nauk Ukrainskoy SSR. Dopovidi
DAN UzbSSR	-	Akademiya nauk Uzbekskoy SSR. Doklady
DBAN	-	Bulgarska akademiya na naukite. Doklady
EOM	-	Elektronnaya obrabotka materialov
FAiO	-	Akademiya nauk SSSR. Izvestiya. Fizika atmosfery i okeana
FGiV	-	Fizika goreniya i vzryva
FiKhOM	-	Fizika i khimiya obrabotka materialov
F-KhMM	-	Fiziko-khimicheskaya mekhanika materialov
FMiM	-	Fizika metallov i metallovedeniye
FTP	-	Fizika i tekhnika poluprovodnikov
FTT	-	Fizika tverdogo tela
FZh	-	Fiziologicheskiy zhurnal
GiA	-	Geomagnetizm i aeronomiya
GiK	-	Geodeziya i kartografiya
IAN Arm	-	Akademiya nauk Armyanskoy SSR. Izvestiya. Fizika
IAN Az	-	Akademiya nauk Azerbaydzhanskoy SSR. Izvestiya. Seriya fiziko-tekhnicheskikh i matematicheskikh nauk

IAN B	-	Akademiya nauk Belorusskoy SSR. Izvestiya. Seriya fiziko-matematicheskikh nauk
IAN Biol	-	Akademiya nauk SSSR. Izvestiya. Seriya biologicheskaya
IAN Energ	-	Akademiya nauk SSSR. Izvestiya. Energetika i transport
IAN Est	-	Akademiya nauk Estonskoy SSR. Izvestiya. Fizika matematika
IAN Fiz	-	Akademiya nauk SSSR. Izvestiya. Seriya fizicheskaya
IAN Fizika zemli	-	Akademiya nauk SSSR. Izvestiya. Fizika zemli
IAN Kh	-	Akademiya nauk SSSR. Izvestiya. Seriya khimicheskaya
IAN Lat	-	Akademiya nauk Latviyskoy SSR. Izvestiya
IAN Met	-	Akademiya nauk SSSR. Izvestiya. Metally
IAN Mold	-	Akademiya nauk Moldavskoy SSR. Izvestiya. Seriya fiziko-tekhnicheskikh i matematicheskikh nauk
IAN SO SSSR	-	Akademiya nauk SSSR. Sibirskoye otdeleniye. Izvestiya
IAN Tadzh	-	Akademiya nauk Tadzhiksoy SSR. Izvestiya. Otdeleniye fiziko-matematicheskikh i geologo-khimicheskikh nauk
IAN TK	-	Akademiya nauk SSSR. Izvestiya. Tekhnicheskaya kibernetika
IAN Turk	-	Akademiya nauk Turkmenskoy SSR. Izvestiya. Seriya fiziko-tekhnicheskikh, khimicheskikh, i geologicheskikh nauk
IAN Uzb	-	Akademiya nauk Uzbekskoy SSR. Izvestiya. Seriya fiziko-matematicheskikh nauk
IBAN	-	Bulgarska akademiya na naukite. Fizicheski institut. Izvestiya na fizicheskaya institut s ANEB
I-FZh	-	Inzhenerno-fizicheskiy zhurnal

IiR	-	Izobretatel' i ratsionalizator
ILEI	-	Leningradskiy elektrotekhnicheskiy institut. Izvestiya
IT	-	Izmeritel'naya tekhnika
IVUZ Avia	-	Izvestiya vysshikh uchebnykh zavedeniy. Aviatsionnaya tekhnika
IVUZ Cher	-	Izvestiya vysshikh uchebnykh zavedeniy. Chernaya metallurgiya
IVUZ Energ	-	Izvestiya vysshikh uchebnykh zavedeniy. Energetika
IVUZ Fiz	-	Izvestiya vysshikh uchebnykh zavedeniy. Fizika
IVUZ Geod	-	Izvestiya vysshikh uchebnykh zavedeniy. Geodeziya i aerofotos"yemka
IVUZ Geol	-	Izvestiya vysshikh uchebnykh zavedeniy. Geologiya i razvedka
IVUZ Gorn	-	Izvestiya vysshikh uchebnykh zavedeniy. Gornyy zhurnal
IVUZ Mash	-	Izvestiya vysshikh uchebnykh zavedeniy. Mashinostroyeniye
IVUZ Priboro	-	Izvestiya vysshikh uchebnykh zavedeniy. Priborostroyeniye
IVUZ Radioelektr	-	Izvestiya vysshikh uchebnykh zavedeniy. Radioelektronika
IVUZ Radiofiz	-	Izvestiya vysshikh uchebnykh zavedeniy. Radiofizika
IVUZ Stroi	-	Izvestiya vysshikh uchebnykh zavedeniy. Stroitel'stvo i arkhitektura
KhVE	-	Khimiya vysokikh energiy
KiK	-	Kinetika i kataliz
KL	-	Knizhnaya letopis'
Kristall	-	Kristallografiya
KSpF	-	Kratkiye soobshcheniya po fizike

LZhS	-	Letopis' zhurnal'nykh statey
MiTOM	-	Metallovedeniye i termicheskaya obrabotka materialov
MP	-	Mekhanika polimerov
MTT	-	Akademiya nauk SSSR. Izvestiya. Mekhanika tverdogo tela
MZhiG	-	Akademiya nauk SSSR. Izvestiya. Mekhanika zhidkosti i gaza
NK	-	Novyye knigi
NM	-	Akademiya nauk SSSR. Izvestiya. Neorganicheskiye materialy
NTO SSSR	-	Nauchno-tekhnicheskiye obshchestva SSSR
OiS	-	Optika i spektroskopiya
OMP	-	Optiko-mekhanicheskaya promyshlennost'
Otkr izobr	-	Otkrytiya, izobreteniya, promyshlennyye obraztsy, tovarnyye znaki
PF	-	Postepy fizyki
Phys abs	-	Physics abstracts
PM	-	Prikladnaya mekhanika
PMM	-	Prikladnaya matematika i mekhanika
PSS	-	Physica status solidi
PSU	-	Pribory i sistemy upravleniya
PTE	-	Pribory i tekhnika eksperimenta
Radiotekh	-	Radiotekhnika
RiE	-	Radiotekhnika i elektronika
RZhAvtom	-	Referativnyy zhurnal. Avtomatika, telemekhanika i vychislitel'naya tekhnika
RZhElektr	-	Referativnyy zhurnal. Elektronika i yeye primeneniye

RZhF	-	Referativnyy zhurnal. Fizika
RZhFoto	-	Referativnyy zhurnal. Fotokinotekhnika
RZhGeod	-	Referativnyy zhurnal. Geodeziya i aeros"-yemka
RZhGeofiz	-	Referativnyy zhurnal. Geofizika
RZhInf	-	Referativnyy zhurnal. Informatics
RZhKh	-	Referativnyy zhurnal. Khimiya
RZhMekh	-	Referativnyy zhurnal. Mekhanika
RZhMetrolog	-	Referativnyy zhurnal. Metrologiya i izmeritel'naya tekhnika
RZhRadiot	-	Referativnyy zhurnal. Radiotekhnika
SovSciRev	-	Soviet science review
TiEKh	-	Teoreticheskaya i eksperimental'naya khimiya
TKiT	-	Tekhnika kino i televideniya
TMF	-	Teoreticheskaya i matematicheskaya fizika
TVT	-	Teplofizika vysokikh temperatur
UFN	-	Uspekhi . icheskikh nauk
UFZh	-	Ukrainskiy fizicheskiy zhurnal
UMS	-	Ustalost' metallov i splavov
UNF	-	Uspekhi nauchnoy fotografii
VAN	-	Akademiya nauk SSSR. Vestnik
VAN BSSR	-	Akademiya nauk Belorusskoy SSR. Vestnik
VAN KazSSR	-	Akademiya nauk Kazakhskoy SSR. Vestnik
VBU	-	Belorusskiy universitet. Vestnik
VNDKh SSSR	-	VNDKh SSSR. Informatsionnyy byulleten'
VLU	-	Leningradskiy universitet. Vestnik. Fizika, khimiya
VMU	-	Moskovskiy universitet. Vestnik. Seriya fizika, astronomiya

ZhETF	-	Zhurnal eksperimental'noy i teoreticheskoy fiziki
ZhETF P	-	Pis'ma v Zhurnal eksperimental'noy i teoreticheskoy fiziki
ZhFKh	-	Zhurnal fizicheskoy khimii
ZhNiPFiK	-	Zhurnal nauchnoy i prikladnoy fotografii i kinematografii
ZhNKh	-	Zhurnal neorganicheskoy khimii
ZhPK	-	Zhurnal prikladnoy khimii
ZhPMTF	-	Zhurnal prikladnoy mekhaniki i tekhnicheskoy fiziki
ZhPS	-	Zhurnal prikladnoy spektroskopii
ZhTF	-	Zhurnal tekhnicheskoy fiziki
ZhVMMF	-	Zhurnal vychislitel'noy matematiki i matematicheskoy fiziki
ZL	-	Zavodskaya laboratoriya

9. AUTHOR INDEX